

NOVEL COPPER-CONTAINING CYTOTOXIC AGENTS BASED ON 2-THIOXOIMIDAZOLONES

Olga Krasnovskaya, Dmitry A Guk, Alexey Naumov, Vita N. Nikitina, Alevtina Semkina, Kseniya Yu. Vlasova, Vadim Pokrovsky, Oksana O Ryabaya, Saida Karshieva, Dmitry A Skvortsov, Irina Zhirkina, Radik Shafikov, Petr Gorelkin, Alexander Vaneev, Alexander Erofeev, Dmitrii Mazur, Viktor Aleksandrovich Tafeenko, Vladimir I. Pergushov, Mikhail Melnikov, Mikhail A. Soldatov, Victor V. Shapovalov, Alexander V. Soldatov, Roman Akasov, Vasily Gerasimov, Dmitry A Sakharov, Anna A. Moiseeva, Nikolay Vasil'evich Zyk, Elena K. Beloglazkina, and Alexander G. Majouga

J. Med. Chem., **Just Accepted Manuscript** • DOI: 10.1021/acs.jmedchem.0c01196 • Publication Date (Web): 28 Sep 2020

Downloaded from pubs.acs.org on September 28, 2020

Just Accepted

"Just Accepted" manuscripts have been peer-reviewed and accepted for publication. They are posted online prior to technical editing, formatting for publication and author proofing. The American Chemical Society provides "Just Accepted" as a service to the research community to expedite the dissemination of scientific material as soon as possible after acceptance. "Just Accepted" manuscripts appear in full in PDF format accompanied by an HTML abstract. "Just Accepted" manuscripts have been fully peer reviewed, but should not be considered the official version of record. They are citable by the Digital Object Identifier (DOI®). "Just Accepted" is an optional service offered to authors. Therefore, the "Just Accepted" Web site may not include all articles that will be published in the journal. After a manuscript is technically edited and formatted, it will be removed from the "Just Accepted" Web site and published as an ASAP article. Note that technical editing may introduce minor changes to the manuscript text and/or graphics which could affect content, and all legal disclaimers and ethical guidelines that apply to the journal pertain. ACS cannot be held responsible for errors or consequences arising from the use of information contained in these "Just Accepted" manuscripts.

	Soldatov, Mikhail; Southern Federal University, The Smart Materials Research Institute
	Shapovalov, Victor; Uznyj federal'nyj universitet, Department of Physics
	Soldatov, Alexander; Uznyj federal'nyj universitet,
	Akasov, Roman; National University of Science and Technology MISIS; I
	M Sechenov First Moscow State Medical University
	Gerasimov, Vasily; Dmitry Mendeleev University of Chemical Technology of Russia
	Sakharov, Dmitry; Dmitry Mendeleev University of Chemical Technology of Russia
	Moiseeva, Anna; Lomonosov Moscow State University Department of Chemistry, Chemistry
	Zyk, Nikolay; Lomonosov Moscow State University Department of Chemistry, Chemistry
	Beloglazkina, Elena; Lomonosov Moscow State University, Chemistry
	Majouga, Alexander; Lomonosov Moscow State University, Chemistry; Dmitry Mendeleev University of Chemical Technology of Russia; National University of Science and Technology MISIS

SCHOLARONE™
Manuscripts

NOVEL COPPER-CONTAINING CYTOTOXIC AGENTS BASED ON 2-THIOXOIMIDAZOLONES

Olga O. Krasnovskaya^{1,2*}‡, Dmitry A. Guk^{2‡}, Alexey E. Naumov², Vita N. Nikitina², Alevtina S. Semkina^{3,4}, Kseniya Yu. Vlasova², Vadim Pokrovsky^{5,6}, Oksana O. Ryabaya⁵, Saida S. Karshieva⁵, Dmitry A. Skvortsov^{2,7}, Irina V. Zhirkina², Radik R. Shafikov², Petr V. Gorelkin¹, Alexander N. Vaneev^{1,2}, Alexander S. Erofeev¹, Dmitrii M. Mazur², Viktor A. Tafenko², Vladimir I. Pergushov², Mikhail Ya. Melnikov², Mikhail A. Soldatov⁸, Victor V. Shapovalov⁸, Alexander V. Soldatov⁸, Roman. A. Akasov^{1,9}, Vasily M. Gerasimov¹⁰, Dmitry A. Sakharov¹⁰, Anna A. Moiseeva², Nikolay V. Zyk², Elena K. Beloglazkina² and Alexander G. Majouga^{1,2,10}

¹National University of Science and Technology MISIS, Department of Materials Science of Semiconductors and Dielectrics, Leninskiy prospect 4, Moscow 101000, Russia

²Lomonosov Moscow State University, Chemistry Department, Leninskie Gory, 1/3, Moscow, 119991, Russia

³Pirogov Russian National Research Medical University, Department of Medical Nanobiotechnologies, Ostrovityanova 1, Moscow 117997, Russia

⁴Serbsky National Medical Research Center for Psychiatry and Narcology, Department of Basic and Applied Neurobiology, Kropotkinskiy 23, Moscow 119991, Russia

⁵N.N. Blokhin National Medical Research Center of Oncology of the Ministry of Health of the Russian Federation, Kashirskoe highway 23, Moscow 115478, Russia

⁶People's Friendship University, Moscow, Russia, Miklukho-Maklaya 6, 117198, Moscow, Russia,

⁷Higher School of Economics, department of biology and biotechnologies, Myasnitskaya 13, Moscow 101000, Russia

⁸The Smart Materials Research Institute Southern Federal University Sladkova, 178/24 Rostov-on-Don, 344090, Russia

⁹I.M. Sechenov First Moscow State Medical University, Trubetskaya 8-2, Moscow 119991, Russia

¹⁰Mendelev University of Chemical Technology of Russia, Miusskaya sq. 9, Moscow 125047, Russia

ABSTRACT: A series of 73 ligands and 73 of their Cu⁺² and Cu⁺¹ copper complexes with different geometries, oxidation states of the metal, and redox activities were synthesized and characterized. The aim of the study was to establish the structure-activity relationship within a series of analogues with different substituents at the N(3) position, which govern the redox potentials of the Cu⁺²/Cu⁺¹ redox couples, ROS generation ability, and intracellular accumulation. Possible cytotoxicity mechanisms, such as DNA damage, DNA intercalation, telomerase inhibition, and apoptosis induction have been investigated. ROS formation in MCF-7 cells and 3D spheroids was proven using Pt-nanoelectrode. Drug accumulation and ROS formation at 40-60 μm spheroid depths was found to be the key factor for the drug efficacy in the 3D tumor model, governed by the Cu⁺²/Cu⁺¹ redox potential. A nontoxic in vivo single dose evaluation for two binuclear mixed-valence Cu⁺¹/Cu⁺² redox-active coordination compounds, **72k** and **61k**, was evaluated.

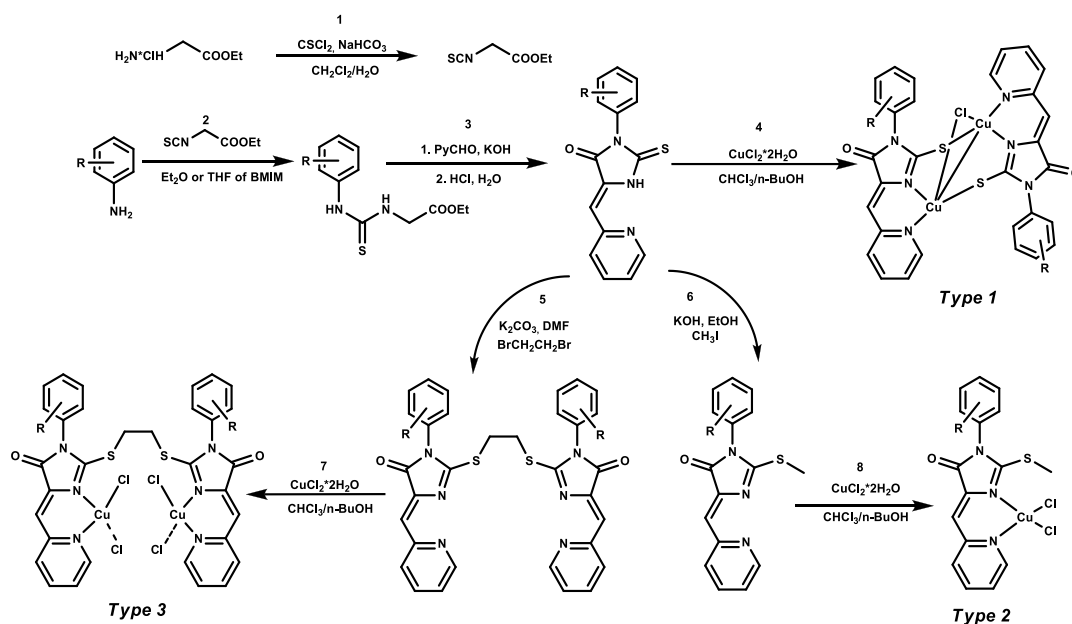
INTRODUCTION

Organometallic complexes are one of the most promising types of anticancer drugs. Monovalent and divalent copper complexes have been investigated in the last few years as less toxic and cheaper alternatives to platinum complexes.^{1,2} Two copper redox states (Cu⁺¹ and Cu⁺²), different possible geometries around the metal center (tetrahedral, square-planar and octahedral) and a variety of cytotoxicity mechanisms (proteasome activity inhibition,² telomerase inhibition,^{3,4} formation of reactive oxygen species (ROS),⁵ DNA degradation,⁶ DNA intercalation,⁷ and paraptosis⁸) make copper coordination compounds especially promising antitumor therapeutic agents.

Copper-containing coordination compounds are not only effective antitumor agents,⁹ but are also effective as antimicrobial,¹⁰ anti-tuberculosis,¹¹ anti-malarial,¹² antifungal¹³ and anti-inflammatory¹⁴ drugs. ⁶⁴Cu-labeled coordination compounds are promising positron emission tomography PET imaging agents for the

diagnosis of malignant pathologies, including head and neck cancer¹⁵, as well as the hallmark of Alzheimer disease, amyloid-β (Aβ).¹⁶⁻¹⁸ The redox properties of copper ions, their ability for intracellular reduction, their selective accumulation in hypoxic areas, and their stability in blood flow means copper-containing therapeutic agents can be used not only for therapeutic purposes but also as diagnostic and theranostic agents.¹⁹ Due to the higher biocompatibility of copper-containing anticancer drugs in comparison with classical platinum agents, Cu-based therapy are supposed to be well tolerated and does not induce substantial body weight loss.²⁰ Several clinical trials of various redox-active disulfiram and copper gluconate combinations are currently ongoing.²¹⁻²³

A key factor for drug toxicity is having a high cellular uptake.²⁴ Drug uptake is influenced by such factors as steric mobility, the oxidation state of the metal cation, the geometry of the coordination compound, ligand

Scheme 1. Synthetic Routes to Type 1-3 coordination compounds.

lipophilicity, and redox activity.²⁵ Cu⁺¹ coordination compounds show higher cytotoxicity and cell accumulation than Cu⁺² analogues.²⁶ Typically, monovalent Cu⁺¹ coordination compounds are phosphine-based due to their high stability²⁷, other Cu⁺¹ coordination compounds are poorly described.

Intracellular redox processes determine cellular viability, where a disturbance in redox homeostasis may affect cell death.²⁸ The biological activity of the copper coordination compound is mostly affected by its intracellular redox activity, therefore the Cu⁺²/Cu⁺¹ redox potential is one of the most important physicochemical parameters upon which the effectiveness of the copper-based drug depends. The relationship between the redox potentials and both the coordination geometry and nature of the donor atoms has long been a subject of interest in copper chemistry,²⁹ especially because copper-containing antitumor drug efficiency correlates with the aforementioned physicochemical parameters.

In this work, we set the task of stabilizing the unstable Cu⁺¹ state by varying the donor atoms and ligand substituent nature in organic core, as well as the geometry and the redox activity of the coordination compounds. We conducted a large-scale study of how the initial ligand structure influences the copper oxidation state and the mechanism of cytotoxicity.

Recently, we have proven that copper 2-thioxoimidazolidone complexes exhibit antitumor activity both *in vitro* and *in vivo*. The binuclear mixed-valence Cu⁺¹/Cu⁺² complex showed a telomerase inhibition ability along with the highest *in vivo* tumor CA-755 growth inhibition.³⁰ In this work, we have greatly expanded this series, having synthesized three types of coordination compounds based on 2-thioxoimidazolidones, which are different in geometry, the oxidation state of copper ions, the redox behavior and a mechanism of cytotoxic activity.

RESULTS AND DISCUSSION

Synthesis and Characterization. Three types of ligands based on 2-thioxoimidazolidin-4-ones (Type 1), 2-(methylthio)-1H-imidazol-5(4H)-ones (Type 2) and 2,2'-(ethane-1,2-diylbis(sulfanediyl))bis-1H-imidazol-

5(4H)-ones (Type 3) were prepared according to Scheme 1. The ¹H and ¹³C NMR and mass spectrometry data were consistent with the proposed structures of the ligands (Tables S1-S3, Figures S46-S118). Purity of targeted compounds was confirmed by HPLC (Tables S4-S15, Figures S1-S8). The type 3 ligands were all *cis*-isomers with magnetically equivalent protons in the ethylene spacer, except for the ortho-fluoro-substituted ligands **60**, **66** and ligand **65**. The Cu⁺², Cu⁺¹ complexes were prepared via solvent layering technique with a copper chloride dihydrate: ligands in a 1:1 (1:2) molar ratio in butanol-1/chloroform system. A series of 73 copper 2-complexes were synthesized and characterized. The color of the complexes obtained differs from bright red to black, depending on the copper oxidation state. By varying the nature of the organic motifs and the donor atom set, we developed three types of copper coordination compounds with different geometries: Type 1 are binuclear Cu^{+1.5}/Cu^{+1.5} coordination compounds, with distorted trigonal bipyramidal geometry, and one bridging chlorine atom located at the same distance from both metal atoms; Type 2 are mononuclear Cu⁺² coordination compounds with tetrahedral geometry; and binuclear type 3 coordination compounds have various oxidation states and geometries of the copper ions: Cu⁺²/Cu⁺², Cu⁺²/Cu⁺¹, Cu⁺¹/Cu⁺¹. UV-Vis data and stability studies of coordination compounds are presented at Figures S14-S24, Table S17.

Organic motif – copper oxidation state. We assumed that the presence of strong electron acceptors (R) in organic core stabilize copper in the monovalent state. Among the three types of coordination compounds (Table 1), the influence of a substituent in the third position of the 2-thioxoimidazolidin-4-one ring on the copper oxidation state is the strongest in type 3, where all three possible subtypes (Cu⁺²/Cu⁺², Cu⁺²/Cu⁺¹, Cu⁺¹/Cu⁺¹) are present. Large electron-withdrawing substituents effectively stabilize Cu⁺¹ (**70k-73k**). Electron-donating groups stabilize Cu⁺² (**52-57k**). **58k-69k** are mixed-valence copper coordination compounds. Butyl alcohol is assumed to be a reducing agent

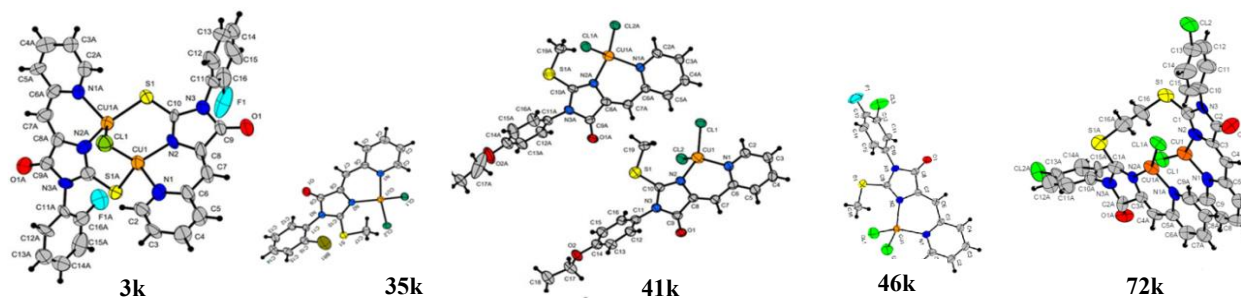


Figure 1. ORTEP representations of the X-ray structure X-ray crystal structure for **3k**, **35k**, **41k**, **46k**, and **72k**.

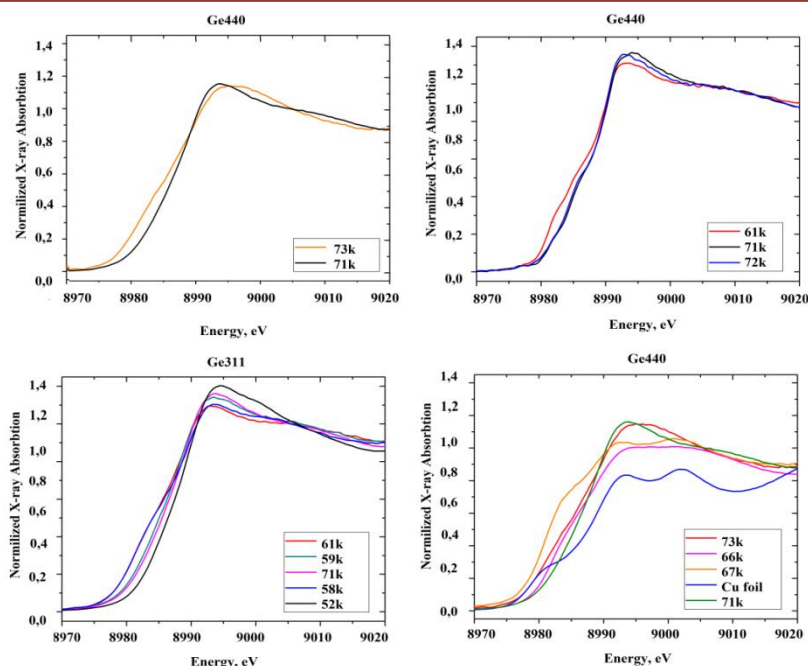


Figure 2. X-ray Absorption Near Edge Structure spectra of Type 3 coordination compounds.

for the copper ion, since the complexation reaction in acetonitrile does not lead to the formation of monovalent copper.³¹ The structures of the five coordination compounds in the solid state were established using X-ray crystallography, the copper oxidation state was determined via X-ray absorption near edge structure (XANES) in solid samples, cyclic voltammetry and electron paramagnetic resonance (EPR) spectra were used for the DMF solutions of the coordination compounds.

Crystallography. Five metal complexes **3k** (Type 1), **35k**, **41k**, **46k** (Type 2), and **72k** (Type 3) were characterized using single-crystal X-ray crystallography. Their thermal ellipsoid plots and atom numberings are shown in Figure 1, and the selected bond lengths are given in Tables 1, S18. Additionally, the X-ray data for **53k** and **54k** have been described previously.³² In the Type 1 coordination compounds (Aba2), copper is coordinated

by two nitrogen atoms and a sulfur atom, which leads to the binuclear coordination compound formation with a Cu – Cu distance of 2.519 Å plus one bridging chlorine atom equidistant from both metal centers (2.346 Å and 2.409 Å).

In Type 2 coordination compounds (P21/n), copper is coordinated through the two N atoms, forming a tetrahedral geometry complex. Coordination compound **72k** is a binuclear Cu⁺/Cu⁺ compound with trigonal-planar coordination geometry, with Cu-Cl bounding 2.151 Å, Cu-N bounding 1.95 Å and 1.97 Å. (P2₁2₁2₁).

XANES spectroscopy. X-ray absorption near edge structure spectroscopic studies gives information on the local chemical environment of the absorbing atom in solids, liquids or gases. At the K (or L3,2-) edges of a selected atom, strong resonances appear below the ionization potential, which are assigned to the transitions of the 1s (or 2p) electron to unoccupied molecular

Table 1. Selected bond lengths (Å) for coordination compounds **3k**, **35k**, **41k**, **46k**, **72k**

	3k	35k	41k	46k	72k
Cu1 – Cl1	2.346(5)	2.214(1)	2.229(2)	2.198(2)	2.154(6)
Cu1 – Cl2	–	2.222(1)	2.216(2)	2.231(1)	–
Cu1 – N1	2.05(1)	2.038(3)	2.029(5)	2.029(4)	1.99(2)
Cu1 – N2	1.94(1)	1.981(3)	2.025(4)	1.964(4)	1.90(1)
Cu1 – Cu1A	2.519(4)	–	–	–	–
Cu1 – S1A	2.291(5)	–	–	–	–
Cl1 – Cu1A	2.409(5)	–	–	–	–
S1 – C10	1.65(1)	1.709(3)	1.707(5)	1.708(5)	1.67(3)
S1A – C10A	1.68(1)	–	–	–	1.70(3)

1
2
3
4
5
6
7
8
9
10
11
12
13
14
15
16
17
18
19
20
21
22
23
24
25
26
27
28
29
30
31
32
33
34
35
36
37
38
39
40
41
42
43
44
45
46
47
48
49
50
51
52
53
54
55
56
57
58
59
60

orbitals. An analysis of these resonances gives information about the electronic structure.³³ Furthermore, in the XANES spectra, the mean free run length of the photoelectron, due to its small kinetic energy ($E_c < 50\text{--}100\text{ eV}$), provides a high contribution to multiple scattering events of the photoelectron allowing to probe the three-dimensional structure (3D) around the absorbing atom.³⁴ The position of the absorption edge not only depends on the charge (oxidation state/valence) of the absorbing atom but also on the local atomic structure (bond lengths and angles, coordination numbers, symmetry, etc.).

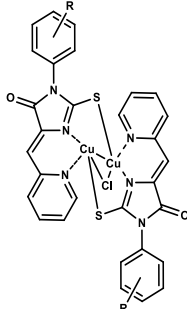
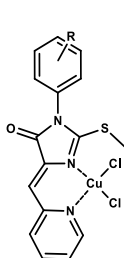
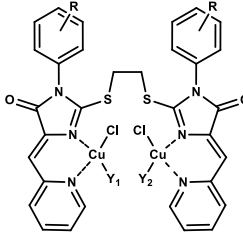
The XANES spectra of Type 3 coordination compounds are presented in Figure 2. Based on an intensity at 8984 eV, we can conclude that the coordination compounds **71k** ($\text{Cu}^{+1}/\text{Cu}^{+1}$) and **73k** ($\text{Cu}^{+1}/\text{Cu}^{+1}$) have similar local atomic and electronic structures for the copper atoms (Figure 2, A). **61k** ($\text{Cu}^{+2}/\text{Cu}^{+1}$), in comparison with samples **71k** and **72k** (Figure 2, B), shows an increase in the “shoulder” height at 8984 eV and a drop in the maximum absorption, which implies a similar ligand environment and different geometries of copper atoms in **72k** and **61k**, while the X-ray absorption data of **71k** and **72k** confirms similar local atomic structures. The X-ray absorption spectra of compounds **59k**, **58k** and **61k** confirm similar local atomic structures of the coordination compounds and demonstrate an increase in the “shoulder” height at 8984 eV and a drop in the maximum absorption when compared with **71k**. The $\text{Cu}^{+2}/\text{Cu}^{+2}$ compound **52k** demonstrates a structural difference from the mixed-valence **58k**, **61k** and monovalent **71k**, which indicates a different geometry and a higher Cu oxidation state (Figure 2, C). The X-ray absorption data of the difluoro-substituted coordination compounds **66k** and **67k** suggests that the complexes are mixed-valence and have different local atomic structures. Considering the NMR spectra, compound **66k** is a trans-isomer, and **67k** has a cis-configuration. The oxidation states of the cations are also determined from the reference samples. The XANES spectra of compounds **3k**, **14k** (Type 1), **43k** (Type 2) and the XANES spectra of Type 3 coordination compounds compared with the reference samples of copper oxides CuO, Cu₂O are given in the SI (Figures S25-S26).

Cyclic voltammetry. To assess the influence of the redox properties on the biological activity, as well as to confirm the oxidation state of copper ions in Type 3 coordination compounds, cyclic voltammetry (CV) and voltammetry with a rotating disk electrode (RDE) were used. Due to the low water solubility of the complexes, DMF was chosen as the solvent, with 0.1 M Bu₄NClO₄ as the supporting electrolyte.

All coordination compounds of Type 1 demonstrated quasi-reversible $\text{Cu}^{+1.5}/\text{Cu}^{+1.5} \rightarrow \text{Cu}^{+1}/\text{Cu}^{+1}$ reduction at potentials $E_{pc} \sim 0.00 - 0.18\text{ V}$, and $\text{Cu}^{+1.5}/\text{Cu}^{+1.5} \rightarrow \text{Cu}^{+2}/\text{Cu}^{+2}$ oxidation at potentials $E_{pa} \sim 0.34 - 0.58\text{ V}$ (Figure S27, Table S19). RDE voltammograms prove the oxidation and reduction process take place in Type 1 coordination compounds (Figure S28).

All coordination compounds of Type 2 showed quasi-reversible cathodic peaks corresponding to the $\text{Cu}^{+2} \rightarrow \text{Cu}^{+1}$ reduction at potentials $E_{pc} \sim 0.32 - 0.41\text{ V}$ in the cathodic region (Figure S29, Table S20). The RDE voltammogram proves that only the oxidation process occurs in the coordination compound of Type 2 (Figure S30).

Table 2. Various types of coordination compounds obtained.

Type 1			Type 2		Type 3			
								
Nº	X	Nº	X	Nº	X	Y1	Y2	
1k	4-F	30k	4-F	52k	4-OMe			
2k	3-F	31k	3-F	53k	4-OEt			
3k	2-F	32k	2-F	54k	3,4-OMe	Cl	Cl	
4k	4-Br	33k	4-Br	55k	4-tBu			
5k	3-Br	34k	3-Br	56k	2,4,6-Me			
6k	2-Br	35k	2-Br	57k	2-tBu			
7k	2-Br, 4-F	36k	2-Br, 4-F	58k	4-F			
8k	4-Cl	37k	4-Cl	59k	3-F			
9k	3-Cl	38k	3-Cl	60k	2-F			
10k	2-Cl	39k	2-Cl	61k	3-Br			
11k	4-OMe	40k	4-OMe	62k	2-Br			
12k	4-OEt	41k	4-OEt	63k	2-Cl			
13k	3, 4-OMe	42k	3, 4-OMe	64k	2-OMe 4-Cl, 5-Me			
14k	4-tBu	43k	4-tBu	65k	2-Br, 4-F			
15k	2-tBu	44k	2-tBu	66k	2,5-F	Cl	-	
16k	4-NO ₂	45k	2-OMe 4-Cl, 5-	67k	3,5-F			
17k	2-Me, 4-NEt ₂	46k	3-Cl, 4-F	68k	2-Me, 3-Cl			
18k	2-OMe, 4-Cl, 5-Me	47k	2-Me, 3-Cl	69k	4-SMe			
19k	3-Cl, 4-F	48k	2,4,6-Me	70k	3-Cl			
20k	2-Me, 3-Cl	49k	4-SMe	71k	4-Br			
21k	2,4,6-Me	50k	2,5-F	72k	4-Cl	-	-	
22k	4-SMe	51k	3,5-F	73k	3-Cl, 4-F			
23k	4-J							
24k	2-Me, 4-NEt ₂							
25k	2,6-Cl							
26k	2,4,6-Cl							
27k	2,6-Br							
28k	2,5-F							
29k	3,5-F							

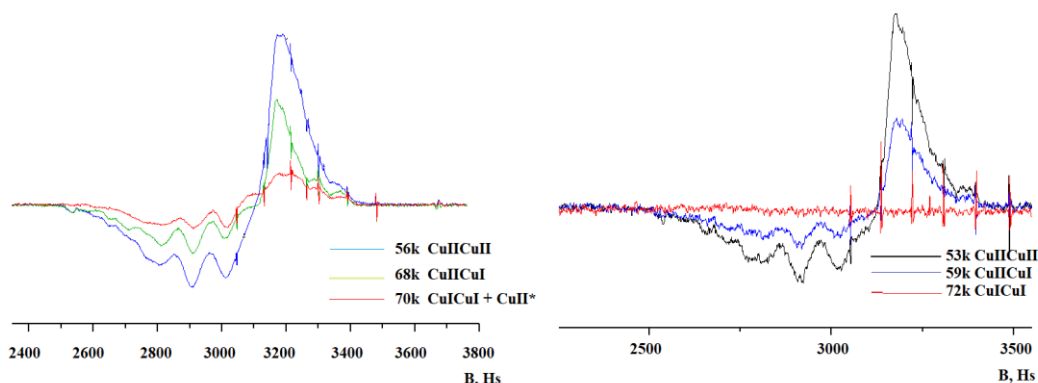


Figure 3. EPR spectra of Type 3 coordination compounds.

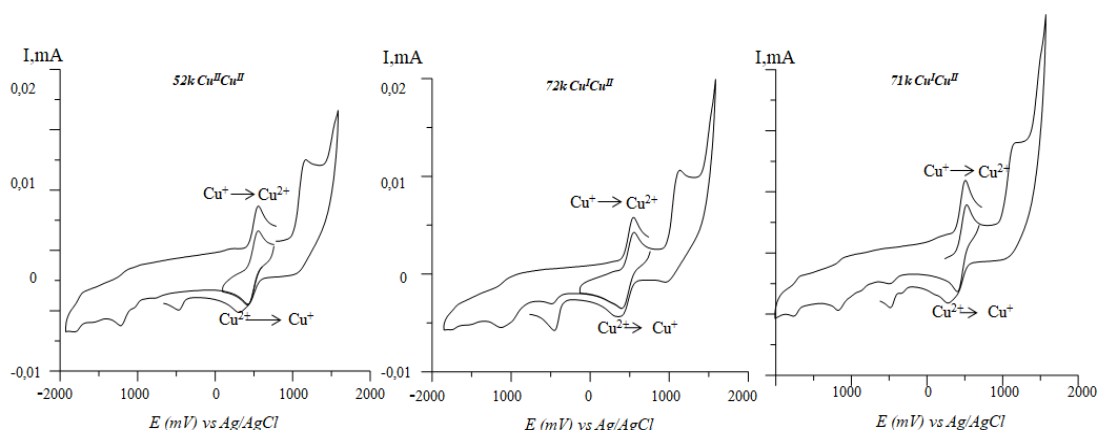


Figure 4. Cyclic voltammograms of Type 3 coordination compounds.

All coordination compounds of Type 3 showed similar voltammograms, regardless of the oxidation state of copper (Figures 4, S31, Table S21). Two reversible waves were observed at the E range 0.3–0.6 mV vs Ag/AgCl, which could be ascribed to the one-electron oxidation of Cu^+ to Cu^{2+} and chlorine oxidation, respectively.³⁵ Recently, Schneider et al. reported a mixed-valence pyridylamide-based complex, and the oxidation of Cu^{2+} , Cu^+ centers was irreversible.³⁶ In our case, both reversible oxidation and reduction are observed.

RDE voltammogram allows for the identification of different redox transition currents $\text{Cu}^{2+}/\text{Cu}^+$ (Figure S32): for Cu^+/Cu^+ complexes (**71k**) only the oxidation current is observed (anodic process $\text{Cu}^+ \rightarrow \text{Cu}^{2+}$), for $\text{Cu}^{2+}/\text{Cu}^{2+}$ (**52k**) complexes only the reduction current is observed (cathodic reaction $\text{Cu}^{2+} \rightarrow \text{Cu}^+$), for mixed-valence complexes $\text{Cu}^+/\text{Cu}^{2+}$ (**61k**) the voltammogram exhibits both anodic and cathodic limiting currents. Most complexes of Type 3 are mixed-valence, which implies the high stability of the resulting $\text{Cu}^{2+}/\text{Cu}^+$ redox system. Despite the fact that **72k** in a solid form is a Cu^+/Cu^+ complex, which was confirmed by the XANES and X-ray data (Figures 1, 2), the resulting rotating ring-disk electrode voltammogram confirms the presence of two copper cations at different oxidation states (Figure S32). Apparently, the instantaneous oxidation of one of the copper cations Cu^+ occurs in solution.

EPR spectroscopy. The EPR spectroscopy is an invaluable method for characterizing the ligand environment and oxidation states of paramagnetic metal complexes.³⁷ EPR spectroscopy enables unambiguously distinguishing Cu^+ ($d10$, $S = 1$) / Cu^{2+} ($d9$, $S = 1/2$) metal

cations in the coordination compound based on their different magnetic susceptibilities. To exclude the spontaneous oxidation of copper cations, which was observed in electrochemical experiments, EPR measurements were made in degassed solutions in the absence of oxygen. The EPR spectra for coordination compounds **53k** ($\text{Cu}^{2+}/\text{Cu}^{2+}$), **56k** ($\text{Cu}^{2+}/\text{Cu}^{2+}$), **58k** ($\text{Cu}^+/\text{Cu}^{2+}$), **59k** ($\text{Cu}^+/\text{Cu}^{2+}$), **70k** (Cu^+/Cu^+), and **72k** (Cu^+/Cu^+) were recorded. In the DMF solution for **70k** there is an admixture of Cu^{2+} (Figure 3), whereas for paramagnetic Cu^{2+} the cations are absent in the degassed DMF solution of the coordination compound **72k** (Cu^+/Cu^+). Despite the fact that the coordination compounds **70k** and **72k** are monovalent Cu^+/Cu^+ when in solid form, as soon as they appear in solution, spontaneous oxidation occurs with the formation of a mixed-valence complex $\text{Cu}^{2+}/\text{Cu}^+$. The coordination compounds **53k** and **56k** are paramagnetic ($\text{Cu}^{2+}/\text{Cu}^{2+}$), and mixed-valence coordination compounds **58k** and **59k** have an intermediate position between them due to the presence of one paramagnetic Cu^{2+} and one diamagnetic Cu^+ centers (Figure 3). Additionally, for coordination compounds **56k** ($\text{Cu}^{2+}/\text{Cu}^{2+}$) and **59k** ($\text{Cu}^+/\text{Cu}^{2+}$), the axial and rhombic symmetry of metal centers was evaluated (Figure S33).

Biological Assays. *In vitro* cytotoxicity, cellular accumulation/distribution, protein binding, DNA intercalation, nuclease activity, apoptosis test, telomerase inhibition, reactive oxygen species formation in the 2D cell monolayer and a 3D spheroid model of the copper complexes (all three types) were studied to clarify the cytotoxicity mechanism of the synthesized coordination compounds.

Table 3. Cytotoxicity data of the coordination compounds.

														IC ₅₀ , μM
	HEK-293	MCF-7	A-549	Va-13		HEK-293	MCF-7	A-549	Va-13		HEK-293	MCF-7	A-549	Va-13
1k	1.9±0.1	3.4±0.4	4.4±0.3	2.6±0.2						54k	9.35±8.23	7.04±1.05	17.08±2.07	5.84±1.95
2k	1.6±0.2	2.8±0.6	4.7±0.3	2.6±0.2	24k	15.3±1.8	18.1±2.2	31.4±4	17.7±1.4	55k	3±1	55±20	102±50	10±2.8
3k	2.1±0.2	9.2±8.1	5.2±0.6	2.5±0.1	28k	-	~10	~14	~16	56k	~14	~12	~54	~17
4k	1.3±0.5	9.6±2.9	24±6.5	9.2±1.8	29k	-	~9	~15	~17	57k	6.48±1.17	19.4±17.87	31.66±3.7	18.17±4.4
5k	2.4±0.4	2.8±0.4	3.0±0.5	2.7±0.5	30k	11±9	1.8±0.5	~10	1.5±0.7	58k	6.8±3.0	6.6±1.4	5.4±2	8.1±2.5
6k	0.9±0.1	2.9±0.3	4.2±1.2	0.9±0.1	31k	3.6±0.5	5±1	7±1	4.0±0.5	59k	1.8±0.2	2.4±0.2	5.1±0.4	~3
7k	6.0±2.5	9.5±0.8	8.3±1.8	2.25±0.1	32k	3.6±0.2	5.2±0.8	6.6±0.4	4.3±0.4	60k	0.8±0.0	2.6±0.4	1.7±0.1	1.1±0.1
8k	2.3±0.3	1.9±0.4	5.7±0.6	1.3±0.2	33k	2.9±0.2	4.4±0.1	9.6±5.3	3.3±0.3	61k	0.3±0.1	0.5±0.1	1±0.4	2.2±0.8
9k	1.1±0.1	1.4±0.1	1.7±0.1	1.9±0.3	34k	4.9±0.6	9.5±0.7	9.8±0.9	9.4±0.7	62k	1.7±0.3	9.2±0.7	8.2±1.3	5.7±0.6
10k	0.8±0.1	2.5±0.5	3.3±0.7	>	35k	4.6±0.6	8.5±0.7	9.8±0.9	9.0±0.7	63k	4.1±0.2	5.1±0.2	8.1±2.3	3.5±0.2
11k	1.6±0.1	2.3±0.2	3.8±1.4	1.7±0.3	36k	1.02±0.47	2.04±0.54	1.85±0.54	0.91±0.23	64k	2.87±1.81	12.11±1.18	18.68±1.32	10.24±3.14
12k	2.6±0.4	6.8±0.6	7.7±0.5	0.2±0	37k	1.05±0.40	~5	1.93±0.40	1.19±0.30	65k	0.49±0.10	1.24±0.20	2.24±0.20	0.73±0.10
13k	5.1±2.4	5.2±1.0	7.7±0.9	3.8±1	38k	-	~12	~54	~48	66k	-	1.6±0.6	1.3±4.7	1±2
15k	6.3±0.3	6.8±0.6	6.7±1.5	4.3±0.3	39k	1.6±0.1	2.6±0.3	4±1	1.4±0.2	67k	-	1.0±2.8	1.4±0.9	2.8±1.2
16	4.1±0.2	5.1±0.2	8.1±2.3	3.5±0.2	40k	1.6±0.1	2.3±0.2	3.8±1.4	1.7±0.3	68k	-	~8	~23	~12
16k	0.07±0.0	1.5±0.2	2.3±0.4	2.3±0.3	41k	2.1±0.3	4.2±0.2	4.6±0.6	2.4±0.1	69k	-	~12	~54	~48
17k	-	~15	~11		46k	-	~19	~14	~16	70k	-	~6	~11	~8
18k	58±4	95±32	45±14	24±7	47k	-	~3	~11	~13	71k	1.5±0.5	2.0±0.4	1.7±0.5	1.3±0.2
19k	-	~13	~57	~31	48k	-	~3	~12	~14	72k	0.5±0.0	0.6±0.0	1.3±0.2	0.8±0.1
20k	-	~3	~8	~4	49k	-	~9	~2	~3	73k	-	~6	~11	~7
21k	-	~55	~75	~66	50k	-	~3	~10	~14					
22k	-	~65	~3	~3	52k	3.38±0.55	5.61±1.21	7.89±0.38	3.03±0.07	Dox	0.01	0.06	0.37±0.19	0.2±0.04
23k	2.9±0.9	4.2±1.0	9.7±2.9	10.7±2.1						CDDP	0.50±0.05	0.62±0.15	10.96±1.42	5.48±1.44
					53k	10.8±3.7	19.7±2.4	>50	21.1±2.7					

In vitro Anticancer Activity. MTT data for the coordination compounds are presented in Table 3. Additionally, for a number of coordination compounds, a fluorescent proteins detection assay was used. The cytotoxicity was measured by the live-imaging of MCF-7 Katushka cells.³⁸ All coordination compounds had a higher toxicity than the original ligands, however, several ligands (**4** - **7**, **10**, and **16**) showed comparable cytotoxicity (Table S22). Most of the compounds **1k** - **73k** have cytotoxicity comparable to cisplatin. The mixed-valence Cu⁺²/Cu⁺¹ coordination compound **61k** and Cu⁺²/Cu⁺¹ **72k** can be considered as lead compounds. Binuclear coordination compounds Cu⁺²/Cu⁺² are generally less toxic than the mixed-valence and monovalent analogs. A change in the substituent's nature and its position has a strong effect on the cytotoxic activity; our task was to establish the nature of this influence and the cytotoxicity mechanism.

Intracellular accumulation/distribution. An intracellular accumulation/distribution of all three types of coordination compounds was studied using the atomic absorption spectroscopy (AAS) technique.

The Type 1 coordination compounds are the most penetrating compounds, with high intracellular accumulation for metal-containing drugs (~40%), accumulating in the nuclei and mitochondria. Type 2 and 3 coordination compounds are also high-penetrating

(except Cu⁺²/Cu⁺² coordination compounds **52k** and **53k**), while demonstrating cytoplasm accumulation. Among the

Type 3 coordination compounds, it is clearly seen that Cu⁺²/Cu⁺² (**52k** and **53k**) coordination compounds are low-penetrating, while Cu⁺¹/Cu⁺¹, Cu⁺²/Cu⁺¹ (**72k** and **61k**) show better cellular accumulation, and as a result are stronger cytotoxic agents (Tables 4, S23).

DNA damage/DNA intercalation. DNA is a therapeutic target for most metal-based agents, where nuclease activity is one of the most common antitumor activities for copper-containing anticancer drugs.³⁹⁻⁴¹ We have tested the DNA cleavage ability of all 3 types of coordination compounds (Tables 4, S24, Figure S34). None of the Type 1 complexes showed nuclease activity, while the representatives of Type 2 proved to be chemical nucleases. The geometry of Type 1 coordination compounds probably does not allow them to exhibit nuclease activity, while the small size of Type 2 coordination compounds allows effective DNA interaction. The lead compound **61k** (type 3) showed a weak nuclease activity, meaning it is not the main mechanism of cytotoxic action. The lead compound **72k** showed no nuclease activity at all. Additionally, DNA intercalation was studied by classic competitive binding assays with ethidium bromide.⁴² Most coordination

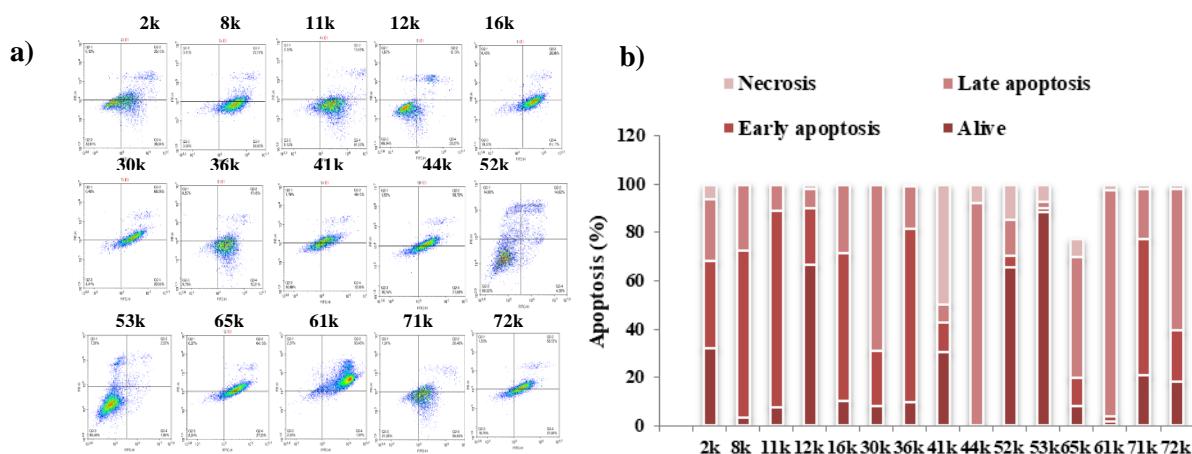


Figure 5. Apoptosis analysis of MCF-7 cells by Annexin V-FITC/PI staining after treatment with coordination compounds.

compounds can intercalate DNA with $K_{app} \sim 10^5$ M, and the values obtained correlate with those obtained for coordination compounds of copper with anticancer

activity.⁴³ Expectedly, organic ligands do not intercalate DNA, except for cytotoxic ligand 16 (Table S25, Figures S35-S37). However, a lack of correlation between the

ability to intercalate DNA and cytotoxicity makes the DNA intercalation ability noncritical for the cytotoxicity of studied ligands and coordination compounds.

BSA binding. BSA is a protein of choice by many biochemists for studying drug-protein interaction and its contribution to the distribution and metabolism of the drug through different organs of the human body.⁴⁴ We have monitored quenching in the fluorescence properties of BSA in the presence of chosen ligands and coordination compounds. It is clear that the fluorescence intensity of BSA

progressively decreases with the binding of copper complexes (Figures S38-S40). Binding constants with albumin were measured by the fluorescence emission spectrum of BSA.⁴⁵ The calculated values ($K_b \sim 10^7$) (Table

S26) suggested significant binding of the selected ligand and complexes to BSA.⁴⁶

Telomerase inhibition. Since the previously described mixed-valence Cu^{+2}/Cu^{+1} 2-thioxoimidazolone-based coordination compound, which was an effective antitumor drug *in vivo*, acted as a telomerase inhibitor,³⁰ the study of the ability of coordination compounds to inhibit telomerase was of particular interest to us. Since an increased telomerase activity in tumor cells has been repeatedly proven,⁴⁷ copper coordination compounds as telomerase inhibitors is of interest.⁴⁸ Among the representatives of all three types, coordination compounds capable of inhibiting the telomerase enzyme were found (1k, 36k and 40k). However, the lead compound 61k showed the highest inhibition rate (Tables 4, S27).

Cell death (apoptosis/necrosis). Induction of the apoptosis by the complexes in the MCF-7 cancer cell line was analyzed with the Annexin V-FITC/PI double staining assay.⁴⁹ The results are presented in the dot plots in Figure 5. The level of phosphatidylserine quantified the treatment of the MCF-7 cells with the complexes for 24

Table 4. Investigation of the intracellular accumulation and various mechanisms of the antiproliferative activity of coordination compounds.

		Intracellular accumulation*	DNA damage (Nuclease activity)**	DNA intercalation***	Apoptosis****	Telomerase inhibition*****
Type 1	Compound tested	6k, 8k, 16k	5k, 8k, 10k, 16k	1k, 2k, 4k-8k, 10k, 12k, 16k	2k, 8k, 11k, 12k, 16k	1k, 5k, 8k, 10k, 16k
$Cu^{+1.5}/Cu^{+1.5}$	Result	~40%	No	$K_b \sim 10^5$, except 2k, 5k	Early apoptosis	1k - average inhibition rate
Type 2	Compound tested	30k, 36k	30k, 36k, 39k, 40k	29k, 30k, 35k, 40k	30k, 36k, 41k, 44k	30k, 36k, 39k, 40k
Cu^{+2}	Result	~25%	Average	$K_b \sim 10^5$, except 40k	Late apoptosis	36k, 40k - average inhibition rate
Type 3	Compound tested	52k, 53k (Cu^{+2}/Cu^{+2}) 57k, 61k, 65k (Cu^{+1}/Cu^{+2}) 72k (Cu^{+1}/Cu^{+1})	61k, 65k, 71k, 72k	53k, 59k, 71k, 72k	53k, 61k, 65k, 71k, 72k	61k, 65k, 71k, 72k
Cu^{+2}/Cu^{+2}	Result	~6%; ~20%; ~24%	Weak, 72k - no nuclease activity	$K_b \sim 10^5$, except 59k	Late Apoptosis, 71k - 56% of necrosis	61k - high inhibition rate

*4T1 breast cancer cells, 24 hours of incubation; ** pUC18 plasmid DNA ***calf thymus DNA+ EB competitive binding method; ***** MCF-7 breast cancer cells, 24 hours of incubation; ***** TRAP method

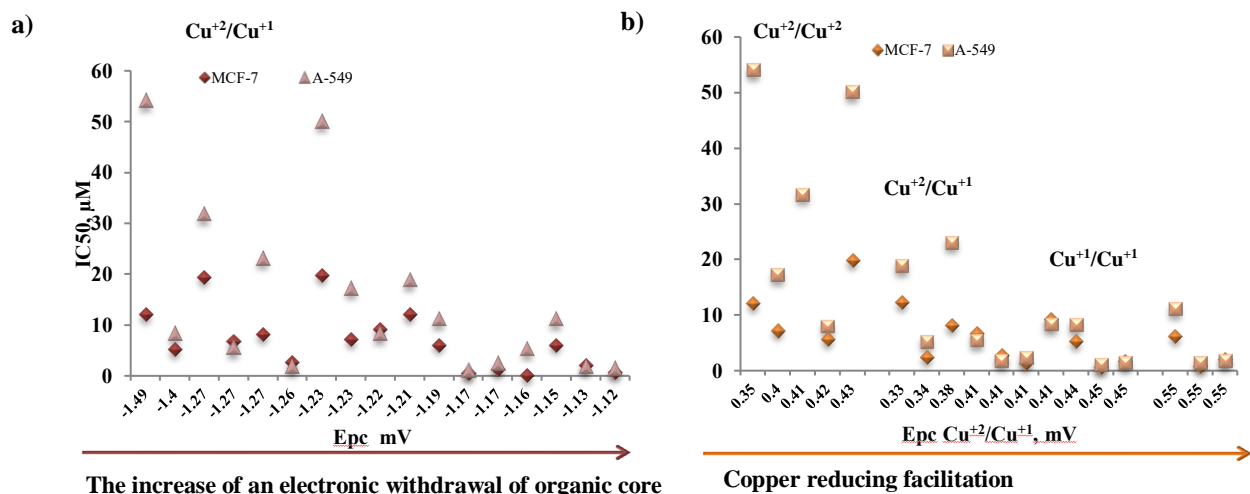


Figure 6. A) The effect of the electron-donor properties of the ligand core on the oxidation state of copper and cytotoxicity of coordination compound. The higher the electron withdrawal of the ligand, the higher the copper reduction potential, the more stable the monovalent state of the copper cation, and the higher the cytotoxicity. B) Dependence of the Cu^{2+}/Cu^{+1} redox potential on cytotoxicity within each subtype. The higher the redox Cu^{2+}/Cu^{+1} potential, the easier the reduction reaction, and the higher the cytotoxicity of the coordination compound.

hours, exhibiting results as viable, early apoptosis, late apoptosis and necrosis, and their percentages (Table S28). All the complexes of Type 1 exhibited early apoptosis; Type 2 and 3 exhibited late apoptosis. Thus, these results confirm that copper complexes induce apoptosis instead of necrosis in MCF-7 cancer cells.

Redox potential as a key factor of drug efficiency. The ability of the organic core to affect the Cu^{2+}/Cu^{+1} redox potential and the drug accumulation was repeatedly proven by the Cu-ATSM series.^{50–53} Radiolabeled ^{64}Cu , ^{62}Cu and ^{60}Cu coordination compounds based on thiosemicarbazone were used as a hypoxia-sensitive PET-imaging agent, capable of accumulation in hypoxic regions.⁵⁰ Dearling et al. proposed a mechanism of trapping and selectivity-based around the redox behavior of the Cu^{2+}/Cu^{+1} couple.⁵¹ In an attempt to further elucidate this proposed mechanism, Blower et al. conducted extensive structure–activity relationship (SAR) studies on a series of thirteen similar CuATSM complexes.⁵² They found that hypoxia selectivity strongly correlated with both the Cu^{2+}/Cu^{+1} reduction potential and the alkyl substitution pattern on the backbone of the ligand. The sensitivity of Cu-ATSM to hypoxia is achieved by irreversible anaerobic

intracellular reduction of a copper-containing drug, along with the inability of the Cu^{+1} -based drug to leave the cell.⁵³ Recently, Anjum et al. reported eight bis(thiosemicarbazone)-based copper coordination compounds, and established some structure-activity ratios.⁵⁴ Electron-donating effects of the disubstitutions on the diamine backbone leads to a lowering in the Cu^{2+}/Cu^{+1} redox potential, and the authors suggested that cytotoxicity could be controlled by the redox potential. Based on this, we also suggested a cytotoxic efficacy to be directly dependent on the electrochemical potential Cu^{2+}/Cu^{+1} .

In all three types of coordination compounds, the redox behavior of copper cations was influenced by a substituent in the aromatic ring. The dependence can be observed when the ortho- and para-halogen-substituted coordination compounds of all three types are compared (Table 5). An increase in the size and mesomeric donation ability of the para-substituent leads to an increase in Epa ($Cu^{+1} \rightarrow Cu^{+2}$) and a decrease in Epc ($Cu^{+2} \rightarrow Cu^{+1}$). The influence of ortho substituents does not coincide with the influence of para-substituents, and in some cases is directly opposite, where an increase in the electron withdrawing ability leads to an increase in Epa ($Cu^{+1} \rightarrow Cu^{+2}$) and a decrease in Epc ($Cu^{+2} \rightarrow Cu^{+1}$) (Table 4).

Table 5. The effect of the substituent in the aromatic ring of the ligand on the redox behavior of copper cations in the coordination compound. (Epa - electron donation, the lower Epa, then the easier the redox-reaction; Epc - Electron acceptance, the higher Epc, then the easier redox-reaction)

Para	Type 1	Epa	$IC_{50}, \mu M$ (MCF-7)	Type 2	Epc	$IC_{50}, \mu M$ (MCF-7)	Type 3	Epa	Epc	$IC_{50}, \mu M$ (MCF-7)
4-F	1k	0.34V	3.4±0.4	30k	0.40/0.55V	1.8±0.5	58k	0.54/0.41	0.41/0.54	6.6±1.4
4-Cl	8k	0.45V	1.9±0.4	37k	0.36/0.58V	~5	72k	0.54/0.40	-	0.6±0.0
4-Br	4k	0.59/0.44V	9.6±2.9	33k	0.32/0.56V	4.4±0.1	71k	0.55/0.45	-	2.0±0.4
<hr/>										
Orto		Epc $Cu^{+2} \rightarrow Cu^{+1}$		Epa $Cu^{+1} \rightarrow Cu^{+2}$		Epc $Cu^{+2} \rightarrow Cu^{+1}$				
2-F	3k	0.55V	9.2±2.1	32k	0.12/0.41V	5.2±0.8	60k	0.41/0.12	0.12/0.41	2.6±0.4
2-Cl	10k	0.53/0.42V	2.5±0.5	39k	0.41/0.56V	2.6±0.3	62k	0.56/0.41	0.41/0.56	9.2±0.7
2-Br	6k	0.52/0.44V	2.9±0.3	35k	0.44/0.55V	8.5±0.7	63k	0.55/0.44	0.44/0.55	5.1±0.2

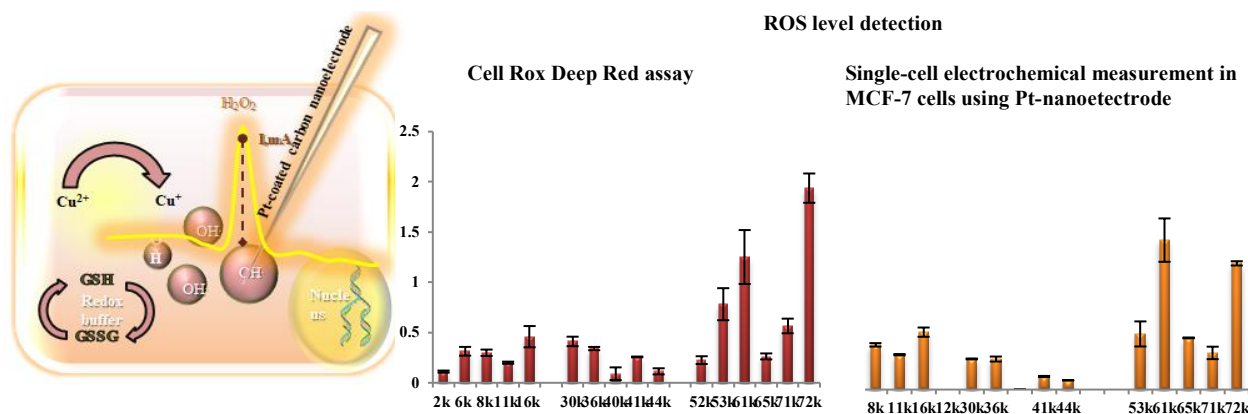


Figure 7. ROS level quantification in MCF-7 cells by single cell H_2O_2 level measurement by Pt-nanoelectrode and Cell Rox Deep Red fluorescent assay.

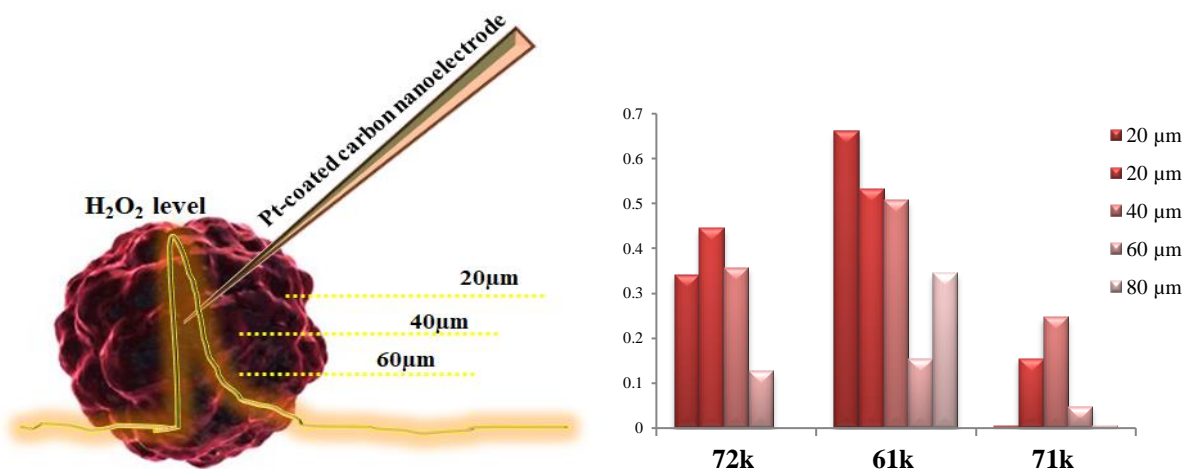


Figure 8. Electrochemical measurement of the ROS level at various depths of an MCF-7 spheroid preincubated with coordination compounds.

The charge state of the binuclear coordination compounds of Type 1 $\text{Cu}^{+1.5}/\text{Cu}^{+1.5}$ makes them different from Type 2 and Type 3 coordination compounds in redox behavior. Type 1 coordination compounds are hardly reduced ($\text{Cu}^{+1.5}/\text{Cu}^{+1.5} \rightarrow \text{Cu}^{+1}/\text{Cu}^{+1}$) in the potential range 0.01 – 0.18 V (Epc) and oxidized ($\text{Cu}^{+1.5}/\text{Cu}^{+1.5} \rightarrow \text{Cu}^{+2}/\text{Cu}^{+2}$) in the potential range 0.32–0.59 V (Epa). These coordination compounds should be prone not to the intracellular reduction, but instead to the electron donation. The lower the oxidation potential Epa ($\text{Cu}^{+1} \rightarrow \text{Cu}^{+2}$), the easier the donation of the electron, and the increased Epa is suggested to negatively affect the cytotoxicity (Tables 5, 3, S19).

Type 2 coordination compounds of Cu^{+2} are capable of a higher reduction to Cu^{+1} than the Type 1 Epc ($\text{Cu}^{+2} \rightarrow \text{Cu}^{+1}$) potential range 0.33–0.42 V (Table S20). Despite the noticeable influence of the ligand environment on the redox potential, this type of coordination compound did not show a noticeable correlation between the redox potential and cytotoxicity. This type contains a labile thiomethyl group, and the formation of a coordination compound with reaction products of ligand hydrolysis can take place in the solution, as described for the disulfiram-based copper antitumor agent.²

Type 3 coordination compounds are capable of $\text{Cu}^{+2} \rightarrow \text{Cu}^{+1}$ reduction in the potential range Epc ($\text{Cu}^{+2}/\text{Cu}^{+2} \rightarrow \text{Cu}^{+1}/\text{Cu}^{+1}$) 0.31–0.44 V, depending on the nature of the substituent in the N3 position (Table S21). Large electron-donor alkyl substituents in the benzene ring lower the Epc ($\text{Cu}^{+2} \rightarrow \text{Cu}^{+1}$), making the reduction of copper difficult, both in the complex itself and inside the cell,

thereby decreasing the antiproliferative activity and intracellular accumulation of the coordination compound. Acceptor substituents in the benzene ring increase the Epc ($\text{Cu}^{+2} \rightarrow \text{Cu}^{+1}$) redox potential, facilitating the copper reduction reaction up to the formation of stable solid monovalent $\text{Cu}^{+1}/\text{Cu}^{+1}$ complexes, such as **71k**, **72k**.

The effect of the substituent on the ligand core is best seen by its electron withdrawal, that is, the ease of reduction. The cyclic voltammetry study of ligands **1–73** (Tables S19–S21) revealed that donor ligands reduce the electron-withdrawing properties of the ligand, while the acceptor substituents, on the contrary, increase. The higher the potential of the first electron addition step, the stronger the electron withdrawal of the ligand. An increase in the electron withdrawal ability of the ligand causes an increase in the copper reduction potential, which contributes to the stabilization of the monovalent state and increases the cytotoxicity (Figure 6, A).

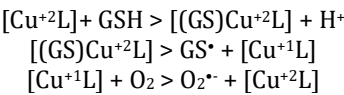
The lower the potential of the $\text{Cu}^{+2}/\text{Cu}^{+1}$, the easier it is to donate electrons. The lower the potential Epc ($\text{Cu}^{+2} \rightarrow \text{Cu}^{+1}$), the worse the antiproliferative activity of the coordination compound, due to the high stability of the Cu^{+2} coordination compound. This dependence can be explained by the low redox activity of the coordination compounds, and the inability to undergo reduction within the cell, which leads to its rapid leaching from the intracellular environment. The electron-withdrawing organic core increases the reduction $\text{Cu}^{+2}/\text{Cu}^{+1}$ potential, providing the high stability of the Cu^{+1} coordination compound, and the high redox activity facilitates an intracellular reduction, which leads to prolonged

Table 6. 3D cytotoxicity (MCF-7 spheroid).

6k	8k	16k	30k	41k	42k	44k	52k	53k	61k	71k	72k
44.3±4.5	96.1±3.0	60.0±4.8	26.3±8.6	22.1±5.0	18.2±6.9	40.5±1.0	34.9±12.4	28.4±1.4	15.8±4.2	17.6±5.8	16.7±4.6

intracellular retention and a high cytotoxicity (Figure 6, B).

ROS generation ability. Copper-containing coordination compounds attract wide attention not only due to the biogenicity of copper ions but also due to the high redox activity.⁵⁵ ROS-mediated nuclease activity,⁵⁶ mitochondrial membrane depolarization,⁵⁷ apoptosis⁵⁸ – all these well-described cytotoxic mechanisms are generally the consequence of the reactive oxygen species formation, which, in turn, is the consequence of redox $\text{Cu}^{+2} \rightarrow \text{Cu}^{+1}$ transitions.⁵⁹ The redox cycle involving copper coordination compounds is based on the Cu^{+2} to Cu^{+1} reduction by intracellular thiols, such as glutathione (GSH), under oxygen-containing conditions. Most coordination compounds of Cu^{+2} after entering the cell quickly form glutathione adducts, which leads to the formation of a coordination compound of Cu^{+1} and glutathione radical GS^{\bullet} . In the presence of oxygen, the Cu^{+1} complex is capable of generating a superoxide anion, which can induce the formation of reactive oxygen species in a fenton-like reaction:⁵⁹



We have tested the representatives of each type of the coordination compounds for their ROS formation ability. To detect the ROS formation in MCF-7 tumor cells, we first used CellRox Deep Red fluorescent probe for all sorts of oxidant species (Figure S41). To detect ROS formation in single tumor cells, we used electrochemical sensor systems for ROS detection, previously described by Erofeev et al.⁶¹ To estimate the amount of ROS and to show the concentration dependence of the current at the platinized electrode, we calibrated the anodic response with H_2O_2 (Figure S42). We measured the ROS level in separate MCF-7 cells using a 60 nm – diameter Pt nanoelectrode for the electrochemical detection of hydrogen peroxide in single cells (Figure S43). A typical intracellular voltammogram is presented in Figure S44.

A comparison of the results of the ROS level detection in the MCF-7 tumor cells quantified by two different methods are presented in Figure 7. The results obtained with the use of a nanoelectrode make it possible to more accurately estimate the number of reactive oxygen species in single cells after incubation with coordination compounds.

As seen from the data obtained, structurally similar coordination compounds are capable of generating ROS differently. In Type 1 coordination compounds, the most active ROS-generator was **16k**. Apparently, a relatively low redox potential (compared with other representatives of this group) ($E_{\text{pa}} = 0.37 \text{ V}$) determines a high electron-donating ability, and, as a result, a high ability to form ROS. For Type1, the ROS generation ability is similar to Type 2, but for the highest of all three types of potentials ($E_{1/2} \sim 0.55 \text{ V}$), the lowest electron-donating ability reduces the ability to generate ROS.

The ability of Type 2 coordination compounds to form ROS inside the cell is also heterogeneous within the group. The lowest ability to generate ROS was expected.

Despite the fact that this type shows the lowest redox potentials ($E_{1/2} \sim 0.44 \text{ V}$), the presence of stable divalent copper does not contribute to the generation of ROS. Obviously, the ligand structure determines both the electrochemical behavior and the ability of coordination compounds to generate ROS. **30k** ($E_{1/2} = 0.48 \text{ V}$) is a more active ROS generator in comparison with **40k** ($E_{1/2} = 0.41 \text{ V}$). Most likely, the more difficulty the coordination compound has in being reduced inside the cell, forming a monovalent copper complex, the worse its ability to generate ROS is. However, for Type 2 there is no apparent correlation between the ability to generate ROS and cytotoxicity, which makes the ability to generate ROS a possibility, but not the main mechanism of action of these Type 2 coordination compounds.

Type 3 coordination compounds were found to be the most active ROS-generators. **61k** and **72k** are active mixed-valence ROS generators. A higher redox potential of **71k** ($E_{1/2} = 0.51 \text{ V}$) in comparison with **72k** ($E_{1/2} = 0.46 \text{ V}$) explains the worse electron-donating ability, and, as a result, a small number of reactive oxygen species are formed. Thus, the difference in redox potentials leads to different behaviors within the cell.

The differences in the ligand structure affect the $\text{Cu}^{+2}/\text{Cu}^{+1}$ redox potential, which apparently affects the ability of the coordination compounds to generate ROS inside the cell. The presence of copper in both oxidation states $\text{Cu}^{+2}/\text{Cu}^{+1}$ in one coordination compound promotes the generation of ROS inside the cell. The electrochemical system containing $\text{Cu}^{+2}/\text{Cu}^{+1}$ can thus be called a redox buffer that maintains a constant equilibrium between oxidized and reduced forms of copper.

Based on RDE voltammograms (Figure S26), the equilibrium potential ($I = 0$) for mixed-valence Type 3 coordination compounds is $\sim 0.5 \text{ V}$, which coincides with the half-wave potential of the $\text{Cu}^{+2}/\text{Cu}^{+1}$ couple for these complexes obtained from CVs. Since the limiting cathodic and anodic currents are equal (as for **72k** and **61k**), the ratio of Cu^{+2} and Cu^{+1} is ≈ 1 . If the potential slightly shifts due to the ROS production in the presence of oxygen, the oxidation of Cu^{+1} occurs, the system tends to restore the equilibrium between Cu^{+2} and Cu^{+1} , which facilitates the regeneration of Cu^{+1} via reduction of Cu^{+2} . The mixed-valence coordination compounds seem to act as a redox buffer and maintain the equilibrium potential in which two copper cations of different valences coexist.

The results obtained by the two ROS-detection methods are well correlated, the difference in the obtained data may be explained by the different sensitivities of the fluorescent dye and the nanoelectrode, as well as by the higher specificity of the nanoelectrode. The H_2O_2 -specific electrode is a direct and reliable method for ROS measuring, while fluorescence peroxide detectors are susceptible to nonspecific oxidation and false-positive reactions.⁶²⁻⁶⁴

ROS detection at different depths of the MCF-7 spheroid. 3D spheroid was chosen as an alternative model to look inside an antitumor drug mechanism of action. The ROS level was detected at different depths of MCF-7 spheroids preincubated with coordination compounds. The measurements were conducted using a Pt-nanoelectrode, capable of measuring the inside of the

spheroid. Cyclic voltammograms were recorded as the electrode deepened for every 10 μm inside the spheroid (Figures 8, S45, Table S29). **61k** proved to be the most effective ROS-generating agent at different depths of the MCF-7 spheroid, where mixed-valence **72k** is slightly inferior to it due to having less redox activity. **71k** expectedly showed less redox activity due to the high stability of the monovalent Cu^+/Cu^+ complex.

3D-Cell Culture/Tumor Spheroids model (MTS assay). The therapeutic efficacy of the drugs in the 3D spheroid model was evaluated (Table 6, Figure S46).

Type 1 coordination compounds showed a moderate efficacy in the 3D model. Previously, Type 1 coordination compounds proved to be highly penetrating (according to cellular accumulation/distribution experiments) and highly cytotoxic (MTT assay). However, experiments on a 3D spheroid model have shown a low efficiency. This fact once again shows the difference between 2D cell experiments and tumor models.

Type 2 coordination compounds showed a high efficiency, along with the inability to generate ROS in the spheroids, confirming the fact that this type of coordination compound exhibits a redox-independent mechanism of cytotoxic action.

Type 3 coordination compounds have been shown to be highly effective in the 3D model. **61k** and **72k** were found to be effective redox-active antitumor agents, showing great cytotoxic ability in MCF-7 spheroids, which confirmed their potential efficiency in solid tumors therapy.

Nontoxic (NOAEL) single dose evaluation *in vivo*. All animal experiments were performed in accordance with Russian law and were approved by the Ethics Committee of the N.N. Blokhin Cancer Research Center. Various doses of **61k** and **72k** (with 3.5 mg/kg as the highest for **61k** and 4.69 mg/kg as the highest for **72k**) were administered intravenously (i.v.) to groups of mice, four animals each. Substances were injected immediately after preparation of the solution. 0.2 ml of solvent were used for i.v. administration in the control group of animals. The animals were placed under observation for 1 hour after administration, then every 2 hours for 12 hours and then a daily monitoring period for 21 days. Behavioral toxicity signs and mortality were recorded. Mice treated with 3.5 mg/kg of **61k** or 4.69 mg/kg of **72k** died immediately after injection (four of four dead). Mice treated with 2.4 and 2.7 mg/kg of **61k** or 2.5 and 3.4 mg/kg **72k** had seizures 20–30 seconds after injection, shallow respiration and then weakness. These seizures lasted for 2–3 minutes (eight of eight mice), but the animals appeared to fully recover 5–10 minutes later and there were no lethal effects during 3 weeks of observation. After i.v. administration of 0.79 mg/kg of **61k** or 1.1 mg/kg **72k** only short-term local convulsions were observed in three of the four mice with complete recovery in 1–2 minutes. These single doses were considered to be tolerable doses with minimum side effects suitable for efficacy experiments.

CONCLUSIONS

In summary, 73 ligands and 73 complexes based on 2-thioxoimidazolidin-4-ones (Type 1), 2-(methylthio)-1H-imidazol-5(4H)-ones (Type 2) and 2,2'-(ethane-1,2-diylbis(sulfanediyl))bis-1H-imidazol-5(4H)-ones (Type 3) were synthesized and characterized by ^1H and ^{13}C NMR

spectra, XANES, EPR spectroscopy, and cyclic voltammetry.

A detailed structure–activity relationships investigation enabled us to suppose the mechanism of cytotoxic action for each type, as well as the factors affecting any antiproliferative activity.

Type 1 binuclear $\text{Cu}^{+1.5}/\text{Cu}^{+1.5}$ coordination compounds showed high 2D cytotoxicity and high intracellular accumulation, the ability to cause early apoptosis, the inability for intracellular reduction, and moderate cytotoxicity in the 3D model of the MCF-7 spheroid.

Type 2 mononuclear Cu^{+2} coordination compounds showed ROS-independent nuclease activity and late apoptosis induction in MCF-7 cells and confirmed their effectiveness in the 3D model MCF-7 spheroid. The data once again confirms that the redox activity of copper cations and the ability to form ROS is an important, but not required mechanism of the cytotoxic action of copper coordination compounds.

Type 3 binuclear coordination compounds showed an evident correlation of $\text{Epc}(\text{Cu}^{+2} \rightarrow \text{Cu}^{+1})$ and an oxidation state of copper with the structure of the initial ligand. Electron-withdrawing substituents in position N3 of the thiohydantoin cycle increased the electron withdrawal of the ligand, which could be observed by an increase in the reduction potential in voltammograms. An increase in the electron withdrawal properties of the organic core facilitated the redox transition $\text{Cu}^{+2} \rightarrow \text{Cu}^{+1}$, up to the complete stabilization of the coordination compound with a monovalent state. The valence state of copper cations in the coordination compounds was confirmed by the cyclic voltammetry with a rotating disk electrode, EPR and XANES data.

It was also shown that the lower the potential $\text{Epc} \text{ Cu}^{+2} \rightarrow \text{Cu}^{+1}$, the more stable the Cu^{+2} complex and the lower the antiproliferative activity of the coordination compound. We suggest that this is due to the rapid leaching of the redox-inactive complex Cu^{+2} from the cell.

Type 3 binuclear mixed-valence coordination compounds **61k** and **72k** are redox active ROS generators and cause apoptosis, while not exhibiting nuclease activity and the ability to intercalate DNA. The redox-buffer system of mixed-valence $\text{Cu}^{+2}/\text{Cu}^{+1}$ in one compound provides high cytotoxicity, both in the 2D monolayer and the 3D tumor spheroid model due to the high ROS-generating ability. The ability of coordination compounds to generate ROS was proven by the classical method with a fluorescent dye, and with the help of a nanoelectrode, capable of single-cell measurements in single MCF-7 cells.

Additionally, ROS accumulation at different MCF-7 spheroid depths was proven using Pt-nanoelectrode, an excellent model for drug penetration investigation possessing the main features of human solid tumors, including structural organization and hypoxia. Both **61k** and **72k** generate ROS up to 100 μm deep in the spheroid, and 3D cytotoxicity confirmed their efficacy.

In vivo maximum tolerated doses of the coordination compounds **72k** and **61k** were determined.

This work is a large-scale study of the cytotoxic properties of copper coordination compounds. The aim of the study was to answer the following question: what affects the cellular accumulation and cytotoxicity of copper coordination compounds? The following SAR were found an increase in the electron-withdrawing properties of the ligand stabilizes the copper in the

monovalent state, which promotes ROS generation. The presence of monovalent copper and a high redox potential $\text{Cu}^{2+}/\text{Cu}^{+1}$ contributes to the intracellular accumulation of the drug and, as a result, its cytotoxic activity. The high drug efficiency is a consequence of the combination of physicochemical properties, which can be tuned by varying the ligand environment and the nature of donor atoms.

EXPERIMENTAL SECTION

General. Unless otherwise noted, all reagents were purchased from Sigma Aldrich (Merck) and used without further purification. NMR spectra were recorded on a Bruker-Avance 400 MHz spectrometer (USA) in $\text{DMSO}-d_6$ and CDCl_3 with TMS as an internal standard. HRMS spectra were obtained with Thermo Scientific Orbitrap Elite (USA) mass spectrometer, ionization: ESI mod with ± 3.5 kV, capillary temperature 275°C . Mass spectra were recorded with an Orbitrap analyzer, resolution: 480000. Internal standards: DMSO and diisooctyl phthalate (m/z 157.03515 and 413.26623) in positive mode and dodecyl sulfate (m/z 265.14790) in negative mode. UV-Vis spectra were recorded on Hitachi U2900 (Japan) spectrophotometer. MALDI Bruker spectra were recorded on Autoflex II (USA). Elemental analysis was performed on ELEMENTAR Vario MICRO Cube (Germany).

Purity of organic ligands. The purities of compounds **1-73** were determined by HPLC. HPLC analysis was carried out on a HPLC system Ultimate 3000 (Thermo Fischer Scientific, USA) with TSQ Endura triple quadrupole mass spectrometer (Thermo Fischer Scientific, USA) equipped with a Column XBridge Peptide BEH C18, 50×2.1 mm, particle size $5 \mu\text{m}$. HPLC profiles were recorded by an UV detector at 260 nm.

The purity of the compounds **1-73** was confirmed to be $\geq 95\%$.

For compounds **1-11, 13-52, 54, 58, 60 - 67, 69, 70**.

Phase A water + 0.1% formic acid, Phase B - acetonitrile + 0.1% formic acid. Elution mode: 0 to 0.5 minutes 5% Phase B, 0.5 to 12.5 minutes Phase B gradient 5 to 100%, 12.5 to 15 minutes 100% Phase B, 15 to 17 minutes Phase B gradient 100 to 5%, 17 - 20 minutes 5% Phase B. Flow rate $300 \mu\text{L}/\text{min}$, column temperature 30°C , injection volume $10 \mu\text{L}$.

For compounds **12, 53, 55-57, 59, 68, 69, 71-73**.

Phase A water + 0.1% formic acid, Phase B - acetonitrile + 0.1% formic acid. Elution mode: 0 to 0.5 minutes 50% Phase B, 0.5 to 12.5 minutes Phase B gradient 50 to 100%, 12.5 to 15 minutes 100% Phase B, 15 to 17 minutes Phase B gradient 100 to 50%, 17 - 20 minutes 50% of Phase B. Flow $300 \mu\text{L}/\text{min}$, column temperature 30°C , injection volume $10 \mu\text{L}$.

MS parameters are the same for all samples: Full Scan Q1, 100 to 1000 Yes, positive ion registration, 3.5 kV, Q1 resolution 0.7 Da, Chrom Filter 1 second. Sheath gas 40 arb, Aux gas 12 arb, Sweep gas 1 arb, capillary temperature 330°C , evaporator temperature 300°C .

Crystallography. The X-ray diffraction study of a single crystal of coordination compounds was conducted on a STOE StadiVari Pilatus 100K diffractometer, Cu-K α radiation (1.54186 \AA), from a GeniX3D Cu HF generator with a microfocus X-ray tube and a Xenocs FOX3DHF multilayer thin-film ellipsoidal monochromator (France). Data collection and processing of the recorded diffraction peaks were performed using the X-Area 1.67 software package (STOE & Cie GmbH, Darmstadt, Germany, 2013). The intensities of the reflections on the frames obtained from the 2D detector were scaled using the LANA program (incorporated in the X-Area package), upon which diffraction data processing minimizes the intensity differences of symmetrically equivalent reflections (multiscan method).

The structural data were deposited with the Cambridge Crystallographic Data Center (CCDC 1874574).

The structure was solved by the direct method implemented in the SHELXS-97 software package.⁶⁵ The positional and thermal parameters of nonhydrogen atoms were refined in the full matrix anisotropic approximation. The positions of hydrogen atoms at heteroatoms (N, O) were determined from the Fourier syntheses and refined freely. The positions of the hydrogen atoms at the carbon atoms were calculated and refined in the isotropic approximation using a riding model. Graphic images of a molecule in the crystal were made using the DIAMOND program.⁶⁶

Cyclic voltammetry. experiments were conducted using an IPC Pro M potentiostat (Russia) with cyclic voltammetry (CV) and rotating disk electrode (RDE) techniques. Glass-carbon ($d =$

2 mm) disks were used as the working electrodes, 0.05 M Bu_4NClO_4 solution in CH_3CN or DMF served as the supporting electrolyte, and $\text{Ag}/\text{AgCl}/\text{KCl}(\text{satur.})$ was used as the reference electrode. The potential scan rates were 200 mV s . Samples were dissolved in the predeaerated solvent.

XANES spectra. The spectra were measured using a Rigaku R-XAS Looper (Japan) X-ray spectrometer equipped with an X-ray tube as the radiation source (cathode and anode material-tungsten). All measurements were made in the geometry of "passing". As an incident radiation intensity detector, an argon-filled ionization chamber (300 mbar) was used, and a scintillation detector was used to detect the transmitted radiation. The size of the X-ray beam on the sample was $10 \times 3 \text{ mm}^2$. For each of the samples, the spectrum was measured in 10 passes with subsequent averaging for reference samples in 4 passes. The approximate time for the measurement of each sample was 15 hours. The measurements of the XAS spectra behind the K-edge of copper were conducted using a crystal-monochromator Ge (440) (second-order reflection of the Ge (220) crystal) in the $8775 - 9500 \text{ eV}$ range. The energy resolution was 0.7 eV . Copper compounds, containing Cu ions with different charge states: Cu(foil), Cu_2O , CuO , and CuCl_2 were used as reference samples.

EPR spectra. were recorded on a Varian E-3 EPR Spectrometer (USA) at the boiling point of liquid nitrogen (77.4 K)

Cytotoxicity in monolayer culture (MTT assay). Human adenocarcinoma MCF-7 cells (5×10^3) were seeded on a 96-well plate and incubated overnight. A freshly prepared stock solution of copper complexes in DMSO (1.0 mg/mL) were diluted in the cell culture media and added to the cells (0.5% DMSO as the maximum concentration). After 72 hours, MTT (3-(4,5-dimethylthiazol-2-yl)-2,5-diphenyltetrazolium bromide) solution was added to the cells to the final concentration of 0.5 mg/mL , according to the standard protocol.⁶⁷ After 2 hours of incubation, the MTT solution was discarded and $140 \mu\text{L}$ of DMSO was added. The plates were shaken (60 rpm) to solubilize the formazan. The absorbance was measured using a microplate reader (VICTOR X5 Plate Reader, PerkinElmer, USA) at a wavelength of 565 nm in order to measure the formazan concentration. IC_{50} values were estimated from the dose-response graph (GraphPad Software, Inc). All measurements were performed in three independent replicates to average the obtained data.

Fluorescent proteins detection assay. Cytotoxicity was measured by the live-imaging of MCF7_Katushka cells in accordance with Kalinina et al.³⁸ using Typhoon FLA scanner (GE Healthcare, USA). Cells were seeded in a 96-well plate ($3,000$ per well) in an F12 medium. After 24 hours, the studied substances diluted in a culture medium were added to cells. The cells were incubated for 72 hours at 37°C in $5\% \text{ CO}_2$ humidified atmosphere and analyzed via a high-resolution scanner at r.t. (less than 30 minutes without CO_2). The obtained plate images were processed using ImageJ software.

Cytotoxicity in tumor spheroids (MTS assay). Tumor spheroid formation was performed using a liquid overlay technique with agarose-coated plates, as described earlier.^{68,69} Briefly, $1.5\% \text{ wt}$ of agarose in PBS ($\text{pH} = 7.4$) was heated on water bath for 15 minutes. Then, $50 \mu\text{L}$ of melted agarose was added to each well of a flat-bottom 96-well plate under sterile conditions. Plates with agarose were cooled down to r.t. for 15 minutes. The cells were seeded on agarose-coated plates ($10,000$ cells/well, $100 \mu\text{L}$ of media per well) and incubated at 37°C and $5\% \text{ CO}_2$ for 72 hours to generate spheroids. The formation of tumor spheroids was then observed using an inverted light microscope. Then, the solutions ($1-50 \mu\text{M}$) of the tested drugs were added to spheroids for 72 hours. The cytotoxicity was evaluated using a colorimetric MTS assay based on the NAD(P)H-dependent dehydrogenase activity, which resulted in the reduction of the MTS tetrazolium compound and generation of the soluble formazan product in the cell culture media. The formazan formation was measured at 490 nm using a Varioskan Flash reader (Thermo Scientific, USA). The IC_{50} values were estimated using the GraphPad Prism Software.

Intracellular accumulation/distribution.

Cell preparation/incubation. The mice 4T1 breast cancer cells were maintained in Roswell Park Memorial Institute medium (RPMI-1640) containing 10% fetal bovine serum (FBS), 2 mM L-glutamine, 100 U/ml penicillin, 100 lg/ml streptomycin, and 0.25 lg/ml amphotericin B, using 25 cm² cell culture flasks (Corning) in a humidified atmosphere (95% air/5% CO₂) at 37°C. The cells were periodically screened for mycoplasma contamination. Exponentially growing cells were harvested by trypsinisation and the resulting single cell suspension was seeded in 25 cm² cell culture flasks at a concentration of 5×10⁵ cells/flask. After 48 hours at 37°C, when the cell culture was 80% confluent, the medium of the subconfluent cells was replaced with 4 ml of a fresh medium containing the desired drug compound at an appropriate concentration in three replicates. The flasks were incubated at 37°C in 5% CO₂ atmosphere for 24 hours. Then, the cells were washed three times with a saline solution (0.9% NaCl), and 1.0 ml of trypsin-EDTA (0.05%) was added to each flask to detach the cells. A complete growth medium (6.0 ml) was added and the cells were aspirated again by gently pipetting. The suspended cells in the growth medium were centrifuged at 800 g (4°C) for 5 minutes. After discarding the supernatant, the cells were dispersed in 500 µl of PBS and the cells were counted using a TC20 automated cell counter (Biorad).

Subcellular fractionation procedure. Samples of the 4T1 cells were subjected to three freezing/thawing cycles at -80°C, treated with 200 µl of PBS supplemented with 0.1 M NaOH and 0.05% Tween-20, and vigorously vortexed to lyse the cells. The homogenate was centrifuged at 600 g for 15 minutes at 4°C to isolate the nuclear fraction. Then, the supernatant was carefully transferred to a new tube and centrifuged at 15000 g for 15 minutes at 4°C to isolate the mitochondria fraction. The supernatant was a cytosol fraction, which was carefully transferred to another tube. All three fractions were treated with highly pure nitric acid (100 µl for nuclear and mitochondria fractions, and 300 µl for cytosol fraction) for at least 48 hours until complete dissolution.

AAS assay. Copper accumulation in cell organelles was measured using an atomic absorption spectrometer (AAS) with KVANT-Z-ETA electrothermal atomization (KORTEK, Russia). 100 µl of the sample were mixed with 500 µl of a 5% pure HNO₃ qualification solution in 1.5 ml Eppendorf tubes, followed by thorough mixing and 10 minutes of incubation at a temperature of 60°C in a water bath. Then, the contents of the tubes were again mixed and centrifuged for 10 minutes at 14500 rpm to separate any possible sediment (no precipitation was observed for any of the samples). 5% extrapure HNO₃ solution was prepared by diluting a 65% HNO₃ solution (Merck KGaA, Germany, Cu ≤ 0.010 ppm) with DI water. The prepared sample was thoroughly mixed immediately prior to measuring the copper content. Resonance copper line λ = 324.8 nm was used for measurements with a preliminary calibration with five solutions (0 µg/l, 5 µg/l, 10 µg/l, 50 µg/l, and 100 µg/l) based on the multielement standard ICP-MS-68 in three replicates. Solution "A" and refinement of the calibration before measuring each sample ("0" is the signal value when measuring double distillate).

DNA degradation. DNA degradatin was detected after agarose gel electrophoresis (Helicon, Russia) by CFX Gel Imager (Biorad, USA). The mixtures (15 µl), containing 150 ng pUC18 plasmid DNA, 20 mM Hepes-KOH (4-(2-hydroxyethyl)-1-piperazineethanesulfonic acid with KOH) pH = 7.8, and 2-200 µM of complexes were prepared. The mixtures were incubated at 37°C for 4 hours and analyzed in 1% agarose gel. The gel densitometry was estimated with ImageQuant software.

DNA intercalation. Competitive binding of ligands and coordination compounds to human DNA intercalated with ethidium bromide was assessed on a Microplate Reader Clariostar (BMG LABTECH, Germany), with scan mode Ethidium homodimer-1, or Agilent Cary Eclipse Fluorescence Spectrophotometer (USA) All operations with human DNA were performed in a Tris-HCl buffer solution (pH = 7.2) supplemented with 5% DMSO. The solutions were used within 30 minutes after preparation. The DNA purity was determined by the ratio of optical absorption values at wavelengths λ = 260 nm and λ = 280 nm (A₂₆₀/A₂₈₀). The ratio did not exceed 1.8, which means that the DNA was not bound to any protein. The DNA concentration was determined by the magnitude of the optical absorption (λ = 260 nm, ε = 6600 M⁻¹cm⁻¹). The initial solutions were prepared by dissolving the test compounds in DMSO. The solutions

for the spectrofluorimetric studies were diluted with a buffer solution. Ethidium bromide was added to a buffer solution containing 2 µM DNA to a concentration of 2 µM. The variable volumes of the test compound in the buffer were added to the resulting solution to obtain a series of samples containing DNA (1 µM), Ethidium bromide (1 µM) and a test compound (0 to 0.9 µM with an increment of 0.1 µM); pure buffer was used as a the control. The solutions were shaken and left for 15 minutes. The interaction between the DNA and coordination compounds (ligands) were evaluated via fluorescence quenching experiments. The DNA solution (2 mM) and EtBr (2 mM) were prepared in 1 M Tris-HCl (pH = 7.0). The spectra of the fluorescence quenching experiments were recorded at r.t. with a DNA excitation wavelength at 502 nm (the emission wavelength at 530-730 nm; step width 1 nm) by keeping the concentration of the DNA constant (1 mM) while varying the concentration of the complexes (ligands) 1-10 mM.

BSA binding. Competitive binding of ligands and coordination compounds to BSA was assessed on Agilent Cary Eclipse Fluorescence Spectrophotometer (USA) All operations with BSA were performed in phosphate buffer (pH = 7.2) with 5% addition of DMSO. All solutions were used within an hour after preparation. Equal volumes of the solutions of the studied compounds and pure phosphate buffer were added to the BSA solution to obtain mixtures containing the final concentrations of 1 µM BSA and 0, 1, 2, 3, 4, 5, 6, 7, 8, 9 µM of the test compound respectively. The solutions were shaken and left for 15 minutes at r.t. to establish equilibrium. The fluorescence spectra were recorded upon excitation at a wavelength of λ = 280 nm in the spectral range of wavelengths 500 - 700 nm. Fluorescence spectra were recorded on an Agilent Cary Eclipse Fluorescence Spectrophotometer without temperature control. The concentration stability constant was calculated using the Skatchard equation:⁷¹

$$\log_{10} \frac{I_0 - I}{I} = \log_{10} K_{app}(BSA) + n * \log_{10} C(X)$$

where I₀ is the fluorescence intensity of a pure BSA solution; I is the intensity at a concentration C (X) of substance X; n is the number of binding sites,

Telomerase inhibition. The telomerase assay was performed with quantitative real-time (RTQ) PCR detection instead of gel modification.⁷⁰ For this, 18 µl of TRAP mixtures were prepared, containing TRAP buffer [20 mM of Hepes-N-Hydroxyethylpiperazine-N-ethane-sulfonate (Hepes-KOH)]; 1.5 mM MgCl₂; 63 mM KCl; 1 mM EGTA; 0.1 mg/ml of bovine serum albumin; 0.005% v/v polyoxyethylene (20) sorbitan monolaurate; 20 µM dNTP; and 0.5 µM TS oligonucleotide (AATCCGTCGAGCAGAGTT). Then, 1 µl of inhibitor solution was added in the sample probes. Water-DMSO solution was added in the control probes instead of the inhibitor. Then, 1 µl of cellular extract 2000/µl cells was added to the sample and the control probes and reaction mixtures were incubated for 30 minutes at 25°C. At the second stage, an equal volume of the inhibitor solution was added to the control probes. Then, two units of Taq DNA polymerase (Fermentas), up to 0.5 µM of ACX oligonucleotide (GCGCGGCTTACCCTTACCCTTACCCTTACCCTAACC), and up to 0.17x Sybr I were added in all probes. RTQ-PCR was performed according to the following scheme: 35 s (94°C), 35 s (50°C), 90 s (72°C) (35 cycles, Thermal cycler CFX96, Biorad, USA). The quantity of the telomerase repeats in comparison to the control without telomerase inhibition was calculated by the formula 1/(2^{ΔCq}[assay with inhibitor addition to telomerase reaction] - Cq[assay with inhibitor addition to the PCR step only])).

Apoptosis/necrosis Annexin V-FITC assay. MCF-7 cells (5×10⁵) were seeded on a 6-well plate and incubated overnight. Then, the cells were treated with drugs at concentrations equal to IC₅₀ values for 24 hours. Then, the cells were detached with trypsin-EDTA and washed with PBS (pH = 7.4). Apoptosis and necrosis were quantified via combined staining of Annexin V-FITC (Molecular probes, Waltham, MA, USA) and propidium iodide (PI) for 15 min at r.t. and in the dark. The FITC and PI fluorescence were measured on a NovoCyte 2000R flow cytometer (ACEA Biosciences, USA), and the percentages of apoptotic and necrotic cells were analyzed using NovoExpress v.1.2.4 software. A minimum of 50,000 cells per sample was acquired and analyzed; acquisition was performed by setting the forward scatter (FSC) and side scatter (SSC) on the dot plot to differentiate the population of

cells from cellular debris (FSC-A vs SSC-A) and doublets (FSC-H vs FSC-W).

ROS level detection in MCF-7 cells preincubated with coordination compounds.

Fluorescent-based ROS measurement. Evaluation of the cytoplasmic ROS was performed using a CellROX Deep Red fluorescent probe (Molecular Probes/Thermo) according to the manufacturer protocol. In brief, the MCF-7 cells (5×10^3) were seeded on a 96-well plate and incubated overnight. Then, the cells were incubated with 2.5 μ M of CellROX Deep Red in DMEM for 30 minutes and washed in PBS three times. After that, the medium was replaced with 100 μ L of drug solutions for 1 hour. The cell nuclei were additionally stained by 50 μ M of Hoechst 33258 dye solution for 15 minutes. Optical images and CellROX Deep Red fluorescence intensity data of the MCF-7 cells were acquired using InCell Analyzer 6000 and the In Cell Analyzer Workstation software v.3.7.3 (GE Healthcare, USA). The ROS level was calculated as a ratio of the CellROX Deep Red fluorescence to the Hoechst 33258 fluorescence to normalize the signal to the cell amount in each image.

Pt-nanoelectrode experiments For the production of platinum electrodes, quartz billets with internal and external diameters of 0.9 mm and 1.2 mm, respectively, were used. These blanks were pulled out on a laser puffer (Sutter, USA), resulting in two nanocapillaries with a diameter of the order of 100-500 nm. Pyrolytic carbon was precipitated on the obtained nanocapillaries with thermal decomposition of the propane-butane mixture in an oxygen-free environment. We used an electrochemical method of creating cavities in the carbon nanoelectrodes with subsequent deposition of platinum. Etching was performed in a solution containing 0.1 mM NaOH and 10 mM KCl. The nanoscale electrode and reference electrode were immersed in the solution; an alternating voltage of a symmetrical V-shape with an amplitude of 1.5 – 2 V was applied to the reference electrode. After soaking in a KCl/NaOH solution, the treated blanks were transferred to a hexachloroplatinic acid solution for further electrochemical deposition of platinum at the tip of the capillary. Both electrodes were placed in a solution with H_2PtCl_6 and platinum was deposited on an etched nanoelectrode by applying a symmetrical sawtooth shape voltage with an amplitude of 0.8 V.

The potential difference between the platinum microelectrode and the reference electrode was recorded by a patch-clamp Model 2400 amplifier ("A-M Systems", USA). The transfer and recording of the measurements to a computer was conducted using a ADC-DAC converter USB-6211 ("National instruments", USA) and the program WinWCP. A micromanipulator PatchStar ("Scientifica", Great Britain) was used to feed the nanosensor. All manipulations were made on the table of an inverted microscope (Nikon, Japan).

Pt-nanoelectrode calibration. The concentration of ROS (hydrogen peroxide) was evaluated at a potential of +800 mV vs. Ag/AgCl. Under the given conditions, the platinum catalyzed reaction $2\text{H}_2\text{O}_2 \leftrightarrow 2\text{H}_2\text{O} + \text{O}_2$ occurs, and since the superoxide radical is rapidly converted in the solution into hydrogen peroxide, the total concentration of peroxide determines the general background of the oxidation processes. Prior to the measurements, each platinum electrode was calibrated using a series of standard H_2O_2 solutions (Figure S25, calibration curve). The levels of peroxides in the samples were determined based on the calibration curve.

DMSO formulation for intravenous administration. The solutions for i.v. administration were prepared using DMSO enriched with auxiliary agents (DMSO: Tween 20: F127 94: 5: 1 by weight). The compositions included DMSO (Ph.Eur 5.0, USP29-NF24), 10% by volume; a nonionic surfactant Tween 20 (Ph. Eur. 8.5, USP29-NF24), 0.5% by volume; and a block copolymer Pluronic F-127 (Ph. Eu. 7.0, USP26-NF21), 1% by volume. We dissolved 1 mg **72k** or **61k** in 300 μ L or 540 μ L of DMSO-based solvent, respectively. The resulting solution was slowly added dropwise by stirring in 2100 μ L of Haemodes-N (FS 42-2620-97, Ph. Eur.8.0), an isotonic agent with a stabilizing, anti-aggregation, detoxification, and plasma substituting effect. The resulting stock solutions were 0.416 mg/ml and 0.379

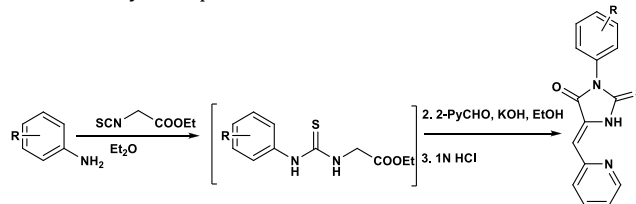
mg/ml for **72k** and **61k**, respectively. The stock solution was adjusted to the desired concentration immediately prior to the experiments using Haemodes-N.

Nontoxic (NOAEL) single dose evaluation in mice. C57Bl6 male mice (six weeks of age, 20–24 g) were obtained from the N.N. Blokhin Cancer Research Center. The mice were housed individually and kept at r.t. (20–22 °C), with a relative humidity of 45–65% and natural lighting. Various doses of test substances (3.5 mg/kg and 4.69 mg/kg as the highest for **61k** and **72k**, respectively) were administered intravenously (0.2 ml in total), and each experimental group included four mice. The i.v. administration of 0.2 ml free DMSO-Haemodes-N solvent was used for a control group. The animals were placed under observation for 1 hour after administration. Then, their conditions were checked every 2 hours for 12 hours followed by a daily monitoring period for 21 days. Behavioral toxicity signs and mortality were recorded.

Syntheses of Compounds 1–15, 17–24, 28, 29

Ethyl isothiocyanatoacetate was synthesized according to the described procedure.⁷²

The synthesis procedure was used in accordance with Kuznetsova et al.⁷² Ethyl isothiocyanatoacetate (1 eq) was added dropwise to a vigorously stirred solution of aniline in ~10 ml of diethyl ether. The mixture was stirred until the white solid precipitate formed, the solvent was evaporated under reduced pressure. The resulted powder was dissolved in ~30 ml of ethanol, 1.1 eq. of solid KOH was added to form a clear red solution. Then, 1.1 eq. of 2-pyridinecarbaldehyde was added dropwise and the mixture was stirred for 3 hours at r.t. 1 M HCl was then added until pH = 7, the precipitate formed was filtered off, washed with water, ethanol, diethyl ether and air-dried. The final products were purified by column chromatography on silica gel, eluent: CH_2Cl_2 : MeOH (10: 1). The products were isolated as a yellow powders.



3-(4-fluorophenyl)-5-((Z)-2-pyridylmethylidene)-2-thioxotetrahydro-4H-imidazol-4-one (1). From 200 mg (1.45 mmol) of 4-fluoroaniline, by the reaction with 210 mg (1.45 mmol) of ethyl isothiocyanatoacetate, followed by addition of 171 mg (1.6 mmol) of pyridine-2-carbaldehyde and 90 mg (1.6 mmol) of solid KOH **1** was obtained as a light yellow powder. Yield: 347 mg (80%) after column chromatography. ¹H NMR (400 MHz, DMSO- d_6 , δ , ppm): 11.87 (brs, 1H, NH), 8.76 (d, 1H, $J=4.89$ Hz, H α -Py), 7.89 (td, 1H, $J_1=7.83$ Hz, $J_2=1.76$ Hz, H β -Py), 7.75 (d, 1H, $J=7.83$ Hz, H β' -Py), 7.47-7.30 (m, 5H, H γ -Py, H α , H α' , H β , H β' -Ph), 6.79 (s, 1H, -CH=). ¹³C NMR (101 MHz, DMSO- d_6 , δ , ppm) 178.2, 161.1, 153.6, 150.3, 137.9, 131.5, 127.1, 123.8, 116.3, 109.0. HRMS (*neg.*) calculated $\text{C}_{15}\text{H}_9\text{FN}_3\text{OS}$: 298.0451 (**1** - H); found 298.0452 (**1** - H); HPLC purity 96.48%.

3-(3-fluorophenyl)-5-((Z)-2-pyridylmethylidene)-2-thioxotetrahydro-4H-imidazol-4-one (2). From 200 mg (1.45 mmol) of 3-fluoroaniline, by the reaction with 210 mg (1.45 mmol) of ethyl isothiocyanatoacetate, followed by addition of 171 mg (1.59 mmol) of pyridine-2-carbaldehyde and 90 mg (1.59 mmol) of solid KOH **2** was obtained as a light yellow powder. Yield: 364 mg (84%) after column chromatography. ¹H NMR (400 MHz, DMSO- d_6 , δ , ppm): 12.71 (brs, 1H, NH), 8.78 (d, 1H, $J=4.89$ Hz, H α -Py), 8.63 (m, 1H, H γ -Py), 7.91 (td, 1H, $J_1=7.82$ Hz, $J_2=1.96$ Hz, H β -Py), 7.79 (m, 1H, H β' -Py), 7.57 (m, 2H, H α , H β -Ph), 7.33 (m, 3H, H β' , H γ -Ph, H α' -Ph), 6.82 (s, 1H, -CH=). ¹³C NMR (101 MHz, DMSO- d_6 , δ , ppm) 177.8, 163.6, 153.5, 150.4, 137.9, 130.9, 130.2, 127.2, 125.7, 123.8, 116.7, 109.2. HRMS (*neg.*) calculated $\text{C}_{15}\text{H}_9\text{FN}_3\text{OS}$: 298.0451 (**2** - H); found 298.0449 (**2** - H); HPLC purity 95.03%.

3-(2-fluorophenyl)-5-((Z)-2-pyridylmethylidene)-2-thioxotetrahydro-4H-imidazol-4-one (3). From 200 mg (1.45

mmol) of 2-fluoroaniline, by the reaction with 210 mg (1.45 mmol) of ethyl isothiocyanatoacetate, followed by addition of 171 mg (1.59 mmol) of pyridine-2-carbaldehyde and 90 mg (1.59 mmol) of solid KOH, **3** was obtained as a yellow powder. Yield: 325 mg (75%) after column chromatography. ¹H NMR (400 MHz, DMSO-d₆, δ, ppm): 12.06 (brs, 1H, NH), 8.76 (d, 1H, J=4.89 Hz, H_α-Py), 7.90 (td, 1H, J₁=7.83 Hz, J₂=1.76 Hz, H_β-Py), 7.77 (m, 1H, H β'-Py), 7.53 (m, 2H, H_β, H_β'-Ph), 7.35 – 7.40 (m, 3H, Hy-Py, H_α, Hy-Ph), 6.85 (s, 1H, -CH=). ¹³C NMR (101 MHz, DMSO-d₆, δ, ppm) 177.3, 163.1, 153.3, 150.4, 145.1, 137.9, 133.4, 132.1, 127.3, 123.9, 116.9, 110.0. HRMS (*neg.*) calculated C₁₅H₉FN₃OS⁺: 298.0451 (**3** - H)⁺, found 298.0453 (**3** - H)⁺. HPLC purity 95.32%.

(Z)-3-(4-bromophenyl)-5-((Z)-2-pyridylmethylidene)-2-thioxotetrahydro-4H-imidazol-4-one (4). From 200 mg (1.16 mmol) of 4-bromoaniline, by the reaction with 168 mg (1.16 mmol) of ethyl isothiocyanatoacetate, followed by addition of 137 mg (1.28 mmol) of pyridine-2-carbaldehyde and 72 mg (1.28 mmol) of solid KOH **4** was obtained as a yellow powder. Yield: 330 mg (79%) after column chromatography. ¹H NMR (400 MHz, DMSO-d₆, δ, ppm): 8.76 (d, 1H, J=4.30 Hz, H_α-Py), 7.89 (td, 1H, J₁=7.83 Hz, J₂=1.96 Hz, H_β-Py), 7.76 (d, 1H, J=7.83 Hz, H_β'-Py), 7.45 (m, 2H, H_β, H_β'-Ph), 7.32 – 7.36 (m, 3H, Hy-Py, H_α, H_α'-Ph), 6.78 (s, 1H, -CH=). ¹³C NMR (101 MHz, DMSO-d₆, δ, ppm) 177.9, 163.6, 153.5, 150.3, 137.9, 132.4, 131.5, 127.2, 123.8, 122.6, 109.1. HRMS (*pos.*) calculated C₁₅H₁₁BrN₃OS⁺: 361.9806 (**4** + H isotopic)⁺, 359.9801 (**4** + H)⁺, found 361.9778, 359.9804 (**4** + H)⁺. HPLC purity 96.72%.

3-(3-bromophenyl)-5-((Z)-2-pyridylmethylidene)-2-thioxotetrahydro-4H-imidazol-4-one (5). From the 200 mg (1.16 mmol) of 3-bromoaniline by the reaction with 168 mg (1.16 mmol) of ethyl isothiocyanatoacetate, followed by addition of 137 mg (1.28 mmol) of pyridine-2-carbaldehyde and 72 mg (1.28 mmol) of solid KOH, **5** was obtained as a yellow powder. Yield: 321 mg (77%) after column chromatography. ¹H NMR (400 MHz, DMSO-d₆, δ, ppm): 8.77 (d, 1H, J=4.37 Hz, H_α-Py), 7.91 (td, 1H, J₁=7.79 Hz, J₂=1.78 Hz, H_β-Py), 7.72 – 7.78 (m, 3H, Hy-Py, H_α, H_α'-Ph), 7.41 (m, 3H, H_β'-Py, H_β-Ph, Hy-Ph), 6.81 (s, 1H, -CH=). ¹³C NMR (101 MHz, DMSO-d₆, δ, ppm) 169.9, 155.8, 154.9, 150.3, 137.8, 135.4, 132.0, 131.1, 128.6, 126.9, 121.4, 109.2. HRMS (*pos.*) calculated C₁₅H₁₁BrN₃OS⁺: 361.9806 (**5** + H isotopic)⁺, 359.9801 (**5** + H)⁺, found 361.9779 (**5** + H)⁺, 359.9804 (**5** + H)⁺. HPLC purity 97.39%.

3-(2-bromophenyl)-5-((Z)-2-pyridylmethylidene)-2-thioxotetrahydro-4H-imidazol-4-one (6). From 200 mg (1.16 mmol) of 2-bromoaniline, by the reaction with 168 mg (1.16 mmol) of ethyl isothiocyanatoacetate, followed by addition of 137 mg (1.28 mmol) of pyridine-2-carbaldehyde and 72 mg (1.28 mmol) of solid KOH **6** was obtained as a yellow powder. Yield: 225 mg (54%) after column chromatography. ¹H NMR (400 MHz, DMSO-d₆, δ, ppm): 8.86 (d, 1H, J=4.69 Hz, H_α-Py), 7.99 (td, 1H, J₁=8.03 Hz, J₂=1.66 Hz, H_β-Py), 7.65 (m, 3H, H_β, H_β'-Ph, H_β'-Py), 7.31 (m, 3H, Hy-Py, H_α, Hy-Ph), 6.78 (s, 1H, -CH=). ¹³C NMR (101 MHz, DMSO-d₆, δ) 177.3, 163.1, 153.3, 150.4, 137.9, 133.4, 132.9, 132.38, 132.37, 132.0, 130.0, 129.2, 127.3, 123.9, 109.8. HRMS (*pos.*) calculated C₁₅H₁₁BrN₃OS⁺: 361.9786 (**6** + H isotopic)⁺, 359.9806 (**6** + H)⁺, found 361.9782 (**6** + H isotopic)⁺, 359.9812 (**6** + H)⁺. HPLC purity 95.06%.

3-(2-bromo-4-fluorophenyl)-5-((Z)-2-pyridylmethylene)-2-thioxoimidazolidin-4-one (7). From 200 mg of (1.06 mmol) 2-bromo-4-fluoroaniline by the reaction with 154 mg (1.06 mmol) of ethyl isothiocyanatoacetate, followed by addition of 125 mg (1.17 mmol) of pyridine-2-carbaldehyde and 66 mg (1.17 mmol) of solid KOH **7** was obtained as light yellow powder. Yield: 248 mg (62%) after column chromatography. ¹H NMR (400 MHz, CDCl₃, δ, ppm): 8.69 (d, 1H, J=3.69 Hz, H_α-Py), 7.76 (td, 1H, J₁=7.74, J₂=1.83 Hz, H_β-Py), 7.43 (m, 3H, H_β-Ph, H_β'-Ph, H_β'-Py), 7.26 (m, 2H, Hy-Py, H_α-Ph), 6.63 (s, 1H, -CH=). ¹³C NMR (101 MHz, CDCl₃, δ, ppm) 176.4, 162.7, 159.1, 153.2, 149.6, 137.4, 131.9, 130.1, 128.1, 126.7, 124.4, 123.3, 120.8, 120.5, 108.6. HRMS (*pos.*) calculated C₁₅H₁₀BrFN₃OS⁺: 379.9687 (**7** + H isotopic)⁺, 377.9707 (**7** + H)⁺, found 379.9718 (**7** + H isotopic)⁺, 377.9706 (**7** + H)⁺. HPLC purity 98.91%

3-(4-chlorophenyl)-5-((Z)-2-pyridylmethylidene)-2-thioxotetrahydro-4H-imidazol-4-one (8). From 200 mg (1.57 mmol) of 4-chloroaniline, by the reaction with 228 mg (1.57 mmol) of ethyl isothiocyanatoacetate, followed by addition of 185 mg (1.72 mmol) of pyridine-2-carbaldehyde and 97 mg (1.72 mmol) of solid KOH **8** was obtained as a white-yellow powder. Yield: 401 mg (81%) after column chromatography. ¹H NMR (400 MHz, DMSO-d₆, δ, ppm): 8.78 (d, 1H, J=4.34 Hz, H_α-Py), 8.58 (m, 1H, H_β-Py) 8.45 (m, 1H, H_β'-Py), 7.45 – 7.34 (m, 5H, J=7.63 Hz, Hy-Py, H_α, H_α', H_β, H_β'-Ph), 6.83 (s, 1H, -CH=). ¹³C NMR (101 MHz, DMSO-d₆, δ, ppm) 177.3, 163.2, 153.3, 150.3, 137.9, 132.8, 132.3, 131.9, 131.2, 130.3, 128.6, 127.3, 123.9, 116.6, 109.9. HRMS (*neg.*) calculated C₁₅H₉ClN₃OS⁺: 316.0125 (**8** - H isotopic)⁺, 314.0155 (**8** - H)⁺, found 316.0125 (**8** - H isotopic)⁺, 314.0158 (**8** - H)⁺. HPLC purity 97.98%

3-(3-chlorophenyl)-5-((Z)-2-pyridylmethylidene)-2-thioxotetrahydro-4H-imidazol-4-one (9). From 200 mg (1.57 mmol) the 4-chloroaniline, by the reaction with 228 mg (1.57 mmol) of ethyl isothiocyanatoacetate, followed by addition of 185 mg (1.72 mmol) of pyridine-2-carbaldehyde and 97 mg (1.72 mmol) of solid KOH **9** was obtained as a white-yellow powder. Yield: 401 mg (81%) after column chromatography. ¹H NMR (400 MHz, CDCl₃, δ, ppm): 8.78 (d, 1H, J=3.91 Hz, H_α-Py), 7.91 (m, 1H, H_β-Py), 7.78 (d, 1H, J=7.82 Hz, H_β'-Py), 7.58 (m, 1H, H_α'-Ph), 7.55 (m, 1H, H_α, H_β-Ph), 7.41 (m, 4H, Hy-Py, Hy-Ph), 6.81 (s, 1H, -CH=). ¹³C NMR (101 MHz, DMSO-d₆, δ, ppm) 177.4, 165.5, 149.9, 137.6, 134.47, 132.9, 130.5, 128.9, 127.9, 126.8, 124.9, 123.4. HRMS (*neg.*) calculated C₁₅H₉ClN₃OS⁺: 314.0125 (**9** - H isotopic)⁺, 314.0155 (**9** - H)⁺, found 314.0129 (**9** - H)⁺, 316.0160 (**9** - H)⁺. HPLC purity 95.22%.

3-(2-chlorophenyl)-5-((Z)-2-pyridylmethylidene)-2-thioxotetrahydro-4H-imidazol-4-one (10). From 200 mg (1.57 mmol) of 2-chloroaniline, by the reaction with 228 mg (1.57 mmol) of ethyl isothiocyanatoacetate, followed by addition of 185 mg (1.72 mmol) of pyridine-2-carbaldehyde and 97 mg (1.72 mmol) of solid KOH **10** was obtained as a white-yellow powder. Yield: 376 mg (76%) after column chromatography. ¹H NMR (400 MHz, DMSO-d₆, δ, ppm): 8.76 (d, 1H, J=4.73 Hz, H_α-Py), 7.89 (td, 1H, J₁=7.91 Hz, J₂=1.94 Hz, H_β-Py), 7.76 (m, 1H, H_β'-Py), 7.47 – 7.43 (m, 2H, H_β, H_β'-Ph), 7.37 – 7.32 (m, 3H, Hy-Py, H_α, Hy-Ph), 6.78 (s, 1H, -CH=). ¹³C NMR (101 MHz, DMSO-d₆, δ, ppm) 177.4, 163.3, 153.3, 150.4, 137.9, 132.3, 132.0, 129.9, 127.3, 125.5, 123.9, 120.8, 120.0, 116.9, 110.0. HRMS (*neg.*) calculated C₁₅H₉ClN₃OS⁺: 316.0125 (**10** - H isotopic)⁺, 314.0155 (**10** - H)⁺, found 314.0159 (**10** - H)⁺, 316.0126 (**10** - H isotopic)⁺. HPLC purity 99.20%.

3-(4-methoxyphenyl)-5-((Z)-2-pyridylmethylidene)-2-thioxotetrahydro-4H-imidazol-4-one (11). From 200 mg (1.63 mmol) of 4-methoxyaniline by the reaction with 236 mg (1.63 mmol) of ethyl isothiocyanatoacetate, followed by addition of 191 mg (1.79 mmol) of pyridine-2-carbaldehyde and 100 mg (1.79 mmol) of solid KOH **11** was obtained as a yellow powder. Yield: 466 mg (92%) after column chromatography. ¹H NMR (400 MHz, DMSO-d₆, δ, ppm): 8.46 (d, 1H, J=3.74 Hz, H_α-Py), 7.73 (td, 1H, J₁=6.91 Hz, J₂=1.73 Hz, H_β-Py), 7.39 (d, 1H, J=6.81 Hz, H_β'-Py), 7.25 (dd, 1H, J₁=7.52 Hz, J₂=2.02 Hz, Hy-Py), 7.17 (m, 2H, H_α, H_α'-Ph), 6.87 (m, 2H, H_β, H_β'-Ph), 6.83 (s, 1H, -CH=), 3.90 (s, 3H, p-OCH₃). ¹³C NMR (101 MHz, DMSO-d₆, δ, ppm) 178.2, 163.6, 159.4, 153.3, 149.9, 137.6, 130.0, 129.9, 126.7, 125.5, 123.3, 114.1, 108.4, 55.5. HRMS (*neg.*) calculated C₁₆H₁₂N₃O₂S⁺: 310.0650 (**11** - H)⁺, found 310.0654 (**11** - H)⁺. HPLC purity 97.31%

3-(4-ethoxyphenyl)-5-((Z)-2-pyridylmethylidene)-2-thioxotetrahydro-4H-imidazol-4-one (12). From 200 mg (1.46 mmol) of 4-ethoxyaniline, by the reaction with 212 mg (1.46 mmol) of ethyl isothiocyanatoacetate, followed by addition of 172 mg (1.60 mmol) of pyridine-2-carbaldehyde and 90 mg (1.60 mmol) of solid KOH **12** was obtained as a yellow powder. Yield: 419 mg (89%) after column chromatography. ¹H NMR (400 MHz, DMSO-d₆, δ, ppm): 8.75 (d, 1H, J=4.40 Hz, H_α-Py), 7.89 (td, 1H, J₁=7.70 Hz, J₂=1.83 Hz, H_β-Py), 7.75 (d, 1H, J=7.89 Hz, H_β'-Py), 7.38 (m, 1H, Hy-Py), 7.26 (m, 2H, H_α, H_α'-Ph), 7.01 (m, 2H, H_β, H_β-Ph), 6.76 (s, 1H, -CH=), 4.05 (q, 2H, J=6.97 Hz, OCH₂-), 1.32 (t, 3H, J=6.97 Hz, -CH₃). ¹³C NMR (101 MHz, DMSO-d₆, δ,

ppm) 178.6, 163.9, 159.1, 153.7, 150.3, 137.9, 130.4, 130.3, 127.1, 125.8, 123.7, 114.9, 108.8, 63.8, 15.1. HRMS (*neg.*) calculated $C_{17}H_{14}O_2N_3S^-$ (**12** - H): 324.0807, found 324.0812 (**12** - H). HPLC purity 95.90%

3-(3,4-dimethoxyphenyl)-5-((Z)-2-pyridylmethylidene)-2-thioxotetrahydro-4H-imidazol-4-one (13). From 200 mg (1.31 mmol) of 3,4-dimethoxyaniline, by the reaction with 190 mg (1.31 mmol) of ethyl isothiocyanatoacetate, followed by addition of 154 mg (1.44 mmol) of pyridine-2-carbaldehyde and 80 mg (1.44 mmol) of solid KOH **13** was obtained as a yellow powder. Yield: 322 mg (72%) after column chromatography. 1H NMR (400 MHz, $CDCl_3$, δ , ppm): 8.69 (d, 1H, $J=4.04$ Hz, $H\alpha$ -Py), 7.77 (td, 1H, $J_1=7.70$ Hz, $J_2=1.65$ Hz, $H\beta$ -Py), 7.44 (d, 1H, $J=7.89$ Hz, $H\beta'$ -Py), 7.29 (dd, 1H, $J_1=7.52$ Hz, $J_2=2.02$ Hz, $H\gamma$ -Py), 6.96 (m, 2H, $H\alpha$, $H\beta$ -Ph), 6.85 (m, 1H, $H\alpha'$ -Ph), 6.60 (s, 1H, -CH=), 3.91 (s, 3H, p -OCH₃), 3.88 (s, 3H, m -OCH₃). ^{13}C NMR (101 MHz, DMSO- d_6 , δ , ppm) 178.6, 163.9, 153.6, 150.3, 149.5, 149.0, 137.9, 130.3, 127.1, 126.0, 123.7, 121.7, 113.0, 111.8, 108.7, 56.1, 56.0. HRMS (*neg.*) calculated $C_{17}H_{14}O_3N_3S^-$: 340.0756 (**13** - H), found 340.0760 (**13** - H). HPLC purity 97.03%

3-(4-*t*-butylphenyl)-5-((Z)-2-pyridylmethylidene)-2-thioxotetrahydro-4H-imidazol-4-one (14). From 200 mg (1.34 mmol) of 4-*tert*-butylaniline, by the reaction with 194 mg (1.34 mmol) of ethyl isothiocyanatoacetate, followed by addition of 158 mg (1.48 mmol) of pyridine-2-carbaldehyde and 83 mg (1.48 mmol) of solid KOH **14** was obtained as a yellow powder. Yield: 402 mg (89%) after column chromatography. 1H NMR (400 MHz, $CDCl_3$, δ , ppm): 8.72 (d, 1H, $J=5.38$ Hz, $H\alpha$ -Py), 7.84 (m, 1H, $H\beta$ -Py), 7.53 (m, 3H, $H\beta$, $H\beta'$ -Ph, $H\beta'$ -Py), 7.33 (m, 3H, $H\gamma$ -Py, $H\alpha$, $H\alpha'$ -Ph), 6.62 (s, 1H, -CH=), 1.36 (m, 9H, *t*-Bu). ^{13}C NMR (101 MHz, DMSO- d_6 , δ , ppm) 179.0, 164.5, 153.1, 149.9, 147.9, 137.6, 132.0, 129.7, 129.2, 126.9, 126.8, 123.4, 108.9, 35.7, 31.5. HRMS (*pos.*) calculated $C_{19}H_{20}N_3OS^+$: 338.1327 (**14** + H)⁺, found 338.1322 (**14** + H)⁺. HPLC purity 98.83%

3-(2-*t*-butylphenyl)-5-((Z)-pyridin-2-ylmethylene)-2-thioxoimidazolidin-4-one (15). From 200 mg (1.34 mmol) of 2-(*tert*-butyl)aniline, by the reaction with 194 mg (1.34 mmol) of ethyl isothiocyanatoacetate, followed by addition of 158 mg (1.48 mmol) of pyridine-2-carbaldehyde and 83 mg (1.48 mmol) of solid KOH **15** was obtained as light yellow powder. Yield: 361 mg (80%) after column chromatography. 1H NMR (400 MHz, $CDCl_3$, δ , ppm): 11.65 (brs, 1H, NH), 8.71 (d, 1H, $J=3.91$ Hz, $H\alpha$ -Py), 7.77 (m, 1H, $H\beta$ -Py), 7.65 (m, 1H, $H\beta'$ -Py), 7.46 (m, 2H, $H\gamma$ -Py, $H\alpha'$ -Ph), 7.27 (m, 2H, $H\beta'$ -Ph, $H\gamma$ -Ph), 7.00 (m, 1H, $H\beta$ -Ph), 6.63 (s, 1H, -CH=), 1.38 (s, 9H, *t*-Bu). ^{13}C NMR (101 MHz, $CDCl_3$, δ , ppm) 179.0, 164.8, 153.6, 149.6, 148.6, 137.2, 131.5, 130.5, 130.3, 130.0, 129.5, 127.2, 126.5, 123.0, 107.8, 36.1, 31.8. HRMS (*pos.*) calculated $C_{19}H_{20}N_3OS^+$: 338.1327 (**15** + H)⁺, found 338.1359 (**15** + H)⁺. HPLC purity 96.97%

3-(2-methyl-4-diethylaminophenyl)-5-((Z)-2-pyridylmethylidene)-2-thioxotetrahydro-4H-imidazol-4-one (17). To a solution of 200 mg (0.93 mmol) of 2-methyl-4-diethylaminoaniline hydrochloride in 10 ml of DI water 40 mg (1.00 mmol) of sodium hydroxide was added. After extraction with diethyl ether (3×10 ml) the organic layers were combined and dried over anhydrous sodium sulfate. Then, 135 mg (0.93 mmol) of ethyl isothiocyanatoacetate was added dropwise to a vigorously stirred solution of 2-methyl-4-diethylaminoaniline in diethyl ether. The mixture was stirred overnight at r.t., the solvent was evaporated under reduced pressure. The resulting oil was dissolved in 10 ml of ethanol, 56 mg (1.00 mmol) of solid KOH was added. After a clear red solution was formed, 107 mg (1.00 mmol) of pyridine-2-carbaldehyde were added dropwise and mixture was stirred for 3 hours at r.t. The solution was then acidified with 1 M HCl until pH = 7. The precipitate formed was filtered off, washed with water, ethanol, diethyl ether and air-dried. **17** was obtained as a light yellow powder. Yield: 276 mg (81%) after column chromatography. 1H NMR (400 MHz, $CDCl_3$, δ , ppm): 11.61 (brs, 1H, NH), 8.70 (d, 1H, $J=3.91$ Hz, $H\alpha$ -Py), 7.76 (t, 1H, $J=9.78$ Hz, $H\beta$ -Py), 7.41 (d, 1H, $J=7.82$ Hz, $H\beta'$ -Py), 7.39 (m, 1H, $H\gamma$ -Py), 6.98 (m, 1H, $H\beta$ -Ph), 6.63 (s, 1H, -CH=), 6.57 (m, 2H, $H\alpha$, $H\beta'$ -Ph), 3.38 (q, 4H, $J=6.84$ Hz, -CH₂-), 1.19 (t, 6H, $J=6.85$ Hz, -CH₃). HRMS (*pos.*) calculated $C_{20}H_{23}N_4OS^+$: 367.1587 (**17** + H)⁺, found 367.1591 (**17** + H)⁺. HPLC purity 95.22%

3-(2-methoxy-4-chloro-5-methylphenyl)-5-((Z)-pyridin-2-ylmethylene)-2-thioxoimidazolidin-4-one (18). From 200 mg (1.17 mmol) of 2-methoxy-4-chloro-5-methyl aniline, by the reaction with 170 mg (1.17 mmol) of ethyl isothiocyanatoacetate, followed by addition of 138 mg (1.30 mmol) of pyridine-2-carbaldehyde and 72 mg (1.30 mmol) of solid KOH **18** was obtained as light yellow powder. Yield: 253 mg (60%) after column chromatography. 1H NMR (400 MHz, $CDCl_3$, δ , ppm): 8.67 (m, 1H, $H\alpha$ -Py), 7.74 (m, 1H, $H\beta$ -Py), 7.42 (m, 1H, $H\beta'$ -Py), 7.25 (m, 1H, $H\gamma$ -Py), 7.11 (s, 1H, $H\beta$ -Ph), 7.04 (s, 1H, $H\alpha'$ -Ph), 6.60 (s, 1H, -CH=), 3.77 (s, 3H, -OCH₃), 2.33 (s, 3H, -CH₃). ^{13}C NMR (101 MHz, $CDCl_3$, δ , ppm) 177.8, 163.5, 153.9, 153.6, 149.6, 137.3, 136.6, 132.1, 130.6, 128.6, 126.5, 123.0, 119.7, 113.5, 107.9, 56.3, 19.2. HRMS (*pos.*) calculated $C_{17}H_{15}ClN_3O_2S^+$: 360.0569 (**18** + H)⁺, found 360.0603 (**18** + H)⁺. HPLC purity 95.14%

3-(3-chloro-4-fluorophenyl)-5-((Z)-pyridin-2-ylmethylene)-2-thioxoimidazolidin-4-one (19). From 200 mg (1.37 mmol) of 3-chloro-4-fluoro aniline, by the reaction with 199 mg (1.37 mmol) of ethyl isothiocyanatoacetate, followed by addition of 161 mg (1.51 mmol) of pyridine-2-carbaldehyde and 85 mg (1.51 mmol) of solid KOH **19** was obtained as light yellow powder. Yield: 366 mg (80%) after column chromatography. 1H NMR (400 MHz, DMSO- d_6 , δ , ppm): 11.91 (br.s., 1H, NH), 8.76 (d, 1H, $J=4.70$ Hz, $H\alpha$ -Py), 7.92 (td, 1H, $J_1=7.43$ Hz, $J_2=1.96$ Hz, $H\beta$ -Py), 7.75 (m, 2H, $H\alpha$, $H\alpha'$ -Ph), 7.58 (m, 1H, $H\beta$ -Ph), 7.51 (m, 1H, $H\gamma$ -Py), 7.40 (m, 1H, $H\beta'$ -Py), 6.80 (c, 1H, -CH=). HRMS (*neg.*) calculated $C_{15}H_8ClFN_3OS^-$: 332.0066 (**19** - H), 334.0031 (**19** - H isotopic), found 332.0065 (**19** - H), 334.0035 (**19** - H isotopic). HPLC purity 96.63%

3-(2-methyl-3-chlorophenyl)-5-((Z)-pyridin-2-ylmethylene)-2-thioxoimidazolidin-4-one (20). From 200 mg (1.41 mmol) of 2-methyl-3-chloro aniline, by the reaction with 204 mg (1.41 mmol) of ethyl isothiocyanatoacetate, followed by addition of 167 mg (1.56 mmol) of pyridine-2-carbaldehyde and 87 mg (1.56 mmol) of solid KOH **20** was obtained as light yellow powder. Yield: 414 mg (89%) after column chromatography. 1H NMR (400 MHz, $CDCl_3$, δ , ppm): 12.23 (br.s., 1H, NH), 8.76 (d, 1H, $J=4.70$ Hz, $H\alpha$ -Py), 7.86 (td, 1H, $J_1=7.73$ Hz, $J_2=1.76$ Hz, $H\beta$ -Py), 7.51 (t, 2H, $J=8.22$ Hz, $H\beta$, $H\gamma$ -Ph), 7.40 (m, 1H, $H\gamma$ -Py), 7.27 (m, 1H, $H\beta'$ -Py), 7.14 (d, 1H, $J=8.22$ Hz, $H\alpha$ -Ph), 6.62 (s, 1H, -CH=), 2.20 (s, 3H, -CH₃). ^{13}C NMR (101 MHz, DMSO- d_6 , δ , ppm) 177.1, 163.2, 153.0, 149.9, 137.6, 134.9, 133.7, 130.4, 129.0, 127.8, 126.8, 123.5, 109.3, 15.0. HRMS (*neg.*) calculated $C_{16}H_{11}ClN_3OS^-$: 328.0311 (**20** - H), 330.0282 (**20** - H isotopic), found 328.0317 (**20** - H), 330.0283 (**20** - H isotopic). HPLC purity 95.12%

3-(2,4,6-methylphenyl)-5-((Z)-pyridin-2-ylmethylene)-2-thioxoimidazolidin-4-one (21). From 200 mg (1.48 mmol) of 2,4,6-methylaniline, by the reaction with 215 mg (1.48 mmol) of ethyl isothiocyanatoacetate, followed by addition of 175 mg (1.63 mmol) of pyridine-2-carbaldehyde and 91 mg (1.63 mmol) of solid KOH **21** was obtained as light yellow powder. Yield: 430 mg (90%) after column chromatography. 1H NMR (400 MHz, $CDCl_3$, δ , ppm): 8.76 (d, 1H, $J=4.70$ Hz, $H\alpha$ -Py), 7.92 (td, 1H, $J_1=8.22$ Hz, $J_2=1.57$ Hz, $H\beta$ -Py), 7.53 (d, 1H, $J=8.22$ Hz, $H\beta'$ -Py), 7.41 (td, 1H, $J_1=7.43$ Hz, $J_2=1.96$ Hz, $H\gamma$ -Py), 7.02 (s, 2H, $H\beta$, $H\beta'$ -Ph), 6.60 (s, 1H, -CH=), 2.32 (s, 3H, -CH₃), 2.10 (s, 6H, 2×-CH₃). ^{13}C NMR (101 MHz, $CDCl_3$, δ , ppm) 176.8, 163.1, 152.9, 149.9, 142.7, 138.9, 137.6, 136.2, 129.6, 128.9, 126.9, 123.5, 109.6, 20.7, 17.3. HRMS (*neg.*) calculated $C_{18}H_{16}N_3OS^-$: 322.1014 (**21** - H), 323.1048 (**21** - H isotopic), found 322.1019 (**21** - H), 323.1052 (**21** - H isotopic). HPLC purity 98.34%

3-(4-methylthiophenyl)-5-((Z)-pyridin-2-ylmethylene)-2-thioxoimidazolidin-4-one (22). From 200 mg (1.44 mmol) of 4-methylthioaniline, by the reaction with 209 mg (1.44 mmol) of ethyl isothiocyanatoacetate, followed by addition of 169 mg (1.58 mmol) of pyridine-2-carbaldehyde and 89 mg (1.58 mmol) of solid KOH **22** was obtained as light yellow powder. Yield: 259 mg (55%) after column chromatography. 1H NMR (400 MHz, $CDCl_3$, δ , ppm): 11.79 (br.s., 1H, NH), 8.71 (d, 1H, $J=4.70$ Hz, $H\alpha$ -Py), 7.80 (td, 1H, $J_1=7.73$ Hz, $J_2=1.76$ Hz, $H\beta$ -Py), 7.47 (td, 1H, $J_1=7.83$ Hz, $J_2=1.96$ Hz, $H\gamma$ -Py), 7.37 (m, 2H, $H\beta'$ -Py), 7.29 (m, 3H, $H\alpha$, $H\alpha'$ -Ph, $H\beta'$ -Ph), 6.63 (s, 1H, -CH=), 2.50 (s, 3H, -SCH₃). ^{13}C NMR (101 MHz, DMSO- d_6 , δ , ppm) 177.8, 163.4, 153.2, 149.9,

139.6, 137.6, 131.3, 129.9, 129.2, 126.8, 125.8, 123.4, 108.6, 14.6. HRMS (*neg.*) calculated $C_{16}H_{12}N_3OS_2$: 326.0422 (**22** - H)⁻; 327.0455 (**22** - H isotopic)⁻; found 326.0427 (**22** - H)⁻; 327.0459 (**22** - H isotopic)⁻. HPLC purity 95.78%

3-(4-iodophenyl)-5-((Z)-2-pyridylmethylidene)-2-thioxotetrahydro-4H-imidazol-4-one (23). From 200 mg (0.91 mmol) of 4-iodoaniline, by the reaction with 146 mg (0.91 mmol) of ethyl isothiocyanatoacetate, followed by addition of 107 mg (1.00 mmol) of pyridine-2-carbaldehyde and 56 mg (1.00 mmol) of solid KOH **23** was obtained as dark yellow powder. Yield: 174 mg (47%) after column chromatography. ¹H NMR (400 MHz, DMSO-*d*₆, δ, ppm): 11.89 (brs, 1H, NH), 8.75 (d, 1H, J=4.70 Hz, H_α-Py), 7.90 – 7.86 (m, 3H, H_β-Py, H_β, H_β'-Ph), 7.75 (d, 1H, J=8.61 Hz, H_β'-Py), 7.38 (m, 1H, H_γ-Py), 7.22 – 7.20 (d, 2H, J=8.22 Hz, H_α, H_α'-Ph), 6.78 (s, 1H, -CH=). ¹³C NMR (101 MHz, DMSO-*d*₆, δ, ppm) 177.5, 164.5, 163.2, 157.8, 153.1, 149.9, 137.6, 131.9, 131.1, 126.8, 123.4, 114.6, 108.8. HRMS (*neg.*) calculated $C_{15}H_9IN_3OS$: 405.9511 (**23** - H)⁻; found 405.9510 (**23** - H)⁻. HPLC purity 97.11%

3-(2-methyl-4-diethylaminophenyl)-5-((Z)-2-pyridylmethylidene)-2-thioxotetrahydro-4H-imidazol-4-one (24). Sodium hydroxide 40 mg (1.00 mmol) was added to a solution of 200 mg (0.93 mmol) of 2-methyl-4-diethylaminoaniline hydrochloride in 10 ml of DI water. After extraction with diethyl ether (3 × 10 ml) the organic layers were combined and dried over anhydrous sodium sulfate. Then, 135 mg (0.93 mmol) of ethyl isothiocyanatoacetate was added dropwise to a vigorously stirred solution of 2-methyl-4-diethylaminoaniline in diethyl ether. The mixture was stirred overnight at r.t., the solvent was evaporated under reduced pressure. Then, 10 ml of EtOH and 56 mg (1.00 mmol) of solid KOH were added to the resulting oil, followed by addition of 107 mg (1.00 mmol) of pyridine-2-carbaldehyde. The mixture was stirred for 3 hours at r.t. The solution was acidified with 1 M HCl until pH = 7. The precipitate formed was filtered off, washed with water, ethanol, diethyl ether and air-dried. **24** was obtained as light yellow powder. Yield: 276 mg (81%). ¹H NMR (400 MHz, CDCl₃, δ, ppm): 11.61 (brs, 1H, NH), 8.70 (d, 1H, J=3.91 Hz, H_α-Py), 7.76 (t, 1H, J₁=9.78 Hz, H_β-Py), 7.41 (d, 1H, J=7.82 Hz, H_β'-Py), 7.39 (m, 1H, H_γ-Py), 6.98 (m, 1H, H_β-Ph), 6.63 (s, 1H, -CH=), 6.57 (m, 2H, H_α, H_β'-Ph), 3.38 (q, 4H, J=6.84 Hz, -CH₂-), 1.19 (t, 6H, J=6.85 Hz -CH₃). ¹³C NMR (101 MHz, CDCl₃, δ, ppm) 171.7, 166.5, 158.2, 149.9, 136.7, 135.1, 130.0, 117.9, 113.5, 112.3, 109.6, 109.1, 108.5, 103.2, 95.6, 43.7, 17.9, 12.6. HRMS (*pos.*) calculated $C_{20}H_{23}N_4OS$: 367.1587 (**24** + H)⁺; found 367.1591 (**24** + H)⁺. HPLC purity 96.91%

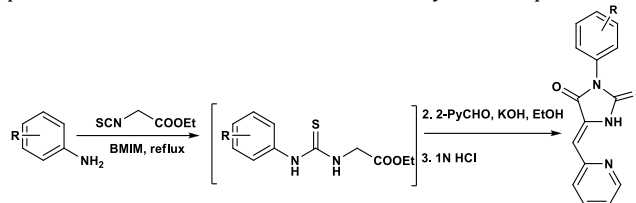
3-(2,5-difluorophenyl)-5-((Z)-pyridin-2-ylmethylene)-2-thioxoimidazolidin-4-one (28). From 200 mg (1.55 mmol) of 2,5-difluoroaniline, by the reaction with 225 mg (1.55 mmol) of ethyl isothiocyanatoacetate, followed by addition of 183 mg (1.71 mmol) of pyridine-2-carbaldehyde and 96 mg (1.71 mmol) of solid KOH **28** was obtained as light yellow powder. Yield: 371 mg (75%) after column chromatography. ¹H NMR (400 MHz, CDCl₃, δ, ppm): 12.06 (br.s, 1H, NH), 8.74 (d, 1H, J=3.91 Hz, H_α-Py), 7.85 (t, 1H, J=7.83 Hz, H_β-Py), 7.51 (d, 1H, J=7.83 Hz, H_β'-Py), 7.36 (m, 1H, H_γ-Py), 7.23 (m, 2H, H_γ, H_β'-Ph), 7.15 (m, 1H, H_α-Ph), 6.65 (s, 1H, -CH=). 174.6, 166.9, 162.7, 158.1, 156.4, 152.8, 149.9, 137.6, 129.4, 128.2, 126.9, 123.6, 118.7, 117.6, 109.9. HRMS (*neg.*) calculated $C_{15}H_8F_2N_3OS$: 316.0362 (**28** - H)⁻; found 316.0361 (**28** - H)⁻. HPLC purity 98.02%

3-(3,5-difluorophenyl)-5-((Z)-pyridin-2-ylmethylene)-2-thioxoimidazolidin-4-one (29). From 200 mg (1.55 mmol) of 3,5-difluoroaniline, by the reaction with 225 mg (1.71 mmol) of ethyl isothiocyanatoacetate, followed by addition of 183 mg (1.71 mmol) of pyridine-2-carbaldehyde and 96 mg (1.71 mmol) of solid KOH **29** was obtained as light yellow powder. Yield: 240 mg (49%) after column chromatography. ¹H NMR (400 MHz, CDCl₃, δ, ppm): 8.73 (d, 1H, J=3.85 Hz, H_α-Py), 7.84 (td, 1H, J₁=7.79 Hz, J₂=1.65 Hz, H_β-Py), 7.50 (d, 1H, J=7.70 Hz, H_β'-Py), 7.35 (dd, 1H, J₁=7.34 Hz, J₂=5.32 Hz, H_γ-Py), 7.02 (m, 2H, H_α, H_α'-Ph), 6.94 (m, 1H, H_γ-Ph), 6.54 (s, 1H, -CH=). ¹³C NMR (101 MHz, DMSO-*d*₆, δ, ppm) 177.0, 168.1, 162.9, 160.8, 149.9, 145.6, 137.6, 129.7, 126.8, 125.9, 123.5, 119.8, 113.4, 113.1, 109.0. HRMS

(*neg.*) calculated $C_{15}H_8F_2N_3OS$: 316.0362 (**29** - H)⁻; found 316.0360 (**29** - H)⁻. HPLC purity 97.50%

Syntheses of compounds 16, 25, 26, and 27

General Protocol (16, 25, 26, 27). In a round bottom flask, 1000 mg of aniline was dissolved in 1 ml of ionic liquid (BMIM-X) and heated to 100°C. Then isothiocyanate ethyl acetate (equimolar amount) was slowly added to the solution and stirred for several hours (TLC control). After the completion of the reaction, the mixture was diluted with 10 ml of ethanol, 1.1 equivalent of pyridine-2-carbaldehyde and 1.1 equivalent of solid KOH were added. The reaction was stirred for several hours at r.t., 1 M HCl was added until pH = 7, the precipitate formed was filtered off, washed with water, ethanol, diethyl ether and air-dried. Final products purified by column chromatography on silica gel, eluent: CH₂Cl₂:MeOH. The products were isolated as a yellow powders.



(Z)-3-(4-nitrophenyl)-5-((Z)-2-pyridylmethylidene)-2-thioxotetrahydro-4H-imidazol-4-one (16). In a round bottom flask, 200 mg (1.45 mmol) of 4-nitroaniline was dissolved in 1 ml of BMIM-N(CN)₂, and heated to 100°C. Then, 210 mg (1.45 mmol) of ethyl isothiocyanatoacetate was added dropwise. The mixture was stirred for 48 hours at 100°C (TLC control). After the completion of the reaction, the mixture was diluted by 10 ml of ethanol, 89 mg (1.59 mmol) of solid KOH and 171 mg (1.59 mmol) of pyridine-2-carbaldehyde was added. The mixture was stirred for 6 hours at r.t. After acidification with 1 M HCl until pH = 7, the precipitate formed was filtered off, washed with ethanol, water, diethyl ether and air-dried. **16** was obtained as a yellow powder. Yield: 137 mg, (29%) after three-time purification by column chromatography (CH₂Cl₂: MeOH 10:1; 15:1; 20:1). ¹H NMR (400 MHz, DMSO-*d*₆, δ, ppm): 8.81 (m, 1H, H_α-Py), 8.40 (m, 3H, H_α, H_β, H_β'-Ph), 7.93 (m, 2H, H_β, H_β'-Py), 7.78 (m, 1H, H_α'-Ph), 7.43 (m, 1H, H_γ-Py), 6.86 (s, 1H, -CH=). ¹³C NMR (101 MHz, DMSO-*d*₆, δ, ppm) 176.9, 163.0, 158.9, 149.9, 147.3, 146.7, 137.6, 130.3, 129.8, 127.6, 126.8, 124.1, 123.5. HRMS (*neg.*) calculated $C_{15}H_9N_4O_3S$: 325.0395 (**16** - H)⁻; found 325.0397 (**16** - H)⁻. HRMS (*pos.*) calculated $C_{15}H_9N_4O_3S$: 327.0552 (**16** + H)⁺; found 327.0544 (**16** + H)⁺. HPLC purity 97.67%

3-(2,6-dichlorophenyl)-5-((Z)-pyridin-2-ylmethylene)-2-thioxoimidazolidin-4-one (25). In a round bottom flask, 1000 mg (6.17 mmol) of 2,6-dichloroaniline was dissolved in 1 ml of BMIM-BF₄ and heated to 100°C. Then, 1.89 g (6.17 mmol) of ethyl isothiocyanatoacetate was added dropwise. The mixture was stirred for 48 hours at 100°C (TLC control). After the completion of the reaction, the mixture was diluted with 10 ml of EtOH and 726 mg (6.79 mmol) of pyridine-2-carbaldehyde and 380 mg (6.79 mmol) of KOH were added. The mixture was stirred for 2 hours at r.t., acidified with 1 M HCl until pH = 7. The precipitate formed was filtered off, washed with ethanol, water, diethyl ether and air-dried. **25** was obtained as a light yellow powder. Yield: 108 mg (5%) after column chromatography. ¹H NMR (400 MHz, CDCl₃, δ, ppm): 11.83 (br.s., 1H, NH), 8.72 (d, 1H, J=3.91 Hz, H_α-Py), 7.80 (td, 1H, J₁=7.83 Hz, J₂=1.96 Hz, H_γ-Py), 7.52 (d, 2H, J=6.85 Hz, H_β', H_β-Ph), 7.48 (m, 2H, H_β'-Py, H_γ-Ph), 7.32 (m, 1H, H_β-Py), 6.67 (s, H, -CH=). HRMS (*pos.*) calculated $C_{15}H_{10}Cl_2N_3OS$: 349.9922 (**25** + H)⁺; found 349.9904 (**25** + H)⁺. HPLC purity 95.94%

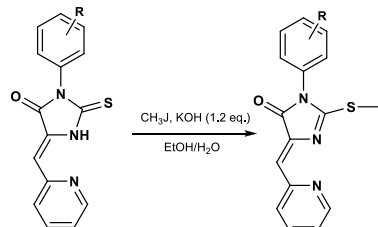
3-(2,4,6-trichlorophenyl)-5-((Z)-pyridin-2-ylmethylene)-2-thioxoimidazolidin-4-one (26). In a round bottom flask, 1000 mg (5.10 mmol) of 2,4,6-trichloroaniline was dissolved in 1 ml of BMIM-BF₄ and heated to 100°C. Then, 740 mg (5.10 mmol) of ethyl isothiocyanatoacetate was added dropwise. The mixture was stirred for 48 hours at 100°C (TLC control). After the completion of the reaction, the mixture was diluted with 10 ml of ethanol, 600 mg (5.61 mmol) of pyridine-2-carbaldehyde

and 314 mg (5.61 mmol) of KOH were added. The reaction was stirred for 2 hours at r.t., acidified with 1 M HCl until pH = 7. The precipitate formed was filtered off, washed with ethanol, water, diethyl ether and air-dried. **26** was obtained as a light yellow powder. Yield: 100 mg (6%) after column chromatography. ¹H NMR (400 MHz, CDCl₃, δ, ppm): 11.91 (br.s, 1H, NH), 8.72 (d, 1H, J=3.91 Hz, H_α-Py), 7.81 (m, 1H, H_β-Py), 7.52 (s, 2H, H_β, H_β'-Ph) 7.46 (d, 1H, J=7.83 Hz, H_β'-Py), 7.31 (m, 1H, H_γ-Py), 6.67 (s, 1H, -CH=). HRMS (*pos.*) calculated C₁₅H₉Cl₃N₃O⁺ 383.9532 (**26** + H)⁺, found 383.9514 (**26** + H)⁺. HPLC purity 96.00%

3-(2,6-dibromophenyl)-5-((Z)-pyridin-2-ylmethylene)-2-thioxoimidazolidin-4-one (27). In a round-bottom flask, 1000 mg (5.10 mmol) of 2,4-dibromaniline was dissolved in 1 ml of BMIM-BF₄ and heated to 100°C. Then, 1.578 mg (3.99 mmol) of ethyl isothiocyanacetate was added dropwise. The mixture was stirred for 48 hours at 100°C (TLC control). After the completion of the reaction, the mixture was diluted with 10 ml of ethanol, 469 mg (4.39 mmol) of pyridine-2-carbaldehyde and 246 mg (4.39 mmol) of solid KOH were added. The mixture was stirred for 2 hours at r.t., acidified with 1 M HCl until pH = 7. The precipitate formed was filtered off, washed with ethanol, water, diethyl ether and air-dried. **27** was obtained as a light yellow powder. Yield: 90 mg (5%) after column chromatography. ¹H NMR (400 MHz, CDCl₃, δ, ppm): 12.05 (br.s, 1H, NH), 8.74 (d, 1H, J=4.89 Hz, H_α-Py), 7.93 (t, 1H, J=7.82 Hz, H_β-Py), 7.71 (d, 1H, J=7.33 Hz, H_β'-Py), 7.56 (d, 2H, J=7.92 Hz, H_β, H_β'-Ph), 7.41 (m, 1H, H_γ-Py), 7.27 (m, 1H, H_γ-Ph), 6.60 (s, 1H, -CH=). HRMS (*pos.*) calculated C₁₅H₁₀Br₂N₃O⁺ 439.8891 (**27** + H)⁺, found 439.8909 (**27** + H)⁺. HPLC purity 97.38%

Syntheses of compounds 30-51

General Protocol. 1.2 eq. of solid KOH was added to a solution of the 3-aryl-5-((Z)-2-pyridylmethylidene)-2-thioxotetrahydro-4H-imidazol-4-one in H₂O/EtOH 1:1 mixture (2 ml per 100 mg of compound). After a clear red solution was formed, methyl iodide (2.3 eq.) was added dropwise and the mixture was stirred for ten minutes. The mixture was placed in a freezer for 1h., the precipitate formed was filtered off, washed with an aqueous 1 M KOH, water, ice-cold ethanol, diethyl ether and air-dried. The products were isolated as a light yellow powders after purification by column chromatography, eluent CH₂Cl₂: MeOH 20:1.



5-(Z)-3-(4-fluorophenyl)-2-(methylthio)-5-(pyridin-2-ylmethylidene)-1H-imidazol-4-one (30). From 100 mg (0.33 mmol) of 3-(4-fluorophenyl)-5-((Z)-2-pyridylmethylidene)-2-thioxotetrahydro-4H-imidazol-4-one **1** as a result of reaction with 110 mg (0.77 mmol) of methyl iodide, in the presence of 22 mg (0.39 mmol) of solid KOH, **30** was obtained as a white-yellow powder. Yield: 39 mg (38%) after column chromatography. ¹H NMR (400 MHz, CDCl₃, δ, ppm): 8.92 (d, 1H, J=8.27 Hz, H_α-Py), 8.81 (d, 1H, J=5.09 Hz, H_β'-Py), 8.04 (t, 1H, J=8.42 Hz, H_γ-Py), 7.48 (m, 1H, H_β-Py), 7.30 (m, 2H, H_β, H_β'-Ph), 7.19 (m, 2H, H_α, H_α'-Ph), 7.12 (s, 1H, -CH=), 2.76 (s, 3H, -SCH₃). ¹³C NMR (101 MHz, DMSO-d₆, δ, ppm) 181.6, 168.4, 165.0, 161.4, 153.5, 150.4, 140.4, 137.0, 130.6, 128.9, 126.8, 124.0, 122.6, 116.8, 13.43. HRMS (*pos.*) calculated for C₁₆H₁₃FN₃O⁺: 314.0758 (**30** + H)⁺, found 314.0761 (**30** + H)⁺. HPLC purity 98.95%

5-(Z)-3-(3-fluorophenyl)-2-(methylthio)-5-(pyridin-2-ylmethylidene)-1H-imidazol-4-one (31). From 100 mg (0.33 mmol) of 3-(3-fluorophenyl)-5-((Z)-2-pyridylmethylidene)-2-thioxotetrahydro-4H-imidazol-4-one **2** as a result of reaction with 110 mg (0.77 mmol) of methyl iodide, in the presence of 22 mg (0.39 mmol) of solid KOH, **31** was obtained as a white-yellow powder. Yield: 43 mg (42%) after column chromatography. ¹H NMR (400 MHz, CDCl₃, δ, ppm): 8.81 (d, 1H, J=8.03 Hz, H_α-Py), 8.68 (d, 1H, J=3.91 Hz, H_β'-Py), 7.76 (t, 1H, J=8.02 Hz, H_γ-Py),

7.44 (m, 1H, H_β-Py), 7.24 - 7.21 (m, 2H, H_α, H_α'-Ph), 7.16 - 7.09 (m, 3H, H_β, H_γ-Ph, -CH=), 2.72 (s, 3H, -SCH₃). ¹³C NMR (101 MHz, DMSO-d₆, δ, ppm) 168.0, 161.2, 153.1, 150.4, 140.3, 137.0, 134.2, 131.6, 126.9, 124.5, 122.8, 116.8, 115.6, 100.3, 87.9, 13.5. HRMS (*pos.*) calculated C₁₆H₁₃FN₃O⁺: 314.0758 (**31** + H)⁺, found 314.0761 (**31** + H)⁺. HPLC purity 98.34%

5-(Z)-3-(2-fluorophenyl)-2-(methylthio)-5-(pyridin-2-ylmethylidene)-1H-imidazol-4-one (32). From 100 mg (0.33 mmol) of 3-(2-fluorophenyl)-5-((Z)-2-pyridylmethylidene)-2-thioxotetrahydro-4H-imidazol-4-one **3** as a result of reaction with 110 mg (0.77 mmol) of methyl iodide, in the presence of 22 mg (0.39 mmol) of solid KOH, **32** was obtained as a white-yellow powder. Yield: 32 mg (31%) after column chromatography. ¹H NMR (400 MHz, CDCl₃, δ, ppm): 8.89 (d, 1H, J=7.82 Hz, H_α-Py), 8.76 (d, 1H, J= 3.91 Hz, H_β'-Py), 7.91 (t, 1H, J=7.82 Hz, H_γ-Py), 7.50 (m, 1H, H_α-Ph), 7.38 - 7.25 (m, 5H, H_β, H_β' , H_γ-Ph, H_β-Py -CH=), 2.76 (s, 3H, -SCH₃). HRMS (*pos.*) calculated C₁₆H₁₃FN₃O⁺: 314.0758 (**32** + H)⁺, found 314.0763 (**32** + H)⁺. HPLC purity 98.20%

5-(Z)-3-(4-bromophenyl)-2-(methylthio)-5-(pyridin-2-ylmethylidene)-1H-imidazol-4-one (33). From 100 mg (0.28 mmol) of 3-(4-bromophenyl)-5-((Z)-2-pyridylmethylidene)-2-thioxotetrahydro-4H-imidazol-4-one **4** as a result of reaction with 93 mg (0.65 mmol) of methyl iodide, in the presence of 19 mg (0.33 mmol) of solid KOH, **33** was obtained as a white-yellow powder. Yield: 42 mg (40%) after column chromatography. ¹H NMR (400 MHz, CDCl₃, δ, ppm): 8.80 (d, 1H, J=8.22 Hz, H_α-Py), 8.68 (d, 1H, J=4.70 Hz, H_β'-Py), 7.76 (dt, 1H, J₁=7.63 Hz, J₂=1.37 Hz, H_γ-Py), 7.61 (m, 2H, H_β-Py, -CH=), 7.25 (m, 2H, H_β, H_β'-Ph), 7.20 (m, 2H, H_α, H_α'-Ph), 2.72 (s, 3H, -SCH₃). ¹³C NMR (101 MHz, DMSO-d₆, δ, ppm) 171.9, 167.6, 152.9, 150.1, 139.8, 136.8, 132.3, 131.5, 129.3, 126.6, 123.9, 123.0, 122.5, 12.9. HRMS (*pos.*) calculated C₁₆H₁₃BrN₃O⁺ 373.9958 (**33** + H)⁺, found 373.9963 (**33** + H)⁺. HPLC purity 95.83%

5-(Z)-3-(3-bromophenyl)-2-(methylthio)-5-(pyridin-2-ylmethylidene)-1H-imidazol-4-one (34). From 100 mg (0.28 mmol) of 3-(3-bromophenyl)-5-((Z)-2-pyridylmethylidene)-2-thioxotetrahydro-4H-imidazol-4-one **5** as a result of reaction with 93 mg (0.65 mmol) of methyl iodide, in the presence of 19 mg (0.33 mmol) of solid KOH, **34** was obtained as a white-yellow powder. Yield: 52 mg (50%) after column chromatography. ¹H NMR (400 MHz, CDCl₃, δ, ppm): 8.80 (d, 1H, J=7.83 Hz, H_α-Py), 8.68 (d, 1H, J=5.67 Hz, H_β'-Py), 7.76 (t, 1H, J=8.23 Hz, H_γ-Py), 7.58 (m, 1H, H_α-Ph), 7.52 (s, 1H, -CH=), 7.36 (m, 1H, H_β-Py), 7.30 (m, 1H, H_α'-Ph), 7.29 - 7.20 (m, 2H, H_β, H_γ-Ph), 2.72 (s, 3H, -SCH₃). ¹³C NMR (101 MHz, DMSO-d₆, δ, ppm) 177.5, 167.5, 150.1, 146.7, 139.7, 136.8, 133.5, 132.3, 131.5, 129.3, 126.6, 123.9, 122.5, 119.1, 110.8, 12.9. HRMS (*pos.*) calculated C₁₆H₁₃BrN₃O⁺ 373.9958 (**34** + H)⁺, found 373.9962 (**34** + H)⁺. HPLC purity 96.16%

5-(Z)-3-(2-bromophenyl)-2-(methylthio)-5-(pyridin-2-ylmethylidene)-1H-imidazol-4-one (35). From 100 mg (0.28 mmol) of 3-(2-bromophenyl)-5-((Z)-2-pyridylmethylidene)-2-thioxotetrahydro-4H-imidazol-4-one **6** as a result of reaction with 93 mg (0.65 mmol) of methyl iodide, in the presence of 19 mg (0.33 mmol) of solid KOH, **35** was obtained as a white-yellow powder. Yield: 30 mg (29%) after column chromatography. ¹H NMR (400 MHz, CDCl₃, δ, ppm): 8.82 (d, 1H, J=9.00 Hz, H_α-Py), 8.69 (d, 1H, J=4.70 Hz, H_β'-Py), 7.74 (m, 2H, H_γ-Py, H_α-Ph), 7.45 (m, 1H, H_β-Py), 7.34 (m, 2H, H_β, H_β'-Ph), 7.21 (m, 2H, H_γ-Ph, -CH=), 2.71 (s, 3H, -SCH₃). ¹³C NMR (101 MHz, DMSO-d₆, δ, ppm) 168.0, 153.2, 150.5, 140.1, 137.1, 133.9, 131.9, 131.9, 131.8, 129.6, 126.9, 124.2, 123.2, 123.0, 122.9, 13.3. HRMS (*pos.*) calculated C₁₆H₁₃BrN₃O⁺ 373.9958 (**35** + H)⁺, found 373.9967 (**35** + H)⁺. HPLC purity 97.01%

5-(Z)-3-(2-bromo-4-fluorophenyl)-2-(methylthio)-5-(pyridin-2-ylmethylene)-1H-imidazol-5(4H)-one (36). From 100 mg (0.27 mmol) of (Z)-3-(2-bromo-4-fluorophenyl)-5-(pyridin-2-ylmethylene)-2-thioxoimidazolidin-4-one **7** as a result of reaction with 90 mg (0.63 mmol) methyl iodide, in the presence of 18 mg (0.33 mmol) of solid KOH, **36** was obtained as a white-yellow powder. Yield: 47 mg (45%) after column chromatography. ¹H NMR (400 MHz, CDCl₃, δ, ppm): 8.85 (d, 1H, J=7.83 Hz, H_α-Py), 8.72 (d, 1H, J=3.91 Hz, H_β'-Py), 7.84 (m, 1H,

Hy-Py), 7.45 (m, 2H, H β -Py, H β -Ph), 7.30 (m, 1H, H β '-Ph), 7.22 (m, 2H, H α -Ph, -CH=), 2.75 (s, 3H, -SCH₃). ¹³C NMR (101 MHz, CDCl₃, δ , ppm) 167.9, 159.0, 156.5, 153.0, 149.3, 139.9, 136.8, 131.0, 128.4, 127.2, 124.4, 123.5, 120.9, 120.7, 116.5, 13.3. HRMS (*pos.*) calculated C₁₆H₁₂BrFN₃O⁺: 393.9843 (**36** + H isotopic)⁺, 391.9863 (**36** + H)⁺, found 393.9879 (**36** + H isotopic)⁺, 391.9902 (**36** + H)⁺. HPLC purity 96.00%

5-(Z)-3-(4-chlorophenyl)-2-(methylthio)-5-(pyridin-2-ylmethylidene)-1H-imidazol-4-one (37). From 100 mg (0.32 mmol) of 3-(4-chlorophenyl)-5-((Z)-2-pyridylmethylidene)-2-thioxotetrahydro-4H-imidazol-4-one **8** as a result of reaction with 103 mg (0.72 mmol) of methyl iodide, in the presence of 21.5 mg (0.38 mmol) of solid KOH, **37** was obtained as a white-yellow powder. Yield: 50 mg (47%) after column chromatography. ¹H NMR (400 MHz, CDCl₃, δ , ppm): 8.82 (d, 1H, J=7.83 Hz, H α -Py), 8.72 (d, 1H, J₁=4.89 Hz, H β '-Py), 7.80 (t, 1H, J=6.85 Hz, Hy-Py), 7.48 (m, 2H, H α , H α '-Ph), 7.42 – 7.30 (m, 3H, H β , H β '-Ph, H β -Py), 7.22 (s, 1H, -CH=), 2.74 (s, 3H, -SCH₃). HRMS (*pos.*) calculated C₁₆H₁₃ClN₃O⁺: 330.0463 (**37** + H)⁺, found 330.0464 (**37** + H)⁺. HPLC purity 96.27%

5-(Z)-3-(3-chlorophenyl)-2-(methylthio)-5-(pyridin-2-ylmethylidene)-1H-imidazol-4-one (38). From 100 mg (0.32 mmol) of 3-(4-chlorophenyl)-5-((Z)-2-pyridylmethylidene)-2-thioxotetrahydro-4H-imidazol-4-one **9** as a result of reaction with 104 mg (0.73 mmol) of methyl iodide, in the presence of 21 mg (0.38 mmol) of solid KOH, **38** was obtained as a white-yellow powder. Yield: 33 mg (31%) after column chromatography. ¹H NMR (400 MHz, CDCl₃, δ , ppm): 8.86 (d, 1H, J=7.83 Hz, H α -Py), 8.73 (d, 1H, J=3.91 Hz, H β '-Py), 7.85 (t, 1H, J=7.83 Hz, Hy-Py), 7.44 (m, 2H, H α , H α '-Ph), 7.38 (m, 1H, H β -Py), 7.28 (m, 3H, H β , Hy-Ph, -CH=), 3.05 (s, 3H, -SCH₃). HRMS (*pos.*) calculated C₁₆H₁₃ClN₃O⁺: 330.0463 (**38** + H)⁺, found 330.0454 (**38** + H)⁺. HPLC purity 96.12%

5-(Z)-3-(2-chlorophenyl)-2-(methylthio)-5-(pyridin-2-ylmethylidene)-1H-imidazol-4-one (39). From 100 mg (0.32 mmol) of 3-(2-chlorophenyl)-5-((Z)-2-pyridylmethylidene)-2-thioxotetrahydro-4H-imidazol-4-one **10** as a result of reaction with 103 mg (0.72 mmol) of methyl iodide, in the presence of 21.5 mg (0.38 mmol) of solid KOH, **39** was obtained as a white-yellow powder. Yield: 52 mg (49%) after column chromatography. ¹H NMR (400 MHz, CDCl₃, δ , ppm): 8.82 (d, 1H, J=7.83 Hz, H α -Py), 8.69 (d, 1H, J=3.91 Hz, H β '-Py), 7.76 (t, 1H, J=7.43 Hz, Hy-Py), 7.56 (m, 1H, H α -Ph), 7.46 – 7.32 (m, 4H, H β -Py, Hy, H β , H β '-Ph), 7.20 (s, 1H, -CH=), 2.71 (s, 3H, -SCH₃). HRMS (*pos.*) calculated C₁₆H₁₃ClN₃O⁺: 330.0463 (**39** + H)⁺, found 330.0468 (**39** + H)⁺. HPLC purity 97.20%

5-(Z)-3-(4-methoxyphenyl)-2-(methylthio)-5-(pyridin-2-ylmethylidene)-1H-imidazol-4-one (40). From 100 mg (0.32 mmol) of 3-(4-methoxyphenyl)-5-((Z)-2-pyridylmethylidene)-2-thioxotetrahydro-4H-imidazol-4-one **11** as a result of reaction with 105 mg (0.74 mmol) of methyl iodide, in the presence of 21 mg (0.38 mmol) of solid KOH, **40** was obtained as a white-yellow powder. Yield: 63 mg (61%) after column chromatography. ¹H NMR (400 MHz, CDCl₃, δ , ppm): 8.87 (d, 1H, J=8.11 Hz, H α -Py), 8.76 (d, 1H, J=4.45 Hz, H β '-Py), 7.93 (t, 1H, J= 8.42 Hz, Hy-Py), 7.27 (m, 4H, H α , H α ', H β , H β '-Ph), 6.96 (m, 2H, H β -Py, -CH=), 2.72 (s, 3H, -SCH₃). ¹³C NMR (101 MHz, DMSO-d₆, δ , ppm) 169.0, 165.1, 160.3, 153.6, 150.4, 140.6, 137.0, 129.6, 126.8, 125.0, 124.8, 122.4, 115.2, 56.0, 13.38. HRMS (*pos.*) calculated C₁₇H₁₆N₃O₂S⁺: 326.0958 (**40** + H)⁺, found 326.0963 (**40** + H)⁺. HPLC purity 96.05%

5-(Z)-3-(4-ethoxyphenyl)-2-(methylthio)-5-(pyridin-2-ylmethylidene)-1H-imidazol-4-one (41). From 100 mg (0.31 mmol) of 3-(4-ethoxyphenyl)-5-((Z)-2-pyridylmethylidene)-2-thioxotetrahydro-4H-imidazol-4-one **12** as a result of reaction with 101 mg (0.71 mmol) of methyl iodide, in the presence of 21 mg (0.37 mmol) of solid KOH, **41** was obtained as a white-yellow powder. Yield: 48 mg (46%) after column chromatography. ¹H NMR (400 MHz, CDCl₃, δ , ppm): 8.86 (d, 1H, J=7.83 Hz, H α -Py), 8.77 (m, 1H, J= 4.45 Hz, H β -Py), 7.92 (t, 1H, J= 8.31 Hz, Hy-Py), 7.34 (m, 2H, H β , H β '-Ph), 7.24 – 7.19 (m, 4H, H β -Py, H α , H α '-Ph, -CH=), 4.06 (q, 2H, J=6.99 Hz, -CH₂-), 2.72 (s, 3H, -SCH₃), 1.42 (t, 3H, J=6.97 Hz, -CH₃). ¹³C NMR (101 MHz, DMSO-d₆, δ , ppm) 168.8,

165.2, 159.6, 153.6, 150.1, 140.5, 136.6, 129.3, 126.8, 124.8, 122.6, 115.5, 63.9, 14.9, 13.34. HRMS (*pos.*) calculated C₁₈H₁₈N₃O₂S⁺: 340.1115 (**41** + H)⁺, found 340.1116 (**41** + H)⁺. HPLC purity 99.30%

5-(Z)-3-(3,4-dimethoxyphenyl)-2-(methylthio)-5-(pyridin-2-ylmethylidene)-1H-imidazol-4-one (42). From 100 mg (0.29 mmol) of 3-(3,4-dimethoxyphenyl)-5-((Z)-2-pyridylmethylidene)-2-thioxotetrahydro-4H-imidazol-4-one **13** as a result of reaction with 95 mg (0.67 mmol) of methyl iodide, in the presence of 19.5 mg (0.35 mmol) of solid KOH, **42** was obtained as a white-yellow powder. Yield: 78 mg (76%) after column chromatography. ¹H NMR (400 MHz, CDCl₃, δ , ppm): 8.90 (m, 2H, J=7.83 Hz, H α , H β -Py), 8.08 (m, 1H, Hy-Py), 7.51 (m, 1H, H β -Py), 6.97 – 6.81 (m, 4H, H α , H α ', H β -Ph, -CH=), 3.93 (s, 3H, p-OCH₃), 3.90 (s, 3H, m-OCH₃), 2.78 (s, 3H, -SCH₃). HRMS (*pos.*) calculated C₁₈H₁₈N₃O₂S⁺: 356.1064 (**42** + H)⁺, found 356.1065 (**42** + H)⁺. HPLC purity 95.02%

5-(Z)-3-(4-tert-butylphenyl)-2-(methylthio)-5-(pyridin-2-ylmethylidene)-1H-imidazol-4-one (43). From 100 mg (0.30 mmol) of 3-(4-tert-butylphenyl)-5-((Z)-2-pyridylmethylidene)-2-thioxotetrahydro-4H-imidazol-4-one **14** as a result of reaction with 98 mg (0.69 mmol) of methyl iodide, in the presence of 20 mg (0.36 mmol) of solid KOH, **43** was obtained as a white-yellow powder. Yield: 96 mg (91%) after column chromatography. ¹H NMR (400 MHz, CDCl₃, δ , ppm): 8.84 (m, 1H, H α -Py), 8.69 (d, 1H, J=4.89 Hz, H β '-Py), 7.78 (m, 1H, H β -Py), 7.50 (m, 2H, H β , H β '-Ph), 7.22 – 7.21 (m, 4H, H β -Py, H α , H α '-Ph, -CH=), 2.72 (s, 3H, -SCH₃), 1.64 (s, 9H, -tBu). HRMS (*pos.*) calculated C₂₀H₂₂N₃O⁺: 352.1479 (**43** + H)⁺, found 352.1479 (**43** + H)⁺. HPLC purity 97.14%

5-(Z)-3-(2-tert-butylphenyl)-2-(methylthio)-5-(pyridin-2-ylmethylidene)-1H-imidazol-5(4H)-one (44). From 100 mg (0.30 mmol) of (Z)-3-(2-(tert-butyl)phenyl)-5-(pyridin-2-ylmethylene)-2-thioxoimidazolidin-4-one **15** as a result of reaction with 100 mg (0.70 mmol) of methyl iodide, in the presence of 20 mg (0.36 mmol) of solid KOH, **44** was obtained as a white-yellow powder. Yield: 42 mg (40%) after column chromatography. ¹H NMR (400 MHz, CDCl₃, δ , ppm): 8.85 (d, 1H, J=7.98 Hz, H α -Py), 8.73 (m, 1H, H β -Py), 7.80 (m, 1H, Hy-Py), 7.64 (m, 1H, H β '-Py), 7.7 (m, 1H, H β '-Ph), 7.32 (m, 1H, Hy-Ph), 7.25 (m, 1H, H α -Ph), 7.21 (s, 1H, -CH=), 7.04-7.00 (m, 1H, H β -Ph), 2.72 (s, 3H, -SCH₃), 1.37 (s, 9H, -tBu). ¹³C NMR (101 MHz, CDCl₃, δ , ppm) 169.1, 153.8, 149.9, 149.3, 140.3, 136.1, 131.5, 130.2, 129.7, 129.5, 127.2, 127.1, 127.0, 123.9, 123.1, 36.1, 31.8, 13.2. HRMS (*pos.*) calculated C₂₀H₂₂N₃O⁺: 352.1479 (**44** + H)⁺, found 352.1515 (**44** + H)⁺. HPLC purity 96.37%

5-(Z)-3-(2-methoxy-4-chloro-5-methylphenyl)-2-(methylthio)-5-(pyridin-2-ylmethylene)imidazolidin-4-one (45). From 100 mg (0.28 mmol) of (Z)-3-(2-methoxy-4-chloro-5-methylphenyl)-5-(pyridin-2-ylmethylene)-2-thioxoimidazolidin-4-one **18** as a result of reaction with 92 mg (0.65 mmol) of methyl iodide, in the presence of 19 mg (0.34 mmol) of solid KOH, **45** was obtained as a white-yellow powder. Yield: 49 mg (47%) after column chromatography. ¹H NMR (400 MHz, CDCl₃, δ , ppm): 8.84 (d, 1H, J=7.98 Hz, H α -Py), 8.69 (d, 1H, J=3.99 Hz, H β '-Py), 7.77 (td, 1H, J₁=7.76 Hz, J₂=1.55 Hz, Hy-Py), 7.22 (ddd, 1H, J₁=7.37 Hz, J₂=4.82 Hz, J₃=1.11 Hz, H β -Py), 7.18 (s, 1H, H β -Ph), 7.10 (s, 1H, H α '-Ph), 7.04 (s, 1H, -CH=), 3.79 (s, 3H, -OCH₃), 2.70 (s, 3H, S-CH₃), 2.33 (s, 3H, Ph-CH₃). ¹³C NMR (101 MHz, CDCl₃, δ , ppm) 168.9, 167.9, 154.0, 153.8, 149.9, 140.2, 136.6, 136.0, 131.6, 128.6, 126.9, 123.8, 123.0, 119.0, 113.4, 56.2, 19.1, 13.1. HRMS (*pos.*) calculated C₁₈H₁₇ClN₃O₂S⁺: 376.0696 (**45** + H isotopic)⁺, 374.0725 (**45** + H)⁺, found 376.0727 (**45** + H isotopic)⁺, 374.0760 (**45** + H)⁺. HPLC purity 95.66%

5-(Z)-3-(3-chloro-4-fluorophenyl)-2-(methylthio)-5-(pyridin-2-ylmethylene)-1H-imidazol-5(4H)-one (46). From 100 mg (0.30 mmol) of (Z)-3-(3-chloro-4-fluorophenyl)-5-(pyridin-2-ylmethylene)-2-thioxoimidazolidin-4-one **19** as a result of reaction with 98 mg (0.69 mmol) of methyl iodide, in the presence of 20 mg (0.36 mmol) of solid KOH, **46** was obtained as a white-yellow powder. Yield: 44 mg (42%) after column chromatography. ¹H NMR (400 MHz, CDCl₃, δ , ppm): 8.87 (d, 1H, J=7.83 Hz, H α -Py), 8.75 (d, 1H, J=4.89 Hz, H β '-Py), 7.93 (t, 1H, J=6.85 Hz, Hy-Py), 7.44 (dd, 2H, J₁=6.85 Hz, J₂=1.96 Hz, H α , H α '-Ph), 7.39 (m, 1H, H β -Ph), 7.31-7.23 (m, 2H, H β -Py, -CH=),

2.76 (s, 3H, -SCH₃). HRMS (*pos.*) calculated C₁₆H₁₂ClFN₃OS⁺: 348.0374 (**46** + H)⁺, 350.0344 (**46** + H isotopic)⁺, found 348.0369 (**46** + H)⁺, 350.0338 (**46** + H isotopic)⁺. HPLC purity 97.19%

5-(Z)-3-(2-methyl-3-chlorophenyl)-2-(methylthio)-5-(pyridin-2-ylmethylene)-1H-imidazol-5(4H)-one (47). From 100 mg (0.30 mmol) of (Z)-3-(2-methyl-3-chlorophenyl)-5-(pyridin-2-ylmethylene)-2-thioxoimidazolidin-4-one **20** as a result of reaction with 98 mg (0.69 mmol) of methyl iodide, in the presence of 20 mg (0.36 mmol) of solid KOH, **47** was obtained as a white-yellow powder. Yield: 62 mg (60%) after column chromatography. ¹H NMR (400 MHz, CDCl₃, δ, ppm): 8.95 (d, 1H, J=7.82 Hz, H_α-Py), 8.83 (d, 1H, J=4.89 Hz, H_β'-Py), 8.05 (t, 1H, J=7.82 Hz, H_γ-Py), 7.50 (m, 2H, -Ph), 7.25 (m, 1H, -Ph), 7.32 (m, 1H, H_β-Py), 7.13 (s, 1H, -CH=), 6.99 (m, 2H, H_β, H_β'-Ph), 2.77 (s, 3H, -SCH₃), 2.24 (s, 3H, -SCH₃). HRMS (*pos.*) calculated C₁₇H₁₅ClN₃OS⁺: 344.0624 (**47** + H)⁺, 346.0595 (**47** + H isotopic)⁺, found 344.0619 (**47** + H)⁺, 346.0589 (**47** + H isotopic)⁺. HPLC purity 96.07%

5-(Z)-3-(2,4,6-trimethylphenyl)-2-(methylthio)-5-(pyridin-2-ylmethylene)-1H-imidazol-5(4H)-one (48). From 100 mg (0.30 mmol) of (Z)-3-(2,4,6-trimethylphenyl)-5-(pyridin-2-ylmethylene)-2-thioxoimidazolidin-4-one **21** as a result of reaction with 101 mg (0.71 mmol) of methyl iodide, in the presence of 21 mg (0.37 mmol) of solid KOH, **48** was obtained as a white-yellow powder. Yield: 52 mg (50%) after column chromatography. ¹H NMR (400 MHz, CDCl₃, δ, ppm): 8.87 (d, 1H, J=7.83 Hz, H_α-Py), 8.76 (d, 1H, J=4.89 Hz, H_β'-Py), 7.90 (t, 1H, J=7.83 Hz, H_γ-Py), 7.34 (m, 1H, H_β-Py), 7.25 (s, 1H, -CH=), 6.99 (m, 2H, H_β, H_β'-Ph), 2.73 (s, 3H, -SCH₃), 2.33 (s, 3H, -SCH₃), 2.14 (s, 6H, 2x-CH₃). HRMS (*pos.*) calculated C₁₉H₂₀N₃OS⁺: 338.1327 (**48** + H)⁺, 339.1361 (**48** + H)⁺, found 338.1322 (**48** + H)⁺, 339.1354 (**48** + H)⁺. HPLC purity 96.80%

5-(Z)-3-(4-methylthiophenyl)-2-(methylthio)-5-(pyridin-2-ylmethylene)-1H-imidazol-5(4H)-one (49). From 100 mg (0.30 mmol) of (Z)-3-(4-methylthiophenyl)-5-(pyridin-2-ylmethylene)-2-thioxoimidazolidin-4-one **22** as a result of reaction with 101 mg (0.71 mmol) of methyl iodide, in the presence of 21 mg (0.37 mmol) of solid KOH, **49** was obtained as a white-yellow powder. Yield: 64 mg (61%) after column chromatography. ¹H NMR (400 MHz, CDCl₃, δ, ppm): 8.87 (d, 1H, J=7.83 Hz, H_α-Py), 8.74 (d, 1H, J=4.89 Hz, H_β'-Py), 7.89 (t, 1H, J=6.85 Hz, H_γ-Py), 7.33 (m, 3H, H_β, H_β'-Ph, H_β-Py), 7.24 (m, 3H, H_α, H_α'-Ph, -CH=), 2.74 (s, 3H, -SCH₃), 2.52 (s, 3H, Ph-SCH₃). HRMS (*pos.*) calculated C₁₇H₁₆N₃OS₂⁺: 342.0735 (**49** + H)⁺, 343.0768 (**49** + H isotopic)⁺, found 342.0730 (**49** + H)⁺, 343.0762 (**49** + H isotopic)⁺. HPLC purity 96.63%

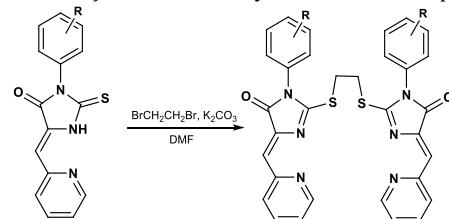
5-(Z)-3-(2,5-difluorophenyl)-2-(methylthio)-5-(pyridin-2-ylmethylene)-1H-imidazol-5(4H)-one (50). From 100 mg (0.30 mmol) of (Z)-3-(2,5-difluorophenyl)-5-(pyridin-2-ylmethylene)-2-thioxoimidazolidin-4-one **28** as a result of reaction with 104 mg (0.73 mmol) of methyl iodide, in the presence of 22 mg (0.38 mmol) of solid KOH, **50** was obtained as a white-yellow powder. Yield: 37 mg (35%) after column chromatography. ¹H NMR (400 MHz, CDCl₃, δ, ppm): 8.87 (d, 1H, J=7.83 Hz, H_α-Py), 8.74 (d, 1H, J=4.89 Hz, H_β'-Py), 7.84 (t, 1H, J=7.82 Hz, H_γ-Py), 7.31-7.17 (m, 3H, H_α, H_β', H_γ-Ph), 7.09 (m, 1H, H_β-Py), 5.30 (s, 1H, -CH=), 2.77 (s, 3H, -SCH₃). HRMS (*pos.*) calculated C₁₆H₁₂F₂N₃OS⁺: 332.0669 (**50** + H)⁺, 333.0703 (**50** + H isotopic)⁺, found 332.0665 (**50** + H)⁺, 333.0698 (**50** + H isotopic)⁺. HPLC purity 96.24%

5-(Z)-3-(3,5-difluorophenyl)-2-(methylthio)-5-(pyridin-2-ylmethylene)-1H-imidazol-5(4H)-one (51). From 100 mg (0.30 mmol) of (Z)-3-(3,5-difluorophenyl)-5-(pyridin-2-ylmethylene)-2-thioxoimidazolidin-4-one **29** as a result of reaction with 104 mg (0.73 mmol) of methyl iodide, in the presence of 22 mg (0.38 mmol) of solid KOH, **51** was obtained as a white-yellow powder. Yield: 41 mg (39%) after column chromatography. ¹H NMR (400 MHz, CDCl₃, δ, ppm): 8.94 (d, 1H, J=7.83 Hz, H_α-Py), 8.81 (d, 1H, J=4.89 Hz, H_β'-Py), 8.05 (d, 1H, J=6.85 Hz, H_γ-Py), 7.35 (m, 1H, H_β-Py), 6.97 (m, 3H, -Ph), 5.31 (m, 1H, -CH=), 2.81 (s, 3H, -SCH₃). HRMS (*pos.*) calculated C₁₆H₁₂F₂N₃OS⁺: 332.0669 (**51** + H)⁺, 333.0703 (**51** + H isotopic)⁺,

found 332.0671 (**51** + H)⁺, 333.0705 (**51** + H isotopic)⁺. HPLC purity 97.09%

Syntheses of compounds 52-73

General protocol. A mixture of 3-aryl-5-((Z)-2-pyridylmethylene)-2-thioxotetrahydro-4H-imidazol-4-one (2 eq.) and dry K₂CO₃ (3 eq.) was dissolved in dimethylformamide (2 ml per 200 mg of the mixture). The mixture was cooled to 0°C, 1,2-dibromoethane (1 eq.) was added dropwise. The mixture was stirred overnight at r.t., and then was quenched with 50 ml of iced water. The precipitate formed was filtered off, washed with 1 M KOH, water, diethyl ester and air-dried. The final products were purified by column chromatography (CH₂Cl₂: MeOH 20:1) and isolated as yellowish or white powders.



(**4Z**, **4'Z**)-2,2'-(ethane-1,2-diyl disulfanediyl)bis(4-(2-pyridylmethylidene)-1-(4-methoxyphenyl)-2,3-dihydro-4H-imidazol-5-one) (**52**). From 100 mg (0.32 mmol) of 3-(4-methoxyphenyl)-5-((Z)-2-pyridylmethylidene)-2-thioxotetrahydro-4H-imidazol-4-one **11** as by reaction with 30 mg (0.16 mmol) of 1,2-dibromoethane, in the presence of 66 mg (0.48 mmol) of solid K₂CO₃, **52** was obtained as a yellow powder. Yield: 71 mg (68%) after column chromatography. ¹H NMR (400 MHz, CDCl₃, δ, ppm): 8.69 (m, 4H, H_α, H_α'-Ph), 7.58 (m, 2H, H_β-Py), 7.25 - 7.17 (m, 8H, H_β, H_β'-Ph, H_β'-Py -CH=), 7.01 (m, 4H, H_γ, H_α-Py), 3.87 (s, 6H, p-OCH₃), 3.83 (s, 4H, -CH₂CH₂-). HRMS (*pos.*) calculated C₃₄H₂₉N₆O₄S₂⁺: 649.1687 (**52** + H)⁺, C₃₄H₂₉N₆O₄S₂²⁺: 325.0880 (**52** + 2H)²⁺, found 649.1688 (**52** + H)⁺, 325.0882 (**52** + 2H)²⁺. HPLC purity 95.26%

(**4Z**, **4'Z**)-2,2'-(ethane-1,2-diyl disulfanediyl)bis(4-(2-pyridylmethylidene)-1-(4-ethoxyphenyl)-2,3-dihydro-4H-imidazol-5-one) (**53**). From 100 mg (0.31 mmol) of 3-(4-ethoxyphenyl)-5-((Z)-2-pyridylmethylidene)-2-thioxotetrahydro-4H-imidazol-4-one **12** by reaction with 29 mg (0.15 mmol) of 1,2-dibromoethane, in the presence of 64 mg (0.46 mmol) of solid K₂CO₃, **53** was obtained as a light yellow powder. Yield: 75.5 mg (72%) after column chromatography. ¹H NMR (400 MHz, CDCl₃, δ, ppm): 8.70 (m, 2H, H_α-Py), 8.64 (d, 2H, J=3.91 Hz, H_β'-Py), 7.58 (m, 4H, J=7.83 Hz, H_α, H_α'-Ph), 7.25-7.17 (m, 4H, H_β, H_β'-Ph), 7.08 (m, 2H, H_β-Py), 6.99 (m, 4H, -CH=, H_γ-Py), 4.09 (m, 4H, -CH₂-), 3.82 (s, 4H, -CH₂CH₂-), 1.46 (m, 6H, J=6.85 Hz, CH₃). HRMS (*pos.*) calculated C₃₆H₃₃O₄N₆S₂⁺: 677.2000 (**53** + H)⁺, C₃₆H₃₃O₄N₆S₂²⁺: 339.1036 (**53** + 2H)²⁺, found 677.1998 (**53** + H)⁺, 339.1038 (**53** + 2H)²⁺. HPLC purity 99.87%

(**4Z**, **4'Z**)-2,2'-(ethane-1,2-diyl disulfanediyl)bis(4-(2-pyridylmethylidene)-1-(3,4-dimethoxyphenyl)-2,3-dihydro-4H-imidazol-5-one) (**54**). From 100 mg (0.29 mmol) of 3-(3,4-dimethoxyphenyl)-5-((Z)-2-pyridylmethylidene)-2-thioxotetrahydro-4H-imidazol-4-one **13** by reaction with 27 mg (0.14 mmol) of 1,2-dibromoethane, in the presence of 60 mg (0.43 mmol) of solid K₂CO₃ was obtained **54** as a white-yellow powder. Yield: 75 mg (73%) after column chromatography. ¹H NMR (400 MHz, CDCl₃, δ, ppm): 8.71 (m, 2H, H_α-Ph), 8.66 (m, 2H, H_β'-Py), 7.59 (m, 2H, H_α'-Ph), 7.20 (s, 4H, H_β-Py), 6.97-6.80 (m, 6H, H_α, H_β, H_γ-Py), 6.80 (s, 2H, -CH=), 3.95 (s, 6H, p-OCH₃), 3.90 (c, 6H, m-OCH₃), 3.84 (s, 4H, -CH₂CH₂-). ¹³C NMR (101 MHz, DMSO-d₆, δ, ppm) 149.3, 136.9, 128.6, 127.0, 123.4, 115.3, 106.9, 63.9, 15.3, 14.7. HRMS (*pos.*) calculated C₃₆H₃₃O₆N₆S₂⁺: 709.1903 (**54** + H)⁺, C₃₆H₃₃O₆N₆S₂²⁺: 355.0990 (**54** + 2H)²⁺, found 709.1896 (**54** + H)⁺, 355.0987 (**54** + 2H)²⁺. HPLC purity 96.78%

(**4Z**, **4'Z**)-2,2'-(ethane-1,2-diyl disulfanediyl)bis(4-(2-pyridylmethylidene)-1-(4-tertbutylphenyl)-2,3-dihydro-4H-imidazol-5-one) (**55**). From 100 mg (0.30 mmol) of 3-(4-tert-butylphenyl)-5-((Z)-2-pyridylmethylidene)-2-thioxotetrahydro-4H-imidazol-4-one **14** by reaction with 28 mg (0.15 mmol) of 1,2-dibromoethane, in the presence of 62 mg (0.45 mmol) of solid K₂CO₃, **55** was obtained as a white powder. Yield: 93 mg (89%) after column chromatography. ¹H NMR (400

MHz, CDCl₃, δ , ppm): 8.69 (m, 4H, H α , H α' -Ph), 7.61 (m, 2H, H α -Py), 7.53 (m, 6H, H β , H β' -Ph), 7.24 – 7.19 (m, 8H, H γ , H β , H β' -Py, -CH=), 3.86 (s, 4H, -CH₂CH₂-), 1.36 (s, 18H, p-tBu). HRMS (*pos.*) calculated C₄₀H₄₁N₆O₂S₂⁺ 701.2727 (**55** + H)⁺, C₄₀H₄₁N₆O₂S₂²⁺ 351.1400 (**55** + 2H)²⁺, found 701.2730 (**55** + H)⁺, 351.1401 (**55** + 2H)²⁺. HPLC purity 95.27%

(4Z, 4'Z)-2,2'-(ethane-1,2-diylbis(sulfanediy))bis(4-(2-pyridylmethylidene)-1-(2,4,6-trimethylphenyl)-2,3-dihydro-4H-imidazol-5-one) (56). From 100 mg (0.31 mmol) of 3-(2,4,6-trimethylphenyl)-5-((Z)-2-pyridylmethylidene)-2-thioxotetrahydro-4H-imidazol-4-one **21** by reaction with 30 mg (0.16 mmol) of 1,2-dibromoethane, in the presence of 66 mg (0.48 mmol) of solid K₂CO₃, **56** was obtained as a yellow powder. Yield: 72 mg (69%) after column chromatography. ¹H NMR (400 MHz, DMSO-d₆, δ , ppm): 8.15 (m, 4H, H β' , H α -Py), 7.07 (t, 2H, J=7.43 Hz, H γ -Py), 6.69 (m, 2H, H β -Py), 6.63 (s, 2H, -CH=), 6.43 (s, 4H, -Ph), 3.29 (m, 4H, -CH₂CH₂-), 1.78 (s, 6H, -CH₃), 1.54 (s, 12H, 2x-CH₃). HRMS (*pos.*) calculated C₃₈H₃₇N₆O₂S₂⁺ 673.2414 (**56** + H)⁺, found 673.2426 (**56** + H)⁺. HPLC purity 95.61%

(4Z,4'Z)-2,2'-(ethane-1,2-diylbis(sulfanediy))bis-4-(pyridin-2-ylmethylene)-1-(2-(t-butylphenyl)-2,3-dihydro-4H-imidazol-5-one) (57). From 100 mg (0.30 mmol) of (Z)-3-(2-(tert-butyl)phenyl)-5-(pyridin-2-ylmethylene)-2-thioxoimidazolidin-4-one **15**, by reaction with 28 mg (0.15 mmol) of 1,2-dibromoethane, in the presence of 62 mg (0.45 mmol) of solid K₂CO₃, **57** was obtained as a bright yellow powder. Yield: 49 mg (46%) after column chromatography. ¹H NMR (400 MHz, CDCl₃, δ , ppm): 8.68 (m, 4H, H α -Ph, H β' -Py), 7.62 (m, 4H, H β -Py, H γ -Py), 7.44 (m, 2H, H α -Py), 7.26 (m, 2H, H β -Ph), 7.23 (m, 2H, H β' -Ph), 7.16 (m, 2H, H γ -Ph), 6.96 (m, 2H, =CH-), 3.84 (s, 4H, -CH₂CH₂-). ¹³C NMR (101 MHz, CDCl₃, δ , ppm) 169.7, 167.4, 153.4, 150.0, 149.2, 139.9, 136.9, 131.5, 130.4, 129.5, 127.3, 127.8, 123.3, 77.00, 36.1, 31.8, 30.1. HRMS (*pos.*) calculated C₄₀H₄₁N₆O₂S₂⁺ 701.2727 (**57** + H)⁺, C₄₀H₄₁N₆O₂S₂²⁺ 351.1400 (**57** + 2H)²⁺, found 701.2783 (**57** + H)⁺, 351.1435 (**57** + 2H)²⁺. HPLC purity 96.19%

(4Z, 4'Z)-2,2'-(ethane-1,2-diylbis(sulfanediy))bis(4-(2-pyridylmethylidene)-1-(4-fluorophenyl)-2,3-dihydro-4H-imidazol-5-one) (58). From 100 mg (0.33 mmol) of 3-(4-fluorophenyl)-5-((Z)-2-pyridylmethylidene)-2-thioxotetrahydro-4H-imidazol-4-one **1**, by reaction with 31 mg (0.16 mmol) of 1,2-dibromoethane, in the presence of 68 mg (0.495 mmol) of solid K₂CO₃, **58** was obtained as a bright yellow powder. Yield: 79 mg (77%) after column chromatography. ¹H NMR (400 MHz, DMSO-d₆, δ , ppm): 8.66 (m, 4H, H α , H α' -Ph), 7.59 (m, 2H, H α -Py), 7.33 – 7.27 (m, 6H, H β , H β' -Ph, -CH=), 7.22 – 7.19 (m, 6H, H γ , H β , H β' -Py), 3.85 (s, 4H, -CH₂CH₂-). HRMS (*pos.*) calculated C₃₂H₂₃F₂N₆O₂S₂⁺ 625.1287 (**58** + H)⁺, C₁₇H₁₃FN₃OS⁺ 326.0763 (1/2 **58** + CH₂)⁺, found 625.1295 (**58** + H)⁺, 326.0762 (1/2 **58** + CH₂)⁺. HPLC purity 95.46%

(4Z, 4'Z)-2,2'-(ethane-1,2-diylbis(sulfanediy))bis(4-(2-pyridylmethylidene)-1-(3-fluorophenyl)-2,3-dihydro-4H-imidazol-5-one) (59). From 100 mg (0.33 mmol) of 3-(3-fluorophenyl)-5-((Z)-2-pyridylmethylidene)-2-thioxotetrahydro-4H-imidazol-4-one **2** by reaction with 31 mg (0.16 mmol) of 1,2-dibromoethane, in the presence of 68 mg (0.49 mmol) of solid K₂CO₃, **59** was obtained as a yellow powder. Yield: 43 mg (42%) after column chromatography. ¹H NMR (400 MHz, CDCl₃, δ , ppm): 8.68 (m, 4H, H α , H α' -Ph), 8.11 (m, 2H, H α -Py), 7.50 (m, 6H, H β , H γ -Ph, H γ -Py), 7.16 (m, 2H, -CH=), 7.11 (m, 4H, H β , H β' -Py), 4.03 (s, 4H, -CH₂CH₂-). HRMS (*pos.*) calculated C₃₂H₂₃F₂N₆O₂S₂⁺ 625.1287 (**59** + H)⁺, C₁₇H₁₃FN₃OS⁺ 326.0763 (1/2 **59** + CH₂)⁺, found 625.1294 (**59** + H)⁺, 326.0761 (1/2 **59** + CH₂)⁺. HPLC purity 98.59%

(4Z, 4'Z)-2,2'-(ethane-1,2-diylbis(sulfanediy))bis(4-(2-pyridylmethylidene)-1-(2-fluorophenyl)-2,3-dihydro-4H-imidazol-5-one) (60). From 100 mg (0.33 mmol) of 3-(2-fluorophenyl)-5-((Z)-2-pyridylmethylidene)-2-thioxotetrahydro-4H-imidazol-4-one **3** as a result of reaction with 31 mg (0.16 mmol) of 1,2-dibromoethane, in the presence of 68 mg (0.49 mmol) of solid K₂CO₃, **60** was obtained as a white-yellow powder. Yield: 74 mg (72%) after column chromatography. ¹H NMR (400 MHz, CDCl₃, δ , ppm): 8.74 (m, 2H, H α -Ph), 8.65 (m, 2H, H γ -Ph), 7.73 (m, 2H, H α -Py), 7.47 (m, 4H,

H β , H β' -Ph), 7.33 (m, 2H, H γ -Py), 7.23 (m, 4H, H β , H β' -Py), 7.17 (s, 2H, -CH=), 3.93 (s, 4H, -CH₂CH₂-). HRMS (*pos.*) calculated C₃₂H₂₃F₂N₆O₂S₂⁺ 625.1287 (**60** + H)⁺, C₁₇H₁₃FN₃OS⁺ 326.0763 (1/2 **60** + CH₂)⁺, found 625.1295 (**60** + H)⁺, 326.0761 (1/2 **60** + CH₂)⁺. HPLC purity 96.10%

(4Z, 4'Z)-2,2'-(ethane-1,2-diylbis(sulfanediy))bis(4-(2-pyridylmethylidene)-1-(3-bromophenyl)-2,3-dihydro-4H-imidazol-5-one) (61). From 100 mg (0.28 mmol) of 3-(3-bromophenyl)-5-((Z)-2-pyridylmethylidene)-2-thioxotetrahydro-4H-imidazol-4-one **5** by reaction with 26 mg (0.14 mmol) of 1,2-dibromoethane, in the presence of 58 mg (0.42 mmol) of solid K₂CO₃, **61** was obtained as a white-yellow powder. Yield: 68 mg (65%) after column chromatography. ¹H NMR (400 MHz, DMSO-d₆, δ , ppm): 8.68 (m, 2H, H α -Ph), 8.58 (m, 2H, H α' -Ph), 7.73 (m, 4H, H β , H γ -Ph), 7.59 (m, 2H, H γ -Py), 7.45 (m, 2H, H α -Py), 7.44 (m, 4H, H β , H β' -Py), 6.74 (s, 2H, -CH=), 3.82 (s, 4H, -CH₂CH₂-). HRMS (*pos.*) calculated C₃₂H₂₃Br₂N₆O₂S₂⁺ 746.9665 (**61** + H)⁺, C₃₂H₂₃Br₂N₆O₂S₂²⁺ 373.9869 (**61** + 2H)²⁺, C₁₇H₁₃BrN₃OS⁺ 385.9963 (1/2 **61** + CH₂)⁺, found 746.9673 (**61** + H)⁺, 373.9879 (**61** + 2H)²⁺, 385.9961 (1/2 **61** + CH₂)⁺. HPLC purity 98.01%

(4Z, 4'Z)-2,2'-(ethane-1,2-diylbis(sulfanediy))bis(4-(2-pyridylmethylidene)-1-(2-bromophenyl)-2,3-dihydro-4H-imidazol-5-one) (62). From 100 mg (0.28 mmol) of 3-(2-bromophenyl)-5-((Z)-2-pyridylmethylidene)-2-thioxotetrahydro-4H-imidazol-4-one **6** as a result of reaction with 26 mg (0.14 mmol) of 1,2-dibromoethane, in the presence of 58 mg (0.42 mmol) of solid K₂CO₃, **62** was obtained as a white-yellow powder. Yield: 74 mg (71%) after column chromatography. ¹H NMR (400 MHz, CDCl₃, δ , ppm): 8.69 (d, 2H, J=8.22 Hz, H α -Ph), 8.61 (m, 2H, H γ -Py), 7.74 (m, 2H, H β -Ph), 7.56 (m, 2H, H α -Py), 7.40 (m, 6H, H β , H β' -Py, H γ -Ph), 7.16 (m, 4H, H β' -Ph, -CH=), 3.83 (s, 4H, -CH₂CH₂-). HRMS (*pos.*) calculated C₃₂H₂₃Br₂N₆O₂S₂⁺ 746.9665 (**62** + H)⁺, C₃₂H₂₃Br₂N₆O₂S₂²⁺ 373.9869 (**62** + 2H)²⁺, C₁₇H₁₃BrN₃OS⁺ 385.9963 (1/2 **62** + CH₂)⁺, found 746.9677 (**62** + H)⁺, 373.9873 (**62** + 2H)²⁺, 385.9961 (1/2 **62** + CH₂)⁺. HPLC purity 96.28%

(4Z, 4'Z)-2,2'-(ethane-1,2-diylbis(sulfanediy))bis(4-(2-pyridylmethylidene)-1-(2-chlorophenyl)-2,3-dihydro-4H-imidazol-5-one) (63). From 100 mg (0.32 mmol) of 3-(2-chlorophenyl)-5-((Z)-2-pyridylmethylidene)-2-thioxotetrahydro-4H-imidazol-4-one **10** by reaction with 30 mg (0.16 mmol) of 1,2-dibromoethane in the presence of 66 mg (0.48 mmol) of solid K₂CO₃, **63** was obtained as a yellow powder. Yield: 67 mg (64%) after column chromatography. ¹H NMR (400 MHz, DMSO-d₆, δ , ppm): 8.73 (d, 2H, J=7.83 Hz, H α -Ph), 7.61 (m, 4H, H β , H β' -Py), 7.56 (m, 2H, H γ -Py), 7.39 (m, 2H, H α -Py), 7.41-7.26 (m, 6H, H γ , H β , H β' -Ph), 6.76 (m, 2H, -CH=), 3.88 (s, 4H, -CH₂CH₂-). HRMS (*pos.*) calculated C₃₂H₂₃Cl₂N₆O₂S₂⁺ 657.0696 (**63** + H)⁺, C₃₂H₂₄Cl₂N₆O₂S₂²⁺ 329.0384 (**63** + 2H)²⁺, found 657.0697 (**63** + H)⁺, 329.0382 (**63** + 2H)²⁺. HPLC purity 96.76%

(4Z,4'Z)-2,2'-(ethane-1,2-diylbis(sulfanediy))bis-4-(pyridin-2-ylmethylene)-1-(2-methoxy-4-chloro-5-methylphenyl)-2,3-dihydro-4H-imidazol-5-one) (64). From 100 mg (0.28 mmol) of (Z)-3-(2-methoxy-4-chloro-5-methylphenyl)-5-(pyridin-2-ylmethylene)-2-thioxoimidazolidin-4-one **18**, by reaction with 26 mg (0.14 mmol) of 1,2-dibromoethane, in the presence of 58 mg (0.42 mmol) of solid K₂CO₃, **64** was obtained as a bright yellow powder. Yield: 79 mg (75%) after column chromatography. ¹H NMR (400 MHz, CDCl₃, δ , ppm): 8.67 (s, 2H, H α -Ph), 8.66 (d, 2H, J=7.83 Hz, H β' -Py), 7.59 (m, 2H, H β -Py), 7.24 (m, H, H γ -Py), 7.11 (s, 2H, H β -Ph), 7.07 (d, 2H, J=7.83 Hz, H α -Py), 7.02 (s, 2H, -CH=) 3.81 (s, 4H, -CH₂CH₂-), 2.32 (s, 6H, -OCH₃), 2.15 (s, 6H, -CH₃). ¹³C NMR (101 MHz, CDCl₃, δ , ppm) 168.3, 167.0, 153.9, 152.7, 149.2, 144.9, 140.2, 136.9, 131.6, 128.8, 127.0, 123.4, 123.0, 118.7, 113.4, 56.2, 30.1, 19.1. HRMS (*pos.*) calculated C₃₆H₃₂Cl₂N₆O₄S₂⁺ 747.1191 (**64** + H isotopic)⁺, 745.1220 (**64** + H)⁺, 374.0632 (**64** + 2H isotopic)²⁺, 373.0347 (**64** + 2H)²⁺, found 747.1253 (**64** + H isotopic)⁺, 745.1287 (**64** + H)⁺, 374.0664 (**64** + 2H isotopic)²⁺, 373.00682 (**64** + 2H)²⁺. HPLC purity 95.16%

(4Z,4'Z)-2,2'-(ethane-1,2-diylbis(sulfanediy))bis(1-(2-bromo-4-fluorophenyl)-4-(pyridin-2-ylmethylene)-1H-imidazol-5(4H)-one) (65). From 100 mg (0.27 mmol) of (Z)-3-

(2-bromo-4-fluorophenyl)-5-(pyridin-2-ylmethylene)-2-thioxoimidazolidin-4-one **7**, by reaction with 25 mg (0.13 mmol) of 1,2-dibromoethane, in the presence of 56 mg (0.40 mmol) of solid K_2CO_3 , **65** was obtained as a bright yellow powder. Yield: 79 mg (75%) after column chromatography. 1H NMR (400 MHz, $CDCl_3$, δ , ppm): 8.74 (m, 2H, H_{α} -Ph), 8.65 (d, 2H, $J=7.83$ Hz, H_{β} -Py), 7.73 (m, 2H, H_{β} -Py), 7.49-7.43 (m, 2H, H_{β} -Ph), 7.32 (m, 4H, H_{γ} -Py, H_{β} -Ph), 7.23 (m, 2H, H_{α} -Py), 7.17 (s, 2H, $-CH=$), 3.90 (m, 4H, $-CH_2CH_2-$). ^{13}C NMR (101 MHz, $DMSO-d_6$, δ , ppm) 167.6, 166.4, 159.0, 156.4, 149.4, 140.0, 137.7, 132.6, 129.3, 127.2, 124.5, 120.8, 119.3, 40.0, 30.3. HRMS (*pos.*) calculated $C_{32}H_{22}Br_2F_2N_6O_2S_2^{2+}$: 391.9775 (**65** + 2H isotopic) $^{2+}$, 390.9785 (**65** + 2H) $^{2+}$, found 391.9798 (**65** + 2H isotopic) $^{2+}$, 390.9807 (**65** + 2H) $^{2+}$. HPLC purity 96.27%

(4Z,4'Z)-2,2'-(ethane-1,2-diylbis(sulfanediyl))bis(1-(2,5-difluorophenyl)-4-(pyridin-2-ylmethylene)-1H-imidazol-5(4H)-one) (**66**). From 100 mg (0.32 mmol) of (Z)-3-(2,5-difluorophenyl)-5-(pyridin-2-ylmethylene)-2-thioxoimidazolidin-4-one **28**, by reaction with 30 mg (0.16 mmol) of 1,2-dibromoethane, in the presence of 66 mg (0.48 mmol) of solid K_2CO_3 , **66** was obtained as a bright yellow powder. Yield: 46 mg (44%) after column chromatography. 1H NMR (400 MHz, $DMSO-d_6$, δ , ppm): 8.69 (d, 2H, $J=7.82$ Hz, H_{β} -Py), 8.59 (m, 2H, H_{α} -Py), 7.68-7.54 (m, 8H, H_{β} -Py, H_{γ} -Py, H_{α} -Ph, H_{γ} -Ph), 7.31 (m, 2H, H_{β} -Ph), 6.79 (s, 2H, $-CH=$), 3.91 (s, 4H, $-CH_2CH_2-$). HRMS (*pos.*) calculated $C_{32}H_{21}F_4N_6O_2S_2^{+}$: 661.1104 (**66** + H) $^{+}$, 662.1137 (**66** + H isotopic) $^{+}$, found 661.1113 (**66** + H) $^{+}$, 662.1129 (**66** + H isotopic) $^{+}$. HPLC purity 95.96%

(4Z,4'Z)-2,2'-(ethane-1,2-diylbis(sulfanediyl))bis(1-(3,5-difluorophenyl)-4-(pyridin-2-ylmethylene)-1H-imidazol-5(4H)-one) (**67**). From 100 mg (0.32 mmol) of (Z)-3-(3,5-difluorophenyl)-5-(pyridin-2-ylmethylene)-2-thioxoimidazolidin-4-one **7**, by reaction with 30 mg (0.6 mmol) of 1,2-dibromoethane, in the presence of 66 mg (0.48 mmol) of solid K_2CO_3 , **67** was obtained as a bright yellow powder. Yield: 65 mg (62%) after column chromatography. 1H NMR (400 MHz, $DMSO-d_6$, δ , ppm): 8.71 (d, 2H, $J=7.83$ Hz, H_{α} -Py), 8.56 (d, 2H, $J=3.91$ Hz, H_{β} -Py), 7.65 (t, 2H, $J=6.85$ Hz, H_{γ} -Py), 7.50 (t, 2H, $J=9.78$ Hz, H_{γ} -Ph), 7.37 (d, 4H, $J=7.83$ Hz, H_{α} -Ph), 7.28 (m, 2H, H_{β} -Py), 6.77 (s, 2H, $-CH=$), 3.89 (s, 4H, $-CH_2CH_2-$). HRMS (*pos.*) calculated $C_{32}H_{21}F_4N_6O_2S_2^{+}$: 661.1104 (**67** + H) $^{+}$, 662.1137 (**67** + H isotopic) $^{+}$, found 661.1096 (**67** + H) $^{+}$, 662.1122 (**67** + H isotopic) $^{+}$. HPLC purity 96.66%

(4Z,4'Z)-2,2'-(ethane-1,2-diylbis(sulfanediyl))bis(1-(2-methyl-3-chlorophenyl)-4-(pyridin-2-ylmethylene)-1H-imidazol-5(4H)-one) (**68**). From 100 mg (0.30 mmol) of (Z)-3-(2-methyl-3-chlorophenyl)-5-(pyridin-2-ylmethylene)-2-thioxoimidazolidin-4-one **20**, by reaction with 28 mg (0.15 mmol) of 1,2-dibromoethane, in the presence of 63 mg (0.45 mmol) of solid K_2CO_3 , **68** was obtained as a bright yellow powder. Yield: 72 mg (70%) after column chromatography. 1H NMR (400 MHz, $DMSO-d_6$, δ , ppm): 8.71 (d, 2H, $J=7.82$ Hz, H_{α} -Py), 8.63 (m, 2H, H_{β} -Py), 7.67-7.57 (m, 4H, H_{β} -Py, H_{β} -Ph), 7.42-7.31 (m, 6H, H_{β} -Ph, H_{γ} -Py, $-CH=$), 6.82 (m, 2H, H_{α} -Ph), 3.88 (m, 4H, $-CH_2CH_2-$). HRMS (*pos.*) calculated $C_{34}H_{27}Cl_2N_6O_2S_2^{+}$: 685.1014 (**68** + H) $^{+}$, 687.0984 (**68** + H isotopic) $^{+}$, found 685.1055 (**68** + H) $^{+}$, 687.1027 (**68** + H isotopic) $^{+}$. HPLC purity 95.83%

(4Z,4'Z)-2,2'-(ethane-1,2-diylbis(sulfanediyl))bis(1-(4-methylthiophenyl)-4-(pyridin-2-ylmethylene)-1H-imidazol-5(4H)-one) (**69**). From 100 mg (0.32 mmol) of (Z)-3-(4-methylthiophenyl)-5-(pyridin-2-ylmethylene)-2-thioxoimidazolidin-4-one **22**, by reaction with 30 mg (0.16 mmol) of 1,2-dibromoethane, in the presence of 64 mg (0.47 mmol) of solid K_2CO_3 , **69** was obtained as a bright yellow powder. Yield: 65 mg (63%) after column chromatography. 1H NMR (400 MHz, $DMSO-d_6$, δ , ppm): 8.72 (d, 2H, $J=7.31$ Hz, H_{α} -Py), 8.60 (m, 2H, H_{β} -Py), 7.67 (t, 2H, $J=7.31$ Hz, H_{γ} -Py), 7.41-7.29 (m, 10H, H_{α} -Ph, H_{α} -Ph, H_{β} -Ph, H_{β} -Ph, H_{β} -Py), 6.77 (s, 2H, $-CH=$), 3.87 (s, 4H, $-CH_2CH_2-$). HRMS (*pos.*) calculated $C_{34}H_{29}N_6O_2S_4^{+}$: 681.1230 (**69** + H) $^{+}$, 682.1263 (**69** + H isotopic) $^{+}$, found 681.1231 (**69** + H) $^{+}$, 682.1271 (**69** + H isotopic) $^{+}$. HPLC purity 97.44%

(4Z, 4'Z)-2,2'-(ethane-1,2-diylbis(sulfanediyl))bis(4-(2-pyridylmethylidene)-1-(3-chlorophenyl)-2,3-dihydro-4H-imidazol-5-one) (**70**). From 100 mg (0.32 mmol) of 3-(3-chlorophenyl)-5-((Z)-2-pyridylmethylidene)-2-thioxotetrahydro-4H-imidazol-4-one **9** by reaction with 30 mg (0.16 mmol) of 1,2-dibromoethane, in the presence of 66 mg (0.48 mmol) of solid K_2CO_3 , **70** was obtained as a white powder. Yield: 73 mg (69%) after column chromatography. 1H NMR (400 MHz, $DMSO-d_6$, δ , ppm): 8.72 (d, 2H, $J=7.83$ Hz, H_{α} -Py), 8.58 (d, 2H, $J=4.89$ Hz, H_{β} -Py), 7.61 (m, 8H, H_{α} -Ph, H_{α} -Ph, H_{β} -Ph, H_{γ} -Py), 7.46 (d, 2H, $J=6.85$ Hz, H_{γ} -Ph), 7.29 (m, 2H, H_{β} -Py), 6.76 (s, 2H, $-CH=$), 3.89 (s, 4H, $-CH_2CH_2-$). HRMS (*pos.*) calculated $C_{32}H_{23}Cl_2N_6O_2S_2^{+}$: 657.0696 (**70** + H) $^{+}$, found 657.0696 (**70** + H) $^{+}$. HPLC purity 95.81%

(4Z, 4'Z)-2,2'-(ethane-1,2-diylbis(sulfanediyl))bis(4-(2-pyridylmethylidene)-1-(4-bromophenyl)-2,3-dihydro-4H-imidazol-5-one) (**71**). From 100 mg (0.28 mmol) of 3-(4-bromophenyl)-5-((Z)-2-pyridylmethylidene)-2-thioxotetrahydro-4H-imidazol-4-one **4** by reaction with 26 mg (0.14 mmol) of 1,2-dibromoethane, in the presence of 58 mg (0.42 mmol) of solid K_2CO_3 , **71** was obtained as a bright yellow powder. Yield: 73 mg (70%) after column chromatography. 1H NMR (400 MHz, $DMSO-d_6$, δ , ppm): 8.68 (m, 2H, H_{α} -Ph), 8.56 (m, 2H, H_{α} -Ph), 7.76-7.73 (m, 4H, H_{β} , H_{β} -Ph), 7.61 (m, 2H, H_{α} -Py), 7.41-7.39 (m, 4H, H_{β} , H_{β} -Py), 7.27 (m, 2H, H_{γ} -Py), 6.75 (s, 2H, $-CH=$), 3.85 (m, 4H, $-CH_2CH_2-$). ^{13}C NMR (101 MHz, $DMSO-d_6$, δ , ppm) 161.7, 158.6, 148.0, 141.3, 136.4, 123.6, 118.9, 96.9, 39.4. HRMS (*pos.*) calculated $C_{32}H_{23}Br_2N_6O_2S_2^{+}$: 746.9665 (**71** + H) $^{+}$, $C_{32}H_{23}Br_2N_6O_2S_2^{2+}$: 373.9869 (**71** + 2H) $^{2+}$, $C_{17}H_{13}BrN_3OS^{+}$: 385.9963 ($1/2$ **71** + CH_2) $^{+}$, found 746.9674 (**71** + H) $^{+}$, 373.9879 (**71** + 2H) $^{2+}$, 385.9962 ($1/2$ **71** + CH_2) $^{+}$. HPLC purity 98.51%

(4Z, 4'Z)-2,2'-(ethane-1,2-diylbis(sulfanediyl))bis(4-(2-pyridylmethylidene)-1-(4-chlorophenyl)-2,3-dihydro-4H-imidazol-5-one) (**72**). From 100 mg (0.32 mmol) of 3-(4-chlorophenyl)-5-((Z)-2-pyridylmethylidene)-2-thioxotetrahydro-4H-imidazol-4-one **8** by reaction with 30 mg (0.16 mmol) of 1,2-dibromoethane, in the presence of 66 mg (0.48 mmol) of solid K_2CO_3 , **72** was obtained as a white powder. Yield: 77 mg (73%) after column chromatography. 1H NMR (400 MHz, $DMSO-d_6$, δ , ppm): 8.66 (m, 4H, H_{α} , H_{α} -Ph), 7.59 (m, 2H, H_{α} -Py), 7.33-7.31 (m, 4H, H_{β} , H_{β} -Ph), 7.22 (m, 2H, $-CH=$), 7.19 (m, 6H, H_{γ} , H_{β} , H_{β} -Py), 3.85 (s, 4H, $-CH_2CH_2-$). ^{13}C NMR (101 MHz, $DMSO-d_6$, δ , ppm) 173.0, 164.9, 150.1, 139.4, 136.4, 129.9, 128.8, 123.5, 111.3, 40.9. HRMS (*pos.*) calculated $C_{32}H_{23}Cl_2N_6O_2S_2^{+}$: 657.0696 (**72** + H) $^{+}$, $C_{32}H_{23}Cl_2N_6O_2S_2^{2+}$: 329.0384 (**72** + 2H) $^{2+}$, found 657.0670 (**72** + H) $^{+}$, 329.0381 (**72** + 2H) $^{2+}$. HPLC purity 98.32%

(4Z, 4'Z)-2,2'-(ethane-1,2-diylbis(sulfanediyl))bis(4-(2-pyridylmethylidene)-1-(3-chloro-4-fluorophenyl)-2,3-dihydro-4H-imidazol-5-one) (**73**). From 100 mg (0.32 mmol) of 3-(3-chloro-4-fluorophenyl)-5-((Z)-2-pyridylmethylidene)-2-thioxotetrahydro-4H-imidazol-4-one **19** by reaction with 30 mg (0.16 mmol) of 1,2-dibromoethane, in the presence of 66 mg (0.48 mmol) of solid K_2CO_3 , **73** was obtained as a white powder. Yield: 77 mg (73%) after column chromatography. 1H NMR (400 MHz, $DMSO-d_6$, δ , ppm): 8.71 (d, 2H, $J=7.83$ Hz, H_{α} -Ph), 8.57 (m, 2H, H_{α} -Ph), 7.86 (m, 2H, H_{γ} -Py), 7.65 (m, 4H, H_{β} , H_{β} -Py), 7.57 (m, 2H, H_{α} -Py), 7.29 (m, 2H, H_{β} -Ph), 6.79 (m, 2H, $-CH=$), 3.89 (s, 4H, $-CH_2CH_2-$). HRMS (*pos.*) calculated $C_{32}H_{23}Cl_2N_6O_2S_2^{+}$: 693.0513 (**73** + H) $^{+}$, 695.0483 (**73** + H isotopic) $^{+}$, found 693.0536 (**73** + H) $^{+}$, 695.0484 (**73** + H isotopic) $^{+}$. HPLC purity 96.97%

Synthesis of coordination compounds 1k-73k

General Protocol. 0.1 ml of butanol-1 was carefully added to a solution of 15 mg of the corresponding ligand in 1.5 ml of dichloromethane* to achieve the separated layers. A solution of copper (II) chloride dihydrate $CuCl_2 \cdot 2H_2O$ in 1.5 ml of butanol-1 is then carefully added to form a two-phase system. The tightly closed reaction mixture was left for 2 - 7 days in the dark, until crystallization occurred. If a clear solution without signs of crystallization or precipitation was formed, crystallization was the activated by ether diffusion. An open vial with a solution of the coordination compound was placed in a larger vial

containing a small amount of diethyl ether, tightly closed and left to stand for 24 hours in the dark. The precipitate was separated by decanting, washed with a small amount of dichloromethane and then with diethyl ether until the washing solvent became colorless. The final products were obtained as dark crystalline powders after drying in air.

* In the case of compounds **66** and **67**, dissolution in dichloromethane was impossible due to the low solubility and the delamination was replaced by boiling with copper chloride in butanol-1 (see procedures **66k** and **67k**).

Preparation of the coordination compound of 3-(4-fluorophenyl)-5-((Z)-2-pyridylmethylidene)-2-thioxotetrahydro-4H-imidazol-4-one 1 with copper (II) chloride dihydrate (1k). **1k** was obtained as a black crystalline precipitate from 15 mg (50 μ mol) 3-(4-fluorophenyl)-5-((Z)-2-pyridylmethylidene)-2-thioxotetrahydro-4H-imidazol-4-one **1** and 8.5 mg (50 μ mol) of copper (II) chloride dihydrate. Yield: 6 mg (32%). MALDI: m/z = 659 ($(1 - H)_2Cu^+$ 32%, 722 ($(1 - H)_2Cu_2^+$ 100%. HRMS (*pos.*) calculated 721.9493 ($C_{30}H_{18}Cu_2F_2N_6O_2S_2$)⁺, found 721.9498 ($C_{30}H_{18}Cu_2F_2N_6O_2S_2$)⁺, UV-vis (λ , nm/ ϵ , l mol⁻¹ cm⁻¹): 432/23834. Elemental analysis: calculated (%) for $C_{30}H_{18}Cu_2ClF_2N_6O_2S_2$: C 47.46, H 2.39, N 11.07, found C 47.42, H 2.36, N 10.78.

Preparation of the coordination compound of 3-(3-fluorophenyl)-5-((Z)-2-pyridylmethylidene)-2-thioxotetrahydro-4H-imidazol-4-one 2 with copper (II) chloride dihydrate (2k). **2k** was obtained as a black crystalline precipitate from 15 mg (50 μ mol) of 3-(3-fluorophenyl)-5-((Z)-2-pyridylmethylidene)-2-thioxotetrahydro-4H-imidazol-4-one **2** and 8.5 mg (50 μ mol) of copper (II) chloride dihydrate. Yield: 5.8 mg (31%). MALDI: m/z = 659 ($(2 - H)_2Cu^+$ 38%, 720 ($(2 - H)_2Cu_2^+$ 100%. HRMS (*pos.*) calculated 721.9493 ($C_{30}H_{18}Cu_2F_2N_6O_2S_2$)⁺, found 721.9512 ($C_{30}H_{18}Cu_2F_2N_6O_2S_2$)⁺, UV-vis (λ , nm/ ϵ , l mol⁻¹ cm⁻¹): 432/22967. Elemental analysis: calculated (%) for $C_{30}H_{20}Cu_2ClF_2N_6O_2S_2 \cdot (H_2O)$: C 46.36, H 2.59, N 10.81, found C 47.74, H 2.36, N 10.85.

Preparation of the coordination compound of 3-(2-fluorophenyl)-5-((Z)-2-pyridylmethylidene)-2-thioxotetrahydro-4H-imidazol-4-one 3 with copper (II) chloride dihydrate (3k). **3k** was obtained as a black crystalline precipitate from 15 mg (50 μ mol) of 3-(2-fluorophenyl)-5-((Z)-2-pyridylmethylidene)-2-thioxotetrahydro-4H-imidazol-4-one **3** and 8.5 mg (50 μ mol) of copper (II) chloride dihydrate. Yield: 6.1 mg (33%). MALDI: m/z = 659 ($(3 - H)_2Cu^+$ 28%, 724 ($(3 - H)_2Cu_2^+$ 100%. HRMS (*pos.*) calculated 721.9493 ($C_{30}H_{18}Cu_2F_2N_6O_2S_2$), found 721.9495 ($C_{30}H_{18}Cu_2F_2N_6O_2S_2$)⁺, UV-vis (λ , nm/ ϵ , l mol⁻¹ cm⁻¹): 432/38497. Elemental analysis: calculated (%) for $C_{30}H_{18}Cu_2ClF_2N_6O_2S_2$: C 47.46, H 2.39, N 11.07, found C 47.85, H 2.41, N 11.00.

Preparation of the coordination compound of 3-(4-bromophenyl)-5-((Z)-2-pyridylmethylidene)-2-thioxotetrahydro-4H-imidazol-4-one 4 with copper (II) chloride dihydrate (4k). **4k** was obtained as a black crystalline precipitate from 15 mg (42 μ mol) of 3-(4-bromophenyl)-5-((Z)-2-pyridylmethylidene)-2-thioxotetrahydro-4H-imidazol-4-one **4** and 7 mg (42 μ mol) of copper (II) chloride dihydrate. Yield: 6.1 mg (33%). MALDI: m/z = 781 ($(4 - H)_2Cu^+$ 32%, 844 ($(4 - H)_2Cu_2^+$ 100%. HRMS (*pos.*) calculated 843.7866 ($C_{30}H_{18}Cu_2Br_2N_6O_2S_2$)⁺, found 843.6904 ($C_{30}H_{18}Cu_2Br_2N_6O_2S_2$)⁺, UV-vis (λ , nm/ ϵ , l mol⁻¹ cm⁻¹): 432/6533. Elemental analysis: calculated (%) for $C_{30}H_{18}Cu_2ClBr_2N_6O_2S_2$: C 40.90, H 2.06, N 9.54, found C 40.61, H 2.02, N 9.82.

Preparation of the coordination compound of 3-(3-bromophenyl)-5-((Z)-2-pyridylmethylidene)-2-thioxotetrahydro-4H-imidazol-4-one 5 with copper (II) chloride dihydrate (5k). **5k** was obtained as a black crystalline precipitate from 15 mg (42 μ mol) of 3-(3-bromophenyl)-5-((Z)-2-pyridylmethylidene)-2-thioxotetrahydro-4H-imidazol-4-one **5** and 7 mg (42 μ mol) of copper (II) chloride dihydrate. Yield: 5.9 mg (32%). MALDI: m/z = 781 ($(5 - H)_2Cu^+$ 18%, 846 ($(5 - H)_2Cu_2^+$ 100%. HRMS (*pos.*) calculated 843.7866 ($C_{30}H_{18}Cu_2Br_2N_6O_2S_2$)⁺, found 843.7813 ($C_{30}H_{18}Cu_2Br_2N_6O_2S_2$)⁺, UV-vis (λ , nm/ ϵ , l mol⁻¹ cm⁻¹): 432/7183. Elemental analysis: calculated (%) for

$C_{30}H_{18}Cu_2ClBr_2N_6O_2S_2$: C 40.90, H 2.06, N 9.54, found C 41.13, H 1.98, N 8.71.

Preparation of the coordination compound of 3-(2-bromophenyl)-5-((Z)-2-pyridylmethylidene)-2-thioxotetrahydro-4H-imidazol-4-one 6 with copper (II) chloride dihydrate (6k). **6k** was obtained as a black crystalline precipitate from 15 mg (42 μ mol) of 3-(2-bromophenyl)-5-((Z)-2-pyridylmethylidene)-2-thioxotetrahydro-4H-imidazol-4-one **6** and 7 mg (42 μ mol) copper (II) chloride dihydrate. Yield: 6.0 mg (32%). MALDI: m/z = 781 ($(6 - H)_2Cu^+$ 32%, 844 ($(6 - H)_2Cu_2^+$ 100%. HRMS (*pos.*) calculated 843.7866 ($C_{30}H_{18}Cu_2Br_2N_6O_2S_2$)⁺, found 843.8512 ($C_{30}H_{18}Cu_2Br_2N_6O_2S_2$)⁺, UV-vis (λ , nm/ ϵ , l mol⁻¹ cm⁻¹): 432/12400. Elemental analysis: calculated (%) for $C_{30}H_{18}Cu_2ClBr_2N_6O_2S_2$: C 40.90, H 2.06, N 9.54, found C 41.02, H 1.98, N 9.91.

Preparation of the coordination compound of 3-(2-bromo-4-fluorophenyl)-5-((Z)-2-pyridylmethylidene)-2-thioxotetrahydro-4H-imidazol-4-one 7 with copper (II) chloride dihydrate (7k). **7k** was obtained as a black crystalline precipitate from 15 mg (42 μ mol) 3-(2-bromo-4-fluorophenyl)-5-((Z)-2-pyridylmethylidene)-2-thioxotetrahydro-4H-imidazol-4-one **7** and 7 mg (42 μ mol) of copper (II) chloride dihydrate. Yield: 7.6 mg (42%). UV-vis (λ , nm/ ϵ , l mol⁻¹ cm⁻¹): 435/16500. HRMS (*pos.*) calculated 439.8816 ($C_{30}H_{16}Br_2Cu_2F_2N_6O_2S_2$)²⁺ found 439.8806 ($C_{30}H_{16}Br_2Cu_2F_2N_6O_2S_2$)²⁺. Elemental analysis: calculated (%) for $C_{30}H_{16}Br_2Cu_2ClF_2N_6O_2S_2$: C 39.29, H 1.76, N 9.17, found C 39.63, H 1.84, N 8.90.

Preparation of the coordination compound of 3-(4-chlorophenyl)-5-((Z)-2-pyridylmethylidene)-2-thioxotetrahydro-4H-imidazol-4-one 8 with copper (II) chloride dihydrate (8k). **8k** was obtained as a black crystalline precipitate from 15 mg (47 μ mol) of 3-(4-chlorophenyl)-5-((Z)-2-pyridylmethylidene)-2-thioxotetrahydro-4H-imidazol-4-one **8** and 8 mg (47 μ mol) of copper (II) chloride dihydrate. Yield: 6.0 mg (32%). MALDI: m/z = 692 ($(8 - H)_2Cu^+$ 13%, 755 ($(8 - H)_2Cu_2^+$ 100%. HRMS (*pos.*) calculated 753.8902 ($C_{30}H_{18}Cu_2Cl_2N_6O_2S_2$)⁺, found 753.8904 ($C_{30}H_{18}Cu_2Cl_2N_6O_2S_2$)⁺, UV-vis (λ , nm/ ϵ , l mol⁻¹ cm⁻¹): 432/9683. Elemental analysis: calculated (%) for $C_{30}H_{18}Cu_2Cl_3N_6O_2S_2$: C 45.49, H 2.29, N 10.61, found C 45.19, H 2.35, N 10.59.

Preparation of the coordination compound of 3-(3-chlorophenyl)-5-((Z)-2-pyridylmethylidene)-2-thioxotetrahydro-4H-imidazol-4-one 9 with copper (II) chloride dihydrate (9k). **9k** was obtained as a black crystalline precipitate from 15 mg (47 μ mol) of 3-(3-chlorophenyl)-5-((Z)-2-pyridylmethylidene)-2-thioxotetrahydro-4H-imidazol-4-one **9** and 8 mg (47 μ mol) of copper (II) chloride dihydrate. Yield: 11.0 mg (50%). MALDI: m/z = 692 ($(9 - H)_2Cu^+$ 15%, 755 ($(9 - H)_2Cu_2^+$ 100%. HRMS (*pos.*) calculated 753.8902 ($C_{30}H_{18}Cu_2Cl_2N_6O_2S_2$)⁺, 755.8884 ($C_{30}H_{18}Cu_2Cl_2N_6O_2S_2$)⁺ isotopic, found 753.8901 ($C_{30}H_{18}Cu_2Cl_2N_6O_2S_2$)⁺, 755.8878 ($C_{30}H_{18}Cu_2Cl_2N_6O_2S_2$)⁺ isotopic. Elemental analysis: calculated (%) for $C_{30}H_{18}Cu_2Cl_3N_6O_2S_2$: C 45.49, H 2.29, N 10.61, found C 45.34, H 2.30, N 10.38.

Preparation of the coordination compound of 3-(2-chlorophenyl)-5-((Z)-2-pyridylmethylidene)-2-thioxotetrahydro-4H-imidazol-4-one 10 with copper (II) chloride dihydrate (10k). **10k** was obtained as a black crystalline precipitate from 15 mg (47 μ mol) of 3-(2-chlorophenyl)-5-((Z)-2-pyridylmethylidene)-2-thioxotetrahydro-4H-imidazol-4-one **10** and 8 mg (47 μ mol) of copper (II) chloride dihydrate. Yield: 5.5 mg (30%). MALDI: m/z = 693 ($(10 - H)_2Cu^+$ 32%, 756 ($(10 - H)_2Cu_2^+$ 100%. HRMS (*pos.*) calculated 753.8902 ($C_{30}H_{18}Cu_2Cl_2N_6O_2S_2$)⁺, found 753.8901 ($C_{30}H_{18}Cu_2Cl_2N_6O_2S_2$)⁺, UV-vis (λ , nm/ ϵ , l mol⁻¹ cm⁻¹): 432/15417. Elemental analysis: calculated (%) for $C_{30}H_{18}Cu_2Cl_3N_6O_2S_2$: C 45.49, H 2.29, N 10.61, found C 45.40, H 2.38, N 10.52.

Preparation of the coordination compound of 3-(4-methoxyphenyl)-5-((Z)-2-pyridylmethylidene)-2-thioxotetrahydro-4H-imidazol-4-one 11 with copper (II) chloride dihydrate (11k). **11k** was obtained as a black crystalline precipitate from 15 mg (44 μ mol) of 3-(4-

methoxyphenyl)-5-(((Z)-2-pyridylmethylidene)-2-thioxotetrahydro-4H-imidazol-4-one **11** and 7.5 mg (44 μmol) of copper (II) chloride dihydrate. Yield: 5.0 mg (29%). MALDI: m/z = 685 (**11** - H_2Cu^+ 32%, 747 (**11** - H_2Cu_2^+ 100%. HRMS (*pos.*) calculated 745.9892 ($\text{C}_{32}\text{H}_{24}\text{Cu}_2\text{N}_6\text{O}_4\text{S}_2$)⁺, found 745.9814 ($\text{C}_{32}\text{H}_{24}\text{Cu}_2\text{N}_6\text{O}_4\text{S}_2$)⁺, UV-vis (λ , nm/ ϵ , l mol⁻¹ cm⁻¹): 441/42859. Elemental analysis: calculated (%) for $\text{C}_{32}\text{H}_{24}\text{Cu}_2\text{ClN}_6\text{O}_4\text{S}_2$ C 49.07, H 3.09, N 10.73, found C 49.43, H 3.22, N 10.61.

Preparation of the coordination compound of 3-(4-ethoxyphenyl)-5-(((Z)-2-pyridylmethylidene)-2-thioxotetrahydro-4H-imidazol-4-one **12 with copper (II) chloride dihydrate (**12k**).** **12k** was obtained as a black crystalline precipitate from 15 mg (47 μmol) of 3-(4-ethoxyphenyl)-5-(((Z)-2-pyridylmethylidene)-2-thioxotetrahydro-4H-imidazol-4-one **12** and 8.1 mg (47 μmol) of copper (II) chloride dihydrate. Yield: 6.0 mg (35%). MALDI: m/z = 711 (**12** - H_2Cu^+ 64%, 776 (**12** - H_2Cu_2^+ 100%. HRMS (*pos.*) calculated 775.0284 ($\text{C}_{34}\text{H}_{29}\text{Cu}_2\text{N}_6\text{O}_4\text{S}_2$)⁺, found 775.0219 ($\text{C}_{34}\text{H}_{29}\text{Cu}_2\text{N}_6\text{O}_4\text{S}_2$)⁺, UV-vis (λ , nm/ ϵ , l mol⁻¹ cm⁻¹): 432/11250. Elemental analysis: calculated (%) for $\text{C}_{35}\text{H}_{32}\text{Cu}_2\text{ClN}_6\text{O}_5\text{S}_2$ (**12k** + CH_3OH) C 49.85, H 3.82, N 9.97, found C 49.98, H 3.39, N 10.02.

Preparation of the coordination compound of 3-(3,4-methoxyphenyl)-5-(((Z)-2-pyridylmethylidene)-2-thioxotetrahydro-4H-imidazol-4-one **13 with copper (II) chloride dihydrate (**13k**).** **13k** was obtained as a black crystalline precipitate from 15 mg (46 μmol) of 3-(3,4-methoxyphenyl)-5-(((Z)-2-pyridylmethylidene)-2-thioxotetrahydro-4H-imidazol-4-one **13** and 8.0 mg (46 μmol) of copper (II) chloride dihydrate. Yield: 7.0 mg (39%). MALDI: m/z = 743 (**13** - H_2Cu^+ 50%, 806 (**13** - H_2Cu_2^+ 100%. HRMS (*pos.*) calculated 806.0104 ($\text{C}_{34}\text{H}_{28}\text{Cu}_2\text{N}_6\text{O}_6\text{S}_2$)⁺, found 806.0100 ($\text{C}_{34}\text{H}_{28}\text{Cu}_2\text{N}_6\text{O}_6\text{S}_2$)⁺, UV-vis (λ , nm/ ϵ , l mol⁻¹ cm⁻¹): 432/33055. Elemental analysis: calculated (%) for $\text{C}_{34}\text{H}_{28}\text{Cu}_2\text{ClN}_6\text{O}_6\text{S}_2$ C 48.42, H 3.35, N 9.97, found C 48.51, H 3.47, N 9.99.

Preparation of the coordination compound of 3-(4-tert-butylphenyl)-5-(((Z)-2-pyridylmethylidene)-2-thioxotetrahydro-4H-imidazol-4-one **14 with copper (II) chloride dihydrate (**14k**).** **14k** was obtained as a black crystalline precipitate from 15 mg (44 μmol) 3-(4-tert-butylphenyl)-5-(((Z)-2-pyridylmethylidene)-2-thioxotetrahydro-4H-imidazol-4-one **14** and 7.5 mg (44 μmol) copper (II) chloride dihydrate. Yield: 10.0 mg (59%). MALDI: m/z = 735 (**14** - H_2Cu^+ 46%, 800 (**14** - H_2Cu_2^+ 100%. HRMS (*pos.*) calculated 737.1788 ($\text{C}_{38}\text{H}_{38}\text{CuN}_6\text{O}_2\text{S}_2$)⁺, found 737.1795 ($\text{C}_{38}\text{H}_{38}\text{CuN}_6\text{O}_2\text{S}_2$)⁺, UV-vis (λ , nm/ ϵ , l mol⁻¹ cm⁻¹): 439/24853. Elemental analysis: calculated (%) for $\text{C}_{38}\text{H}_{44}\text{Cu}_2\text{ClN}_6\text{O}_2\text{S}_2$ (**14k** + $4\text{H}_2\text{O}$) C 50.29, H 4.89, N 9.26, found C 50.64, H 4.22, N 9.36.

Preparation of the coordination compound of 3-(2-tert-butylphenyl)-5-(((Z)-2-pyridylmethylidene)-2-thioxotetrahydro-4H-imidazol-4-one **15 with copper (II) chloride dihydrate (**15k**).** **15k** was obtained as a black crystalline precipitate from 15 mg (44 μmol) of 3-(2-tert-butylphenyl)-5-(((Z)-2-pyridylmethylidene)-2-thioxotetrahydro-4H-imidazol-4-one **15** and 7.5 mg (44 μmol) of copper (II) chloride dihydrate. Yield: 11 mg (50%) HRMS calculated 399.0449 ($\text{C}_{38}\text{H}_{38}\text{CuN}_6\text{O}_2\text{S}_2$)²⁺, found 399.0461 ($\text{C}_{38}\text{H}_{38}\text{CuN}_6\text{O}_2\text{S}_2$)²⁺. UV-vis (λ , nm/ ϵ , l mol⁻¹ cm⁻¹): 434/28800. Elemental analysis: calculated (%) for $\text{C}_{38}\text{H}_{38}\text{Cu}_2\text{ClN}_6\text{O}_2\text{S}_2$ C 54.63, H 4.34, N 10.06, found C 54.25, H 4.30, N 10.34.

Preparation of the coordination compound of 3-(4-nitrophenyl)-5-(((Z)-2-pyridylmethylidene)-2-thioxotetrahydro-4H-imidazol-4-one **16 with copper (II) chloride dihydrate (**16k**).** **16k** was obtained as a black crystalline precipitate from 15 mg (46 μmol) of 3-(4-nitrophenyl)-5-(((Z)-2-pyridylmethylidene)-2-thioxotetrahydro-4H-imidazol-4-one **16** and 7.8 mg (46 μmol) of copper (II) chloride dihydrate. Yield: 6.0 mg (35%). MALDI: m/z = 778 (**16** - H_2Cu_2^+ 100%. UV-vis (λ , nm/ ϵ , l mol⁻¹ cm⁻¹): 432/10583. Elemental analysis: calculated (%) for $\text{C}_{30}\text{H}_{18}\text{Cu}_2\text{ClN}_8\text{O}_6\text{S}_2$ C 44.31, H 2.23, N 13.78, found C 44.30, H 2.22, N 13.80.

Preparation of the coordination compound of 3-(2-methyl-4-diethylaminophenyl)-5-(((Z)-2-pyridylmethylidene)-2-thioxotetrahydro-4H-imidazol-4-

one **17 with copper (II) chloride dihydrate (**17k**).** **17k** was obtained as a black crystalline precipitate from 15 mg (41 μmol) of 3-(2-methyl, 4-diethylaminophenyl)-5-(((Z)-2-pyridylmethylidene)-2-thioxotetrahydro-4H-imidazol-4-one **17** and 6.9 mg (41 μmol) of copper(II) chloride dihydrate. Yield: 6.2 mg (35%). MALDI: m/z = 333 (**17-H**)⁺ 98%, 856 (**17** - H_2Cu_2^+ 100%. HRMS (*pos.*) calculated 856.1464 ($\text{C}_{40}\text{H}_{42}\text{Cu}_2\text{N}_8\text{O}_2\text{S}_2$)⁺, found 856.1484 ($\text{C}_{40}\text{H}_{42}\text{Cu}_2\text{N}_8\text{O}_2\text{S}_2$)⁺, UV-vis (λ , nm/ ϵ , l mol⁻¹ cm⁻¹): 432/25240. Elemental analysis: calculated (%) for $\text{C}_{40}\text{H}_{42}\text{Cu}_2\text{ClN}_8\text{O}_2\text{S}_2$ C 53.77, H 4.74, N 12.54, found C 53.43, H 4.88, N 12.17.

Preparation of the coordination compound of 3-(2-methoxy-4-chloro-5-methylphenyl)-5-(((Z)-2-pyridylmethylidene)-2-thioxotetrahydro-4H-imidazol-4-one **18 with copper (II) chloride dihydrate (**18k**).** **18k** was obtained as a black crystalline precipitate from 15 mg (47 μmol) of 3-(2-methoxy-4-chloro-5-methylphenyl)-5-(((Z)-2-pyridylmethylidene)-2-thioxotetrahydro-4H-imidazol-4-one **18** and 8 mg (47 μmol) of copper (II) chloride dihydrate. Yield: 5.5 mg (30%). MALDI: m/z = 693 (**18** - H_2Cu^+ 32%, 756 (**18** - H_2Cu_2^+ 100%. HRMS (*pos.*) calculated 753.8902 ($\text{C}_{30}\text{H}_{18}\text{Cu}_2\text{Cl}_2\text{N}_6\text{O}_2\text{S}_2$)⁺, found 753.8901 ($\text{C}_{30}\text{H}_{18}\text{Cu}_2\text{Cl}_2\text{N}_6\text{O}_2\text{S}_2$)⁺. UV-vis (λ , nm/ ϵ , l mol⁻¹ cm⁻¹): 436/34300. Elemental analysis: calculated (%) for $\text{C}_{30}\text{H}_{18}\text{Cu}_2\text{Cl}_3\text{N}_6\text{O}_2\text{S}_2$ C 46.40, H 2.98, N 9.55, found C 46.31, H 2.93, N 9.32.

Preparation of the coordination compound of 3-(3-chloro-4-fluorophenyl)-5-(((Z)-2-pyridylmethylidene)-2-thioxotetrahydro-4H-imidazol-4-one **19 with copper (II) chloride dihydrate (**19k**).** **19k** was obtained as a black crystalline precipitate from 15 mg (45 μmol) of 3-(3-chloro-4-fluorophenyl)-5-(((Z)-2-pyridylmethylidene)-2-thioxotetrahydro-4H-imidazol-4-one **19** and 7.6 mg (45 μmol) of copper (II) chloride dihydrate. Yield: 9 mg (45%). HRMS (*pos.*) calculated 789.8713 ($\text{C}_{30}\text{H}_{16}\text{Cu}_2\text{Cl}_2\text{F}_2\text{N}_6\text{O}_2\text{S}_2$)⁺, found 789.8615 ($\text{C}_{30}\text{H}_{16}\text{Cu}_2\text{Cl}_2\text{F}_2\text{N}_6\text{O}_2\text{S}_2$)⁺. Elemental analysis: calculated (%) for $\text{C}_{30}\text{H}_{16}\text{Cu}_2\text{Cl}_3\text{F}_2\text{N}_6\text{O}_2\text{S}_2$ C 43.51, H 1.95, N 10.15, found C 43.90, H 2.12, N 10.05.

Preparation of the coordination compound of 3-(2-methyl-3-chlorophenyl)-5-(((Z)-2-pyridylmethylidene)-2-thioxotetrahydro-4H-imidazol-4-one **20 with copper (II) chloride dihydrate (**20k**).** **20k** was obtained as a black crystalline precipitate from 15 mg (47 μmol) of 3-(2-methyl-3-chlorophenyl)-5-(((Z)-2-pyridylmethylidene)-2-thioxotetrahydro-4H-imidazol-4-one **20** and 8 mg (47 μmol) of copper (II) chloride dihydrate. Yield: 14 mg (61%). HRMS (*pos.*) calculated 781.9215 ($\text{C}_{32}\text{H}_{22}\text{Cl}_2\text{Cu}_2\text{N}_6\text{O}_2\text{S}_2$)⁺, 783.9197 ($\text{C}_{32}\text{H}_{22}\text{Cl}_2\text{Cu}_2\text{N}_6\text{O}_2\text{S}_2$ ⁺ isotopic), found 781.9179 ($\text{C}_{32}\text{H}_{22}\text{Cl}_2\text{Cu}_2\text{N}_6\text{O}_2\text{S}_2$)⁺, 783.9213 ($\text{C}_{32}\text{H}_{22}\text{Cl}_2\text{Cu}_2\text{N}_6\text{O}_2\text{S}_2$ ⁺ isotopic). Elemental analysis: calculated (%) for $\text{C}_{36}\text{H}_{32}\text{Cu}_2\text{Cl}_3\text{N}_6\text{O}_2\text{S}_2$ (**20k** + Et_2O) C 48.35, H 3.61, N 9.40, found C 48.38, H 3.87, N 9.37.

Preparation of the coordination compound of 3-(2,4,6-trimethylphenyl)-5-(((Z)-2-pyridylmethylidene)-2-thioxotetrahydro-4H-imidazol-4-one **21 with copper (II) chloride dihydrate (**21k**).** **21k** was obtained as a black crystalline precipitate from 15 mg (46 μmol) of 3-(2,4,6-trimethylphenyl)-5-(((Z)-2-pyridylmethylidene)-2-thioxotetrahydro-4H-imidazol-4-one **21** and 7.8 mg (46 μmol) of copper (II) chloride dihydrate. Yield: 13 mg (59%). HRMS (*pos.*) calculated 770.0620 ($\text{C}_{36}\text{H}_{32}\text{Cu}_2\text{N}_6\text{O}_2\text{S}_2$)⁺, 772.0602 ($\text{C}_{36}\text{H}_{32}\text{Cu}_2\text{N}_6\text{O}_2\text{S}_2$ ⁺ isotopic), found 770.0624 ($\text{C}_{36}\text{H}_{32}\text{Cu}_2\text{N}_6\text{O}_2\text{S}_2$)⁺, 772.0604 ($\text{C}_{36}\text{H}_{32}\text{Cu}_2\text{N}_6\text{O}_2\text{S}_2$ ⁺ isotopic). Elemental analysis: calculated (%) for $\text{C}_{36}\text{H}_{32}\text{Cu}_2\text{ClN}_6\text{O}_2\text{S}_2$ C 53.56, H 4.00, N 10.41, found C 53.40, H 3.97, N 10.30.

Preparation of the coordination compound of 3-(4-methylthiophenyl)-5-(((Z)-2-pyridylmethylidene)-2-thioxotetrahydro-4H-imidazol-4-one **22 with copper (II) chloride dihydrate (**22k**).** **22k** was obtained as a black crystalline precipitate from 15 mg (46 μmol) of 3-(4-methylthiophenyl)-5-(((Z)-2-pyridylmethylidene)-2-thioxotetrahydro-4H-imidazol-4-one **22** and 7.8 mg (46 μmol) of copper (II) chloride dihydrate. Yield: 10 mg (45%). HRMS (*pos.*) calculated 777.9436 ($\text{C}_{32}\text{H}_{24}\text{Cu}_2\text{N}_6\text{O}_2\text{S}_4$)⁺, 779.9418 ($\text{C}_{32}\text{H}_{24}\text{Cu}_2\text{N}_6\text{O}_2\text{S}_4$ ⁺ isotopic), found 777.9442 ($\text{C}_{32}\text{H}_{24}\text{Cu}_2\text{N}_6\text{O}_2\text{S}_4$)⁺, 779.9406 ($\text{C}_{32}\text{H}_{24}\text{Cu}_2\text{N}_6\text{O}_2\text{S}_4$ ⁺ isotopic).

Elemental analysis: calculated (%) for $C_{32}H_{28}Cu_2ClN_6O_4S_4$ (**22k** + $2H_2O$): C 45.14, H 3.31, N 9.87, found C 44.83, H 2.95, N 9.96.

Preparation of the coordination compound of 3-(4-iodophenyl)-5-((Z)-2-pyridylmethylidene)-2-thioxotetrahydro-4H-imidazol-4-one 23 with copper (II) chloride dihydrate (23k). **23k** was obtained as a black crystalline precipitate from 15 mg (16.5 μ mol) of 3-(4-iodophenyl)-5-((Z)-2-pyridylmethylidene)-2-thioxotetrahydro-4H-imidazol-4-one **23** and 3 mg (16.5 μ mol) of copper (II) chloride dihydrate. Yield: 6.0 mg (32%). MALDI: m/z = 877 (**23** - H) $_2Cu^+$ 6%, 940 (**23** - H) $_2Cu_2^+$ 100%. HRMS (*pos.*) calculated 937.7614 ($C_{30}H_{18}Cu_2I_2N_6O_2S_2$) $^+$, found 937.7643 ($C_{30}H_{18}Cu_2I_2N_6O_2S_2$) $^+$, UV-vis (λ , nm/ ϵ , l mol $^{-1}$ cm $^{-1}$): 438/19622. Elemental analysis: calculated (%) for $C_{30}H_{18}Cu_2ClI_2N_6O_2S_2$ C 36.96, H 1.86, N 8.62, found C 36.76, H 1.70, N 8.49.

Preparation of the coordination compound of 3-(2-methyl-4-diethylaminophenyl)-5-((Z)-2-pyridylmethylidene)-2-thioxotetrahydro-4H-imidazol-4-one 24 with copper (II) chloride dihydrate (24k). **24k** was obtained as a black crystalline precipitate from 15 mg (41 μ mol) of 3-(2-methyl, 4-diethylaminophenyl)-5-((Z)-2-pyridylmethylidene)-2-thioxotetrahydro-4H-imidazol-4-one **17** and 6.9 mg (41 μ mol) of copper (II) chloride dihydrate. Yield: 6.2 mg (35%). MALDI: m/z = 856 (**24** - H) $_2Cu_2^+$ 100%. HRMS (*pos.*) calculated 856.1464 ($C_{40}H_{42}Cu_2N_8O_2S_2$) $^+$, found 856.1484 ($C_{40}H_{42}Cu_2N_8O_2S_2$) $^+$, UV-vis (λ , nm/ ϵ , l mol $^{-1}$ cm $^{-1}$): 432/25240. Elemental analysis: calculated (%) for $C_{40}H_{42}Cu_2Cl_2N_8O_2S_2$ C 53.77, H 4.74, N 12.54, found C 54.01, H 5.02, N 12.90.

Preparation of the coordination compound of 3-(2,6-dichlorophenyl)-5-((Z)-2-pyridylmethylidene)-2-thioxotetrahydro-4H-imidazol-4-one 25 with copper (II) chloride dihydrate (25k). **25k** was obtained as a black crystalline precipitate from 15 mg (43 μ mol) of 3-(2,6-dichlorophenyl)-5-((Z)-2-pyridylmethylidene)-2-thioxotetrahydro-4H-imidazol-4-one **25** and 7.3 mg (43 μ mol) of copper (II) chloride dihydrate. Yield: 5 mg (27%). HRMS (*pos.*) calculated 858.7781 ($C_{30}H_{16}Cl_2Cu_2N_6O_2S_2$) $^+$, found 858.8301 ($C_{30}H_{16}Cl_2Cu_2N_6O_2S_2$) $^+$. Elemental analysis: calculated (%) for $C_{30}H_{16}Cl_2Cu_2N_6O_2S_2$ C 41.85, H 1.87, N 9.76, found C 42.05, H 1.79, N 9.68.

Preparation of the coordination compound of 3-(2,4,6-trichlorophenyl)-5-((Z)-2-pyridylmethylidene)-2-thioxotetrahydro-4H-imidazol-4-one 26 with copper (II) chloride dihydrate (26k). **26k** was obtained as a black crystalline precipitate from 15 mg (39 μ mol) of 3-(2,4,6-trichlorophenyl)-5-((Z)-2-pyridylmethylidene)-2-thioxotetrahydro-4H-imidazol-4-one **26** and 6.6 mg (39 μ mol) of copper (II) chloride dihydrate. Yield: 6 mg (33%). HRMS (*pos.*) calculated 891.7313 ($C_{30}H_{16}Cl_3Cu_2N_6O_2S_2$) $^+$, found 891.7231 ($C_{30}H_{16}Cl_3Cu_2N_6O_2S_2$) $^+$. Elemental analysis: calculated (%) for $C_{30}H_{16}Cl_3Cu_2N_6O_2S_2$ C 38.75, H 1.52, N 9.04, found C 38.70, H 1.43, N 9.06.

Preparation of the coordination compound of 3-(2,6-dibromophenyl)-5-((Z)-2-pyridylmethylidene)-2-thioxotetrahydro-4H-imidazol-4-one 27 with copper (II) chloride dihydrate (27k). **27k** was obtained as a black crystalline precipitate from 15 mg (34 μ mol) of 3-(2,6-dibromophenyl)-5-((Z)-2-pyridylmethylidene)-2-thioxotetrahydro-4H-imidazol-4-one **27** and 5.8 mg (34 μ mol) of copper (II) chloride dihydrate. Yield: 9 mg (51%). HRMS (*pos.*) calculated 1001.6061 ($C_{30}H_{16}Br_2Cu_2N_6O_2S_2$) $^+$, found 1001.6035 ($C_{30}H_{16}Br_2Cu_2N_6O_2S_2$) $^+$. Elemental analysis: calculated (%) for $C_{30}H_{16}Cu_2ClBr_2N_6O_2S_2$ C 34.69, H 1.55, N 8.09, found C 34.80, H 1.69, N 8.20.

Preparation of the coordination compound of 3-(2,5-difluorophenylphenyl)-5-((Z)-2-pyridylmethylidene)-2-thioxotetrahydro-4H-imidazol-4-one 28 with copper (II) chloride dihydrate (28k). **28k** was obtained as a black crystalline precipitate from 15 mg (45 μ mol) of 3-(2,5-difluorophenylphenyl)-5-((Z)-2-pyridylmethylidene)-2-thioxotetrahydro-4H-imidazol-4-one **28** and 7.6 mg (45 μ mol) of copper (II) chloride dihydrate. Yield: 5 mg (24%). HRMS calculated 757.9299 ($C_{30}H_{16}Cu_2F_4N_6O_2S_2$) $^+$, found 757.9292 ($C_{30}H_{16}Cu_2F_4N_6O_2S_2$) $^+$. Elemental analysis: calculated (%) for

$C_{30}H_{16}Cu_2ClF_4N_6O_2S_2$ C 45.31, H 2.03, N 10.50, found C 45.38, H 2.13, N 10.41.

Preparation of the coordination compound of 3-(3,5-difluorophenylphenyl)-5-((Z)-2-pyridylmethylidene)-2-thioxotetrahydro-4H-imidazol-4-one 29 with copper (II) chloride dihydrate (29k). **29k** was obtained as a black crystalline precipitate from 15 mg (46 μ mol) of 3-(3,5-difluorophenylphenyl)-5-((Z)-2-pyridylmethylidene)-2-thioxotetrahydro-4H-imidazol-4-one **29** and 7.8 mg (46 μ mol) of copper (II) chloride dihydrate. Yield: 10 mg (47%). HRMS calculated 757.9299 ($C_{30}H_{16}Cu_2F_4N_6O_2S_2$) $^+$, found 757.9289 ($C_{30}H_{16}Cu_2F_4N_6O_2S_2$) $^+$. Elemental analysis: calculated (%) for $C_{30}H_{16}Cu_2ClF_4N_6O_2S_2$ C 45.31, H 2.03, N 10.57, found C 45.32, H 2.12, N 10.18.

Preparation of the coordination compound 5-(Z)-3-(4-fluorophenyl)-2-(methylthio)-5-(pyridin-2-ylmethylidene)-1H-imidazol-4-one 30 with copper (II) chloride dihydrate (30k). **30k** was obtained as a black crystalline precipitate from 15 mg (50 μ mol) of 5-(Z)-3-(4-fluorophenyl)-2-(methylthio)-5-(pyridin-2-ylmethylidene)-1H-imidazol-4-one **30** and 8.5 mg (50 μ mol) of copper (II) chloride dihydrate. Yield: 6.0 mg (32%). MALDI: m/z = 314 (**30** + H) $^+$ 100%, 376 **30** Cu^+ 70%, 690 (**30**) $_2Cu^+$ 100%. HRMS (*pos.*) calculated 423.0114 ($C_{16}H_{13}CuFN_3OS^*HCOOH$) $^+$, found 423.0111 ($C_{16}H_{13}CuFN_3OS^*HCOOH$) $^+$, UV-vis (λ , nm/ ϵ , l mol $^{-1}$ cm $^{-1}$): 392/20417. Elemental analysis: calculated (%) for $C_{16}H_{13}CuCl_2FN_3OS$ C 42.91, H 2.70, N 9.38, found C 42.94, H 2.67, N 9.22.

Preparation of the coordination compound 5-(Z)-3-(3-fluorophenyl)-2-(methylthio)-5-(pyridin-2-ylmethylidene)-1H-imidazol-4-one 31 with copper (II) chloride dihydrate (31k). **31k** was obtained as a black crystalline precipitate from 15 mg (50 μ mol) of 5-(Z)-3-(3-fluorophenyl)-2-(methylthio)-5-(pyridin-2-ylmethylidene)-1H-imidazol-4-one **31** and 8.5 mg (50 μ mol) of copper (II) chloride dihydrate. Yield: 5.8 mg (32%). MALDI: m/z = 313 (**31**) $^+$ 20%, 376 **31** Cu^+ 68%, 690 (**31**) $_2Cu^+$ 100%. HRMS (*pos.*) calculated 423.0114 ($C_{16}H_{13}CuFN_3OS^*HCOOH$) $^+$, found 423.0074 ($C_{16}H_{13}CuFN_3OS^*HCOOH$) $^+$, UV-vis (λ , nm/ ϵ , l mol $^{-1}$ cm $^{-1}$): 392/13583. Elemental analysis: calculated (%) for $C_{16}H_{13}CuCl_2FN_3OS$ C 42.91, H 2.70, N 9.38, found C 42.86, H 2.69, N 9.31.

Preparation of the coordination compound 5-(Z)-3-(2-fluorophenyl)-2-(methylthio)-5-(pyridin-2-ylmethylidene)-1H-imidazol-4-one 32 with copper (II) chloride dihydrate (32k). **32k** was obtained as a black crystalline precipitate from 15 mg (50 μ mol) of 5-(Z)-3-(2-fluorophenyl)-2-(methylthio)-5-(pyridin-2-ylmethylidene)-1H-imidazol-4-one **32** and 8.5 mg (50 μ mol) of copper (II) chloride dihydrate. Yield: 6.1 mg (33%). MALDI: m/z = 374 (**32**) Cu^+ 11%, 692 (**32**) $_2Cu^+$ 100%. HRMS (*pos.*) calculated 423.0114 ($C_{16}H_{13}CuFN_3OS^*HCOOH$) $^+$, found 423.0109 ($C_{16}H_{13}CuFN_3OS^*HCOOH$) $^+$, UV-vis (λ , nm/ ϵ , l mol $^{-1}$ cm $^{-1}$): 392/14883. Elemental analysis: calculated (%) for $C_{16}H_{13}CuCl_2FN_3OS$ C 42.91, H 2.70, N 9.38, found C 42.95, H 2.90, N 9.41.

Preparation of the coordination compound 5-(Z)-3-(4-bromophenyl)-2-(methylthio)-5-(pyridin-2-ylmethylidene)-1H-imidazol-4-one 33 with copper (II) chloride dihydrate (33k). **33k** was obtained as a black crystalline precipitate from 15 mg (42 μ mol) of 5-(Z)-3-(4-bromophenyl)-2-(methylthio)-5-(pyridin-2-ylmethylidene)-1H-imidazol-4-one **33** and 7 mg (42 μ mol) of copper (II) chloride dihydrate. Yield: 6.1 mg (33%). MALDI: m/z = 390 (**33** + CH_3) $^+$ 100%, 478 (**33**) Cu^+ 12%, 814 (**33**) $_2Cu^+$ 100%. HRMS (*pos.*) calculated 482.9314 ($C_{16}H_{13}CuBrN_3OS^*HCOOH$) $^+$, found 482.9303 ($C_{16}H_{13}CuBrN_3OS^*HCOOH$) $^+$, UV-vis (λ , nm/ ϵ , l mol $^{-1}$ cm $^{-1}$): 393/12157. Elemental analysis: calculated (%) for $C_{16}H_{13}CuCl_2BrN_3OS$ C 37.78, H 2.38, N 8.26, found C 37.85, H 2.39, N 8.31.

Preparation of the coordination compound 5-(Z)-3-(3-bromophenyl)-2-(methylthio)-5-(pyridin-2-ylmethylidene)-1H-imidazol-4-one 34 with copper (II) chloride dihydrate (34k). **34k** was obtained as a black crystalline precipitate from 15 mg (42 μ mol) of 5-(Z)-3-(3-

bromophenyl)-2-(methylthio)-5-(pyridin-2-ylmethylidene)-1H-imidazol-4-one **34** and 7 mg (42 μ mol) of copper (II) chloride dihydrate. Yield: 5.9 mg (32%). MALDI: m/z = 375 (**34** + H)⁺ 80%, 438 (**34**) Cu⁺ 32%, 815 (**34**)₂Cu⁺ 100%. HRMS (*pos.*) calculated 482.9314 (C₁₆H₁₃CuBrN₃OS*HCOOH)⁺, found 482.9310 (C₁₆H₁₃CuBrN₃OS*HCOOH)⁺, UV-vis (λ , nm/ ϵ , l mol⁻¹ cm⁻¹): 392/11917. Elemental analysis: calculated (%) for C₁₆H₁₃CuCl₂BrN₃OS C 37.78, H 2.38, N 8.26, found C 37.75, H 2.29, N 8.27.

Preparation of the coordination compound 5-(Z)-3-(2-bromophenyl)-2-(methylthio)-5-(pyridin-2-ylmethylidene)-1H-imidazol-4-one 35 with copper (II) chloride dihydrate (35k). **35k** was obtained as a black crystalline precipitate from 15 mg (42 μ mol) of 5-(Z)-3-(2-bromophenyl)-2-(methylthio)-5-(pyridin-2-ylmethylidene)-1H-imidazol-4-one **35** and 7 mg (42 μ mol) of copper (II) chloride dihydrate. Yield: 6.0 mg (32%). MALDI: m/z = 375 (**35** + H)⁺ 34%, 475 (**35**)CuCl⁺ 18%, 814 (**35**)₂Cu⁺ 100%. HRMS (*pos.*) calculated 482.9314 (C₁₆H₁₃CuBrN₃OS*HCOOH)⁺, found 482.9307 (C₁₆H₁₃CuBrN₃OS*HCOOH)⁺, UV-vis (λ , nm/ ϵ , l mol⁻¹ cm⁻¹): 392/5950. Elemental analysis: calculated (%) for C₁₆H₁₃CuCl₂BrN₃OS C 37.78, H 2.38, N 8.26, found C 37.79, H 2.36, N 8.30.

Preparation of the coordination compound 5-(Z)-3-(2-bromo-4-fluorophenyl)-2-(methylthio)-5-(pyridin-2-ylmethylidene)-1H-imidazol-4-one 36 with copper (II) chloride dihydrate (36k). **36k** was obtained as a black crystalline precipitate from 15 mg (42 μ mol) of 5-(Z)-3-(2-bromophenyl)-2-(methylthio)-5-(pyridin-2-ylmethylidene)-1H-imidazol-4-one **36** and copper (II) chloride dihydrate 7 mg (42 μ mol). Yield: 5 mg (25%) HRMS (*pos.*) calculated 523.8458 (C₁₆H₁₁BrCl₂CuFN₃OS)⁺, found 523.8463 (C₁₆H₁₁BrCl₂CuFN₃OS)⁺. UV-vis (λ , nm/ ϵ , l mol⁻¹ cm⁻¹): 386/37800. Elemental analysis: calculated (%) for C₁₆H₁₁CuCl₂BrFN₃OS C 36.49, H 2.11, N 7.98, found C 36.55, H 2.24, N 7.96.

Preparation of the coordination compound 5-(Z)-3-(4-chlorophenyl)-2-(methylthio)-5-(pyridin-2-ylmethylidene)-1H-imidazol-4-one 37 with copper (II) chloride dihydrate (37k). **37k** was obtained as a black crystalline precipitate from 15 mg (47 μ mol) of 5-(Z)-3-(4-chlorophenyl)-2-(methylthio)-5-(pyridin-2-ylmethylidene)-1H-imidazol-4-one **37** and 8 mg (47 μ mol) of copper (II) chloride dihydrate. Yield: 6.0 mg (32%). MALDI: m/z = 330 (**37** + H)⁺ 100%, 392 (**37**) Cu⁺ 82%, 814 (**37**)₂Cu⁺ 100%. HRMS (*pos.*) calculated 438.9814 (C₁₆H₁₄CuClN₃OS*HCOOH)⁺, found 438.9811 (C₁₆H₁₃CuClN₃OS*HCOOH)⁺, UV-vis (λ , nm/ ϵ , l mol⁻¹ cm⁻¹): 382/18034. Elemental analysis: calculated (%) for C₁₆H₁₃CuCl₃N₃OS C 41.39, H 2.61, N 9.05, found C 41.44, H 2.67, N 9.11.

Preparation of the coordination compound 5-(Z)-3-(3-chlorophenyl)-2-(methylthio)-5-(pyridin-2-ylmethylidene)-1H-imidazol-4-one 38 with copper (II) chloride dihydrate (38k). **38k** was obtained as a black crystalline precipitate from 15 mg (45 μ mol) of 5-(Z)-3-(4-chlorophenyl)-2-(methylthio)-5-(pyridin-2-ylmethylidene)-1H-imidazol-4-one **38** and 7.6 mg (45 μ mol) of copper (II) chloride dihydrate. Yield: 11 mg (50%). HRMS (*pos.*) calculated 437.9735 (C₁₆H₁₃CuClN₃OS*HCOOH)⁺, found 437.9739 (C₁₆H₁₃CuClN₃OS*HCOOH)⁺, UV-vis (λ , nm/ ϵ , l mol⁻¹ cm⁻¹): 392/14567. Elemental analysis: calculated (%) for C₁₆H₁₃CuCl₃N₃OS C 41.39, H 2.61, N 9.05, found C 41.31, H 2.58, N 9.01.

Preparation of the coordination compound 5-(Z)-3-(2-chlorophenyl)-2-(methylthio)-5-(pyridin-2-ylmethylidene)-1H-imidazol-4-one 39 with copper (II) chloride dihydrate (39k). **39k** was obtained as a black crystalline precipitate from 15 mg (47 μ mol) of 5-(Z)-3-(2-chlorophenyl)-2-(methylthio)-5-(pyridin-2-ylmethylidene)-1H-

imidazol-4-one **39** and 8 mg (47 μ mol) of copper (II) chloride dihydrate. Yield: 5.5 mg (30%). MALDI: m/z = 330 (**39** + H)⁺ 37%, 392 (**39**)Cu⁺ 100%, 814 (**39**)₂Cu⁺ 73%. HRMS (*pos.*) calculated 438.9814 (C₁₆H₁₄CuClN₃OS*HCOOH)⁺, found 438.9815 (C₁₆H₁₄CuClN₃OS*HCOOH)⁺, UV-vis (λ , nm/ ϵ , l mol⁻¹ cm⁻¹): 382/17298. Elemental analysis: calculated (%) for C₁₆H₁₃CuCl₃N₃OS C 41.39, H 2.61, N 9.05, found C 41.35, H 2.59, N 9.01.

Preparation of the coordination compound 5-(Z)-3-(4-methoxyphenyl)-2-(methylthio)-5-(pyridin-2-ylmethylidene)-1H-imidazol-4-one 40 with copper (II) chloride dihydrate (40k). **40k** was obtained as a black crystalline precipitate from 15 mg (44 μ mol) of 5-(Z)-3-(4-methoxyphenyl)-2-(methylthio)-5-(pyridin-2-ylmethylidene)-1H-imidazol-4-one **40** and 7.5 mg (44 μ mol) of copper (II) chloride dihydrate. Yield: 5.0 mg (29%). MALDI: m/z = 326 (**40** + H)⁺ 100%, 388 (**40**)Cu⁺ 47%, 423 (**40**)CuCl⁺, 649 (**40**-OMe)₂Cu⁺ 51%. HRMS (*pos.*) calculated 435.0314 (C₁₇H₁₇CuN₃O₂S*HCOOH)⁺, found 435.0316 (C₁₇H₁₇CuN₃O₂S*HCOOH)⁺, UV-vis (λ , nm/ ϵ , l mol⁻¹ cm⁻¹): 392/13400. Elemental analysis: calculated (%) for C₁₇H₁₇CuCl₂N₃O₂S C 44.40, H 3.29, N 9.14, found C 44.44, H 3.32, N 9.15.

Preparation of the coordination compound 5-(Z)-3-(4-ethoxyphenyl)-2-(methylthio)-5-(pyridin-2-ylmethylidene)-1H-imidazol-4-one 41 with copper (II) chloride dihydrate (41k). **41k** was obtained as a black crystalline precipitate from 15 mg (47 μ mol) of 5-(Z)-3-(4-ethoxyphenyl)-2-(methylthio)-5-(pyridin-2-ylmethylidene)-1H-imidazol-4-one **41** and 8.1 mg (47 μ mol) of copper (II) chloride dihydrate. Yield: 6.0 mg (35%). MALDI: m/z = 342 (**41** + H)⁺ 50%, 441 (**41**)CuCl⁺ 32%, 747 (**41**)₂Cu⁺ 100%. HRMS (*pos.*) calculated 449.0471 (C₁₈H₁₉CuN₃O₂S*HCOOH)⁺, found 449.0471 (C₁₈H₁₉CuN₃O₂S*HCOOH)⁺, UV-vis (λ , nm/ ϵ , l mol⁻¹ cm⁻¹): 392/13233. Elemental analysis: calculated (%) for C₁₈H₁₉CuCl₂N₃O₂S C 45.62, H 3.62, N 8.87, found C 45.44, H 3.50, N 8.75.

Preparation of the coordination compound 5-(Z)-3-(3,4-dimethoxyphenyl)-2-(methylthio)-5-(pyridin-2-ylmethylidene)-1H-imidazol-4-one 42 with copper (II) chloride dihydrate (42k). **42k** was obtained as a black crystalline precipitate from 15 mg (46 μ mol) of 5-(Z)-3-(3,4-dimethoxyphenyl)-2-(methylthio)-5-(pyridin-2-ylmethylidene)-1H-imidazol-4-one **42** and 8.0 mg (46 μ mol) of copper (II) chloride dihydrate. Yield: 7.0 mg (39%). MALDI: m/z = 356 (**42** + H)⁺ 100%, 418 (**42**)Cu⁺ 22%, 453 (**42**)CuCl⁺ 36%, 709 (**42**-OMe)₂Cu⁺ 49%. HRMS (*pos.*) calculated 465.0420 (C₁₈H₁₉CuN₃O₃S*HCOOH)⁺, found 465.0411 (C₁₈H₁₉CuN₃O₃S*HCOOH)⁺, UV-vis (λ , nm/ ϵ , l mol⁻¹ cm⁻¹): 368/149756. Elemental analysis: calculated (%) for C₁₈H₁₉CuCl₂N₃O₃S C 44.13, H 3.50, N 8.58, found C 44.22, H 3.60, N 8.62.

Preparation of the coordination compound 5-(Z)-3-(4-*t*-butylphenyl)-2-(methylthio)-5-(pyridin-2-ylmethylidene)-1H-imidazol-4-one 43 with copper (II) chloride dihydrate (43k). **43k** was obtained as a black crystalline precipitate from 15 mg (44 μ mol) of 5-(Z)-3-(4-*t*-butylphenyl)-2-(methylthio)-5-(pyridin-2-ylmethylidene)-1H-imidazol-4-one **43** and 7.5 mg (44 μ mol) of copper (II) chloride dihydrate. Yield: 10.0 mg (59%). MALDI: m/z = 353 (**43** + H)⁺ 53%, 669 ((**43**-*t*Bu)-Me)Cu⁺ 27%, 685 (**43**-*t*Bu)₂CuCl⁺ 100%, 701 (**31**-*t*Bu)₂Me)Cu⁺ 27%. HRMS (*pos.*) calculated 461.0834 (C₂₀H₂₂CuN₃OS*HCOOH)⁺, found 461.0833 (C₂₀H₂₂CuN₃OS*HCOOH)⁺, UV-vis (λ , nm/ ϵ , l mol⁻¹ cm⁻¹): 366/13487. Elemental analysis: calculated (%) for C₂₀H₂₁CuCl₂N₃OS C 49.44, H 4.36, N 8.65, found C 49.56, H 4.39, N 8.72.

Preparation of the coordination compound 5-(Z)-3-(2-*t*-butylphenyl)-2-(methylthio)-5-(pyridin-2-ylmethylidene)-1H-imidazol-4-one 44 with copper (II) chloride dihydrate (44k). **44k** was obtained as a black crystalline precipitate from 15 mg (44 μ mol) of 5-(Z)-3-(4-*t*-butylphenyl)-2-(methylthio)-5-(pyridin-2-ylmethylidene)-1H-imidazol-4-one **44** and 7.5 mg (44 μ mol) of copper (II) chloride dihydrate. Yield: 9.5 mg (46%).

HRMS (*pos.*) calculated 415.0775 ($C_{20}H_{22}CuN_3OS$)⁺, found 415.0769 ($C_{20}H_{22}CuN_3OS$)⁺, UV-vis (λ , nm/ ϵ , l mol⁻¹ cm⁻¹): 392/11350. Elemental analysis: calculated (%) for $C_{20}H_{21}CuCl_2N_3OS$ C 49.44, H 4.36, N 8.65, found C 49.43, H 4.28, N 8.65.

Preparation of the coordination compound 5-(Z)-3-(2-methoxy-4-chloro-5-methylphenyl)-2-(methylthio)-5-(pyridin-2-ylmethylidene)-1H-imidazol-4-one 45 with copper (II) chloride dihydrate (45k). 45k was obtained as a black crystalline precipitate from 15 mg (47 μ mol) of 5-(Z)-3-(4-chlorophenyl)-2-(methylthio)-5-(pyridin-2-ylmethylidene)-1H-imidazol-4-one 45 and 8 mg (47 μ mol) of copper (II) chloride dihydrate. Yield: 5.0 mg (27%). HRMS (*pos.*) calculated 481.9998 ($C_{18}H_{16}CuN_3O_2S + HCOOH$)⁺, found 481.9989 ($C_{18}H_{16}CuN_3O_2S + HCOOH$)⁺, UV-vis (λ , nm/ ϵ , l mol⁻¹ cm⁻¹): 392/9467. Elemental analysis: calculated (%) for $C_{18}H_{16}CuCl_3N_3O_2S$ C 42.53, H 3.17, N 8.27, found C 42.57, H 3.20, N 8.33.

Preparation of the coordination compound 5-(Z)-3-(3-chloro-4-fluorophenyl)-2-(methylthio)-5-(pyridin-2-ylmethylidene)-1H-imidazol-4-one 46 with copper (II) chloride dihydrate (46k). 46k was obtained as a black crystalline precipitate from 15 mg (44 μ mol) of 5-(Z)-3-(3-chloro-4-fluorophenyl)-2-(methylthio)-5-(pyridin-2-ylmethylidene)-1H-imidazol-4-one 46 and 7.5 mg (44 μ mol) copper (II) chloride dihydrate. Yield: 9.5 mg (46%). HRMS (*pos.*) calculated 409.9591 ($C_{16}H_{11}ClCuFN_3OS$)⁺, found 409.9590 ($C_{16}H_{11}ClCuFN_3OS$)⁺, UV-vis (λ , nm/ ϵ , l mol⁻¹ cm⁻¹): 392/12217. Elemental analysis: calculated (%) for $C_{17}H_{19}CuCl_3FN_3O_4S$ (46k + 2H₂O + CH₃OH): C 37.10, H 3.48, N 7.64, found C 36.50, H 3.38, N 7.76.

Preparation of the coordination compound 5-(Z)-3-(2-methyl-3-chlorophenyl)-2-(methylthio)-5-(pyridin-2-ylmethylidene)-1H-imidazol-4-one 47 with copper (II) chloride dihydrate (47k). 47k was obtained as a black crystalline precipitate from 15 mg (44 μ mol) of 5-(Z)-3-(2-methyl-3-chlorophenyl)-2-(methylthio)-5-(pyridin-2-ylmethylidene)-1H-imidazol-4-one 47 and 7.4 mg (44 μ mol) of copper (II) chloride dihydrate. Yield: 9.5 mg (46%). HRMS calculated 405.9842 ($C_{17}H_{14}ClCuN_3OS$)⁺, found 405.9836 ($C_{17}H_{14}ClCuN_3OS$)⁺. Elemental analysis: calculated (%) for $C_{17}H_{14}CuCl_3N_3OS$: C 42.69, H 2.95, N 8.79, found C 42.70, H 2.91, N 8.81.

Preparation of the coordination compound 5-(Z)-3-(2,4,6-methylphenyl)-2-(methylthio)-5-(pyridin-2-ylmethylidene)-1H-imidazol-4-one 48 with copper (II) chloride dihydrate (48k). 48k was obtained as a black crystalline precipitate from 15 mg (45 μ mol) 5-(Z)-3-(2,4,6-methylphenyl)-2-(methylthio)-5-(pyridin-2-ylmethylidene)-1H-imidazol-4-one 48 and 7.6 mg (45 μ mol) of copper (II) chloride dihydrate. Yield: 12 mg (52%). HRMS calculated 400.0545 ($C_{19}H_{19}CuN_3OS$)⁺, found 400.0536 ($C_{19}H_{19}CuN_3OS$)⁺. Elemental analysis: calculated (%) for $C_{19}H_{19}CuCl_2N_3OS$ C 48.36, H 4.06, N 8.90, found C 48.30, H 3.77, N 8.87.

Preparation of the coordination compound 5-(Z)-3-(4-methylthiophenyl)-2-(methylthio)-5-(pyridin-2-ylmethylidene)-1H-imidazol-4-one 49 with copper (II) chloride dihydrate (49k). 49k was obtained as a black crystalline precipitate from 15 mg (44 μ mol) of 5-(Z)-3-(4-methylthiophenyl)-2-(methylthio)-5-(pyridin-2-ylmethylidene)-1H-imidazol-4-one 49 and 7.4 mg (44 μ mol) of copper (II) chloride dihydrate. Yield: 9 mg (43%). HRMS calculated 403.9953 ($C_{17}H_{15}CuN_3OS_2$)⁺, found 403.9946 ($C_{17}H_{15}CuN_3OS_2$)⁺. Elemental analysis: calculated (%) for $C_{17}H_{15}CuCl_2N_3OS_2$ C 42.90, H 3.18, N 8.83, found C 42.93, H 3.20, N 8.86.

Preparation of the coordination compound 5-(Z)-3-(2,5-difluorophenyl)-2-(methylthio)-5-(pyridin-2-ylmethylidene)-1H-imidazol-4-one 50 with copper (II) chloride dihydrate (50k). 50k was obtained as a black crystalline precipitate from 15 mg (45 μ mol) of 5-(Z)-3-(2,5-difluorophenyl)-2-(methylthio)-5-(pyridin-2-ylmethylidene)-1H-imidazol-4-one 50 and 7.6 mg (45 μ mol) of copper (II) chloride dihydrate. Yield: 5 mg (24%). HRMS calculated 393.9882 ($C_{16}H_{11}CuF_2N_3OS$)⁺, found 393.9892

($C_{16}H_{11}CuF_2N_3OS$)⁺, UV-vis (λ , nm/ ϵ , l mol⁻¹ cm⁻¹): 392/11583. $C_{16}H_{11}CuCl_2F_2N_3OS$ C 41.26, H 2.38, N 9.02, found C 41.30, H 2.41, N 9.01.

Preparation of the coordination compound 5-(Z)-3-(3,5-difluorophenyl)-2-(methylthio)-5-(pyridin-2-ylmethylidene)-1H-imidazol-4-one 51 with copper (II) chloride dihydrate (51k). 51k was obtained as a black crystalline precipitate from 15 mg (45 μ mol) of 5-(Z)-3-(3,5-difluorophenyl)-2-(methylthio)-5-(pyridin-2-ylmethylidene)-1H-imidazol-4-one 51 and 7.6 mg (45 μ mol) of copper (II) chloride dihydrate. Yield: 10 mg (47%). HRMS calculated 393.9882 ($C_{16}H_{11}CuF_2N_3OS$)⁺, found 393.9872 ($C_{16}H_{11}CuF_2N_3OS$)⁺. Elemental analysis: calculated (%) for $C_{16}H_{11}CuCl_2F_2N_3OS$ C 41.26, H 2.38, N 9.02, found C 41.33, H 2.34, N 9.40.

Preparation of the coordination compound (4Z,4'Z)-2,2'-(ethane-1,2-diyldisulfanediy)bis(4-(2-pyridylmethylidene)-1-(4-methoxyphenyl)-2,3-dihydro-4H-imidazol-5-one) 52 with copper (II) chloride dihydrate (52k). 52k was obtained as a black crystalline precipitate from 15 mg (22 μ mol) of (4Z, 4'Z)-2,2'-(ethane-1,2-diyl disulfandiy)bis(4-(2-pyridylmethylidene)-1-(4-methoxyphenyl)-2,3-dihydro-4H-imidazole-5-one) 52 as a result of reaction with 7.5 mg (44 μ mol) copper (II) chloride dihydrate. Yield: 5.1 mg (30%). MALDI: m/z = 712 52Cu⁺ 100%, 775 52Cu₂⁺ 22%. HRMS (*pos.*) calculated 711.0909 ($C_{34}H_{28}O_4N_6CuS_2$)⁺, found 711.0910 ($C_{34}H_{28}O_4N_6CuS_2$)⁺, UV-vis (λ , nm/ ϵ , l mol⁻¹ cm⁻¹): 395/31517. Elemental analysis: calculated (%) for $C_{34}H_{28}Cu_2Cl_4N_6O_4S_2$ C 44.50, H 3.08, N 9.16, found C 44.61, H 3.15, N 9.19.

Preparation of the coordination compound (4Z,4'Z)-2,2'-(ethane-1,2-diyldisulfanediy)bis(4-(2-pyridylmethylidene)-1-(4-ethoxyphenyl)-2,3-dihydro-4H-imidazol-5-one) 53 with copper (II) chloride dihydrate (53k). 53k was obtained as a black crystalline precipitate from 15 mg (23.5 μ mol) of (4Z, 4'Z)-2,2'-(ethane-1,2-diyl disulfandiy)bis(4-(2-pyridylmethylidene)-1-(4-ethoxyphenyl)-2,3-dihydro-4H-imidazole-5-one) 53 as a result of reaction with 8.1 mg (47 μ mol) of copper (II) chloride dihydrate. Yield: 6.3 mg (37%). MALDI: m/z = 739 53Cu⁺ 100%, 801 53Cu₂⁺ 23%. HRMS (*pos.*) calculated 738.1222 ($C_{36}H_{32}O_4N_6CuS_2$)⁺, found 739.1221 ($C_{36}H_{32}O_4N_6CuS_2$)⁺, UV-vis (λ , nm/ ϵ , l mol⁻¹ cm⁻¹): 395/34383. Elemental analysis: calculated (%) for $C_{36}H_{32}Cu_2Cl_4N_6O_4S_2$ C 45.72, H 3.41, N 8.89, found C 45.75, H 3.45, N 8.93.

Preparation of the coordination compound (4Z,4'Z)-2,2'-(ethane-1,2-diyldisulfanediy)bis(4-(2-pyridylmethylidene)-1-(3,4-dimethoxyphenyl)-2,3-dihydro-4H-imidazol-5-one) 54 with copper (II) chloride dihydrate (54k). 54k was obtained as a black crystalline precipitate from 15 mg (23 μ mol) of (4Z, 4'Z)-2,2'-(ethane-1,2-diyl disulfandiy)bis(4-(2-pyridylmethylidene)-1-(3,4-dimethoxyphenyl)-2,3-dihydro-4H-imidazole-5-one) 54 as a result of reaction with 8.0 mg (46 μ mol) of copper (II) chloride dihydrate. Yield: 5.1 mg (30%). MALDI: m/z = 772 54 Cu⁺ 100%, 834 54 Cu₂⁺ 15%. HRMS (*pos.*) calculated 771.1121 ($C_{36}H_{32}O_6N_6CuS_2$)⁺, found 771.1121 ($C_{36}H_{32}O_6N_6CuS_2$)⁺, UV-vis (λ , nm/ ϵ , l mol⁻¹ cm⁻¹): 395/4233. Elemental analysis: calculated (%) for $C_{36}H_{32}Cu_2Cl_4N_6O_6S_2$ C 44.22, H 3.30, N 8.60, found C 44.19, H 3.26, N 8.59.

Preparation of the coordination compound (4Z,4'Z)-2,2'-(ethane-1,2-diyldisulfanediy)bis(4-(2-pyridylmethylidene)-1-(4-*t*-butylphenyl)-2,3-dihydro-4H-imidazol-5-one) 55 with copper (II) chloride dihydrate (55k). 55k was obtained as a black crystalline precipitate from 15 mg (22 μ mol) of (4Z, 4'Z)-2,2'-(ethane-1,2-diyl disulfandiy)bis(4-(2-pyridylmethylidene)-1-(4-*t*-butylphenyl)-2,3-dihydro-4H-imidazole-5-one) 55 as a result of reaction with 7.5 mg (44 μ mol) of copper (II) chloride dihydrate. Yield: 6.1 mg (33%). MALDI: m/z = 763 55Cu⁺ 100%, 825 55Cu₂⁺ 20%. HRMS (*pos.*) calculated 763.1950 ($C_{40}H_{40}O_2N_6CuS_2$)⁺, found 763.1948 ($C_{40}H_{40}O_2N_6CuS_2$)⁺, UV-vis (λ , nm/ ϵ , l mol⁻¹ cm⁻¹): 375/46311. Elemental analysis:

calculated (%) for $C_{40}H_{40}Cu_2Cl_4N_6O_2S_2$ C 49.54, H 4.16, N 8.67, found C 49.59, H 4.20, N 8.72.

Preparation of the coordination compound (4Z,4'Z)-2,2'-(ethane-1,2-diyl disulfanediy)bis(4-(2-pyridylmethylidene)-1-(2,4,6-trimethylphenyl)-2,3-dihydro-4H-imidazol-5-one) 56 with copper (II) chloride dihydrate (56k). 56k was obtained as a black crystalline precipitate from 15 mg (22 μ mol) of (4Z, 4'Z)-2,2'-(ethane-1,2-diyl disulfandiy)bis(4-(2-pyridylmethylidene)-1-(2,4,6-trimethylphenyl)-2,3-dihydro-4H-imidazole-5-one) **56** as a result of reaction with 7.5 mg (44 μ mol) of copper (II) chloride dihydrate. Yield: 10 mg (49%) HRMS (*pos.*) calculated 718.9919 ($C_{32}H_{22}Cl_2CuN_6O_2S_2$)⁺, found 718.9883 ($C_{32}H_{22}Cl_2CuN_6O_2S_2$)⁺ Elemental analysis: calculated (%) for $C_{32}H_{22}Cu_2Cl_4N_6O_2S_2$ C 48.46, H 3.85, N 8.92, found C 48.52, H 4.10, N 8.69.

Preparation of the coordination compound (4Z,4'Z)-2,2'-(ethane-1,2-diyl disulfanediy)bis(4-(2-pyridylmethylidene)-1-(2-t-butylphenyl)-2,3-dihydro-4H-imidazol-5-one) 57 with copper (II) chloride dihydrate (57k). 57k was obtained as a black crystalline precipitate from 15 mg (22 μ mol) of (4Z, 4'Z)-2,2'-(ethane-1,2-diyl disulfandiy)bis(4-(2-pyridylmethylidene)-1-(4-tretbutylphenyl)-2,3-dihydro-4H-imidazole-5-one) **57** as a result of reaction with 7.5 mg (44 μ mol) of copper (II) chloride dihydrate. Yield: 7 mg (35%) HRMS (*pos.*) calculated 763.2023 ($C_{40}H_{41}CuN_6O_2S_2$)⁺, found 763.1978 ($C_{40}H_{41}CuN_6O_2S_2$)⁺. UV-vis (λ , nm/ ϵ , l mol⁻¹ cm⁻¹): 367/43300. Elemental analysis: calculated (%) for $C_{42}H_{48}Cu_2Cl_4N_6O_4S_2$ (**57k** + 2CH₃OH) C 48.79, H 4.68, N 8.13, found C 48.57, H 4.67, N 8.24.

Preparation of the coordination compound (4Z,4'Z)-2,2'-(ethane-1,2-diyl disulfanediy)bis(4-(2-pyridylmethylidene)-1-(4-fluorophenyl)-2,3-dihydro-4H-imidazol-5-one) 58 with copper (II) chloride dihydrate (58k). 58k was obtained as a black crystalline precipitate from 15 mg (25 μ mol) of (4Z, 4'Z)-2,2'-(ethane-1,2-diyl disulfandiy)bis(4-(2-pyridylmethylidene)-1-(4-fluorophenyl)-2,3-dihydro-4H-imidazole-5-one) **58** as a result of reaction with 8.5 mg (50 μ mol) of copper (II) chloride dihydrate. Yield: 5.8 mg (30%). MALDI: m/z = 687 **58Cu**⁺ 100%, 750 **58Cu**₂⁺ 10%. HRMS (*pos.*) calculated 739.1034 ($C_{32}H_{22}O_2N_6CuF_2S_2$ + CH₃OH + H₂O)⁺, found 739.1253 ($C_{32}H_{22}O_2N_6CuF_2S_2$ + CH₃OH + H₂O)⁺, UV-vis (λ , nm/ ϵ , l mol⁻¹ cm⁻¹): 470/37109. Elemental analysis: calculated (%) for $C_{32}H_{22}Cu_2Cl_3F_2N_6O_2S_2$ C 44.79, H 2.58, N 9.79, found C 44.85, H 2.60, N 9.82.

Preparation of the coordination compound (4Z,4'Z)-2,2'-(ethane-1,2-diyl disulfanediy)bis(4-(2-pyridylmethylidene)-1-(3-fluorophenyl)-2,3-dihydro-4H-imidazol-5-one) 59 with copper (II) chloride dihydrate (59k). 59k was obtained as a black crystalline precipitate from 15 mg (25 μ mol) of (4Z, 4'Z)-2,2'-(ethane-1,2-diyl disulfandiy)bis(4-(2-pyridylmethylidene)-1-(3-fluorophenyl)-2,3-dihydro-4H-imidazole-5-one) **59** as a result of reaction with 8.5 mg (50 μ mol) of copper (II) chloride dihydrate. Yield: 5.9 mg (32%). MALDI: m/z = 686 **59Cu**⁺ 100%, 749 **59Cu**₂⁺ 13%. HRMS (*pos.*) calculated 739.1034 ($C_{32}H_{22}O_2N_6CuF_2S_2$ + CH₃OH + H₂O)⁺, found 739.1233 ($C_{32}H_{22}O_2N_6CuF_2S_2$ + CH₃OH + H₂O)⁺, UV-vis (λ , nm/ ϵ , l mol⁻¹ cm⁻¹): 395/24800. Elemental analysis: calculated (%) for $C_{32}H_{22}Cu_2Cl_3F_2N_6O_2S_2$ C 44.79, H 2.58, N 9.79, found C 44.81, H 2.63, N 9.81.

Preparation of the coordination compound (4Z,4'Z)-2,2'-(ethane-1,2-diyl disulfanediy)bis(4-(2-pyridylmethylidene)-1-(2-fluorophenyl)-2,3-dihydro-4H-imidazol-5-one) 60 with copper (II) chloride dihydrate (60k). 60k was obtained as a black crystalline precipitate from 15 mg (25 μ mol) of (4Z, 4'Z)-2,2'-(ethane-1,2-diyl disulfandiy)bis(4-(2-pyridylmethylidene)-1-(2-fluorophenyl)-2,3-dihydro-4H-imidazole-5-one) **60** as a result of reaction with 8.5 mg (50 μ mol) of copper (II) chloride dihydrate. Yield: 6.1 mg (33%). MALDI: m/z = 687 **60Cu**⁺ 100%, 750 **60Cu**₂⁺ 16%. HRMS (*pos.*) calculated 739.1034 ($C_{32}H_{22}O_2N_6CuF_2S_2$ + CH₃OH + H₂O)⁺, found 739.1053 ($C_{32}H_{22}O_2N_6CuF_2S_2$ + CH₃OH + H₂O)⁺, UV-vis (λ , nm/ ϵ , l mol⁻¹ cm⁻¹): 364/36150. Elemental analysis: calculated (%) for $C_{32}H_{22}Cu_2Cl_3F_2N_6O_2S_2$ C 44.79, H 2.58, N 9.79, found C 44.85, H 2.67, N 9.83.

Preparation of the coordination compound (4Z,4'Z)-2,2'-(ethane-1,2-diyl disulfanediy)bis(4-(2-pyridylmethylidene)-1-(3-bromophenyl)-2,3-dihydro-4H-imidazol-5-one) 61 with copper (II) chloride dihydrate (61k). 61k was obtained as a black crystalline precipitate from 15 mg (21 μ mol) of (4Z, 4'Z)-2,2'-(ethane-1,2-diyl disulfandiy)bis(4-(2-pyridylmethylidene)-1-(3-bromophenyl)-2,3-dihydro-4H-imidazole-5-one) **61** as a result of reaction with 7.0 mg (42 μ mol) of copper (II) chloride dihydrate. Yield: 5.7 mg (30%). MALDI: m/z = 806 **61Cu**⁺ 100%, 869 **61Cu**₂⁺ 5%. HRMS (*pos.*) calculated 858.9433 ($C_{32}H_{22}O_2N_6CuBr_2S_2$ + CH₃OH + H₂O)⁺, found 858.9431 ($C_{32}H_{22}O_2N_6CuBr_2S_2$ + CH₃OH + H₂O)⁺, UV-vis (λ , nm/ ϵ , l mol⁻¹ cm⁻¹): 395/28600. Elemental analysis: calculated (%) for $C_{32}H_{22}Cu_2Cl_3Br_2N_6O_2S_2$ C 39.22, H 2.26, N 8.58, found C 39.25, H 2.26, N 8.60.

Preparation of the coordination compound (4Z,4'Z)-2,2'-(ethane-1,2-diyl disulfanediy)bis(4-(2-pyridylmethylidene)-1-(2-bromophenyl)-2,3-dihydro-4H-imidazol-5-one) 62 with copper (II) chloride dihydrate (62k). 62k was obtained as a black crystalline precipitate from 15 mg (21 μ mol) of (4Z, 4'Z)-2,2'-(ethane-1,2-diyl disulfandiy)bis(4-(2-pyridylmethylidene)-1-(2-bromophenyl)-2,3-dihydro-4H-imidazole-5-one) **62** as a result of reaction with 7.0 mg (42 μ mol) of copper (II) chloride dihydrate. Yield: 6.1 mg (33%). MALDI: m/z = 806 **62Cu**⁺ 100%, 870 **62Cu**₂⁺ 5%. HRMS (*pos.*) calculated 858.9433 ($C_{32}H_{22}O_2N_6CuBr_2S_2$ + CH₃OH + H₂O)⁺, found 858.9435 ($C_{32}H_{22}O_2N_6CuBr_2S_2$ + CH₃OH + H₂O)⁺, UV-vis (λ , nm/ ϵ , l mol⁻¹ cm⁻¹): 395/36083. Elemental analysis: calculated (%) for $C_{32}H_{22}Cu_2Cl_3Br_2N_6O_2S_2$ C 39.22, H 2.26, N 8.58, found C 39.24, H 2.25, N 8.61.

Preparation of the coordination compound (4Z,4'Z)-2,2'-(ethane-1,2-diyl disulfanediy)bis(4-(2-pyridylmethylidene)-1-(2-chlorophenyl)-2,3-dihydro-4H-imidazol-5-one) 63 with copper (II) chloride dihydrate (63k). 63k was obtained as a black crystalline precipitate from 15 mg (23.5 μ mol) of (4Z, 4'Z)-2,2'-(ethane-1,2-diyl disulfandiy)bis(4-(2-pyridylmethylidene)-1-(2-chlorophenyl)-2,3-dihydro-4H-imidazole-5-one) **63** as a result of reaction with 8.0 mg (47 μ mol) of copper (II) chloride dihydrate. Yield: 5.7 mg (32%). MALDI: m/z = 717 **63Cu**⁺ 100%, 781 **63Cu**₂⁺ 15%. HRMS (*pos.*) calculated 771.0443 ($C_{32}H_{22}O_2N_6CuCl_2S_2$ + CH₃OH + H₂O)⁺, found 771.0440 ($C_{32}H_{22}O_2N_6CuCl_2S_2$ + CH₃OH + H₂O)⁺, UV-vis (λ , nm/ ϵ , l mol⁻¹ cm⁻¹): 370/10874. Elemental analysis: calculated (%) for $C_{32}H_{22}Cu_2Cl_5N_6O_2S_2$ C 43.13, H 2.49, N 9.43, found C 43.17, H 2.51, N 9.41.

Preparation of the coordination compound (4Z,4'Z)-2,2'-(ethane-1,2-diyl disulfanediy)bis(4-(2-pyridylmethylidene)-1-(2-methoxy-4-chloro-5-methylphenyl)-2,3-dihydro-4H-imidazol-5-one) 64 with copper (II) chloride dihydrate (64k). 64k was obtained as a black crystalline precipitate from 15 mg (23.5 μ mol) of (4Z, 4'Z)-2,2'-(ethane-1,2-diyl disulfandiy)bis(4-(2-pyridylmethylidene)-1-(2-methoxy-4-chloro-5-methylphenyl)-2,3-dihydro-4H-imidazole-5-one) **64** as a result of reaction with 8.0 mg (47 μ mol) of copper (II) chloride dihydrate. Yield: (after purification by column chromatography CH₂Cl₂:MeOH 40:1) 6.1 mg (31%). HRMS (*pos.*) calculated 808.0516 ($C_{36}H_{31}Cl_2CuN_6O_4S$)⁺, found 808.0518 ($C_{36}H_{31}Cl_2CuN_6O_4S$)⁺. UV-vis (λ , nm/ ϵ , l mol⁻¹ cm⁻¹): 367/45000. Elemental analysis: calculated (%) for $C_{43}H_{47}Cu_2Cl_6N_7O_6S_2$ (**64k** + 2Et₂O + CH₃OH + CH₃CN): C 44.45, H 4.08, N 8.44, found C 44.14, H 4.02, N 8.33.

Preparation of the coordination compound (4Z,4'Z)-2,2'-(ethane-1,2-diyl disulfanediy)bis(4-(2-pyridylmethylidene)-1-(2-bromo-4-fluorophenyl)-2,3-dihydro-4H-imidazol-5-one) 65 with copper (II) chloride dihydrate (65k). 65k was obtained as a black crystalline precipitate from 15 mg (21 μ mol) of (4Z, 4'Z)-2,2'-(ethane-1,2-diyl disulfandiy)bis(4-(2-pyridylmethylidene)-1-(2-bromo-4-fluorophenyl)-2,3-dihydro-4H-imidazole-5-one) **65** as a result of reaction with 7.0 mg (42 μ mol) of copper (II) chloride dihydrate. Yield: 8.2 mg (32%) HRMS (*pos.*) calculated 845.8817 ($C_{32}H_{21}Br_2CuF_2N_6O_2S_2$)⁺, found 845.8860 ($C_{32}H_{21}Br_2CuF_2N_6O_2S_2$)⁺. UV-vis (λ , nm/ ϵ , l mol⁻¹ cm⁻¹): 367/44700. Elemental analysis: calculated (%) for

$C_{32}H_{20}Cu_2Cl_3Br_2F_2N_6O_2S_2$ C 37.83, H 1.98, N 8.27, found C 37.89, H 2.10, N 8.34.

Preparation of the coordination compound (4Z,4'Z)-2,2'-(ethane-1,2-diyl disulfanediy)bis(4-(2-pyridylmethylidene)-1-(2,5-difluorophenyl)-2,3-dihydro-4H-imidazol-5-one) 66 with copper (II) chloride dihydrate (66k). 66k was obtained as a black crystalline precipitate from 15 mg (23 μ mol) of (4Z, 4'Z)-2,2'-(ethane-1,2-diyl disulfandiy)bis(4-(2-pyridylmethylidene)-1-(2,5-difluorophenyl)-2,3-dihydro-4H-imidazole-5-one) 66 as a result of reaction with 7.0 mg (45 μ mol) of copper (II) chloride dihydrate in boiling butanol-1. After solvent evaporation, solid residue was washed with MeOH and dried on air. Yield: 5 mg (24%) HRMS (*pos.*) calculated 723.0316 ($C_{32}H_{20}CuF_4N_6O_2S_2$)*, found 723.0308 ($C_{32}H_{20}CuF_4N_6O_2S_2$)*. Elemental analysis: calculated (%) for $C_{32}H_{20}Cu_2Cl_3F_4N_6O_2S_2$ C 42.99, H 2.25, N 9.40, found C 43.19, H 2.36, N 9.36.

Preparation of the coordination compound (4Z,4'Z)-2,2'-(ethane-1,2-diyl disulfanediy)bis(4-(2-pyridylmethylidene)-1-(3,5-difluorophenyl)-2,3-dihydro-4H-imidazol-5-one) 67 with copper (II) chloride dihydrate (67k). 67k was obtained as a black crystalline precipitate from 15 mg (23 μ mol) of (4Z, 4'Z)-2,2'-(ethane-1,2-diyl disulfandiy)bis(4-(2-pyridylmethylidene)-1-(3,5-difluorophenyl)-2,3-dihydro-4H-imidazole-5-one) 67 as a result of reaction with 7.0 mg (45 μ mol) of copper (II) chloride dihydrate in boiling butanol-1. After solvent evaporation, solid residue was washed with MeOH and dried on air. Yield: 9 mg (41%) HRMS (*pos.*) calculated 723.0316 ($C_{32}H_{20}CuF_4N_6O_2S_2$)*, found 723.0323 ($C_{32}H_{20}CuF_4N_6O_2S_2$)*. Elemental analysis: calculated (%) for $C_{32}H_{20}Cu_2Cl_3F_4N_6O_2S_2$ C 42.99, H 2.25, N 9.40, found C 43.14, H 2.41, N 9.58.

Preparation of the coordination compound (4Z,4'Z)-2,2'-(ethane-1,2-diyl disulfanediy)bis(4-(2-pyridylmethylidene)-1-(2-methyl-3-chlorophenyl)-2,3-dihydro-4H-imidazol-5-one) 68 with copper (II) chloride dihydrate (68k). 68k was obtained as a black crystalline precipitate from 15 mg (21 μ mol) of (4Z, 4'Z)-2,2'-(ethane-1,2-diyl disulfandiy)bis(4-(2-pyridylmethylidene)-1-(2-methyl-3-chlorophenyl)-2,3-dihydro-4H-imidazole-5-one) 68 as a result of reaction with 7.1 mg (42 μ mol) of copper (II) chloride dihydrate. Yield: 11 mg (55%) HRMS (*pos.*) calculated 743.0453 ($C_{34}H_{28}CuN_6O_2S_2$)*, found 743.0453 ($C_{34}H_{28}CuN_6O_2S_2$)*, UV-vis (λ , nm/ ϵ , l mol⁻¹ cm⁻¹): 395/25000. Elemental analysis: calculated (%) for $C_{34}H_{26}Cu_2Cl_5N_6O_2S_2$ C 44.43, H 2.85, N 9.14, found C 44.49, H 2.97, N 9.05.

Preparation of the coordination compound (4Z,4'Z)-2,2'-(ethane-1,2-diyl disulfanediy)bis(4-(2-pyridylmethylidene)-1-(4-methylthiophenyl)-2,3-dihydro-4H-imidazol-5-one) 69 with copper (II) chloride dihydrate (69k). 69k was obtained as a black crystalline precipitate from 15 mg (22 μ mol) of (4Z, 4'Z)-2,2'-(ethane-1,2-diyl disulfandiy)bis(4-(2-pyridylmethylidene)-1-(4-methylthiophenyl)-2,3-dihydro-4H-imidazole-5-one) 69 as a result of reaction with 7.5 mg (44 μ mol) of copper (II) chloride dihydrate. Yield: 10 mg (50%) HRMS (*pos.*) calculated 743.0453 ($C_{34}H_{28}CuN_6O_2S_4$)*, found 743.0453 ($C_{34}H_{28}CuN_6O_2S_4$)*. Elemental analysis: calculated (%) for $C_{34}H_{28}Cu_2Cl_3N_6O_2S_4$ C 44.66, H 3.09, N 9.19, found 44.87, H 3.19, N 9.08.

Preparation of the coordination compound (4Z,4'Z)-2,2'-(ethane-1,2-diyl disulfanediy)bis(4-(2-pyridylmethylidene)-1-(3-chlorophenyl)-2,3-dihydro-4H-imidazol-5-one) 70 with copper (II) chloride dihydrate (70k). 70k was obtained as a red crystalline precipitate from 15 mg (22 μ mol) of (4Z, 4'Z)-2,2'-(ethane-1,2-diyl disulfandiy)bis(4-(2-pyridylmethylidene)-1-(3-chlorophenyl)-2,3-dihydro-4H-imidazole-5-one) 70 as a result of reaction with 7.6 mg (45 μ mol) of copper (II) chloride dihydrate. Yield: 8 mg (36%) HRMS (*pos.*) calculated 718.9919 ($C_{32}H_{22}Cl_2CuN_6O_2S_2$)*, found 718.9883 ($C_{32}H_{22}Cl_2CuN_6O_2S_2$)*, UV-vis (λ , nm/ ϵ , l mol⁻¹ cm⁻¹): 395/16400. Elemental analysis: calculated (%) for $C_{32}H_{22}Cu_2Cl_4N_6O_2S_2$ C 44.92, H 2.59, N 9.82, found C 45.17, H 2.63, N 9.75.

Preparation of the coordination compound (4Z,4'Z)-2,2'-(ethane-1,2-diyl disulfanediy)bis(4-(2-pyridylmethylidene)-1-(4-bromophenyl)-2,3-dihydro-4H-imidazol-5-one) 71 with copper (II) chloride dihydrate (71k). 71k was obtained as a red crystalline precipitate from 15 mg (21 μ mol) of (4Z, 4'Z)-2,2'-(ethane-1,2-diyl disulfandiy)bis(4-(2-pyridylmethylidene)-1-(4-bromophenyl)-2,3-dihydro-4H-imidazole-5-one) 71 as a result of reaction with 7.0 mg (42 μ mol) of copper (II) chloride dihydrate. Yield: 6.3 mg (35%). MALDI: m/z = 809 71Cu⁺ 100%. HRMS (*pos.*) calculated 858.9433 ($C_{32}H_{22}O_2N_6CuBr_2S_2 + CH_3OH + H_2O$)*, found 858.9443 ($C_{32}H_{22}O_2N_6CuBr_2S_2 + CH_3OH + H_2O$)*, UV-vis (λ , nm/ ϵ , l mol⁻¹ cm⁻¹): 395/28967. Elemental analysis: calculated (%) for $C_{32}H_{22}Cu_2Cl_2Br_2N_6O_2S_2$ C 40.69, H 2.35, N 8.90, found C 40.47, H 2.10, N 8.73.

Preparation of the coordination compound (4Z,4'Z)-2,2'-(ethane-1,2-diyl disulfanediy)bis(4-(2-pyridylmethylidene)-1-(4-chlorophenyl)-2,3-dihydro-4H-imidazol-5-one) 72 with copper (II) chloride dihydrate (72k). 72k was obtained as a dark-red crystalline precipitate from 15 mg (23.5 μ mol) of (4Z, 4'Z)-2,2'-(ethane-1,2-diyl disulfandiy)bis(4-(2-pyridylmethylidene)-1-(4-chlorophenyl)-2,3-dihydro-4H-imidazole-5-one) 72 as a result of reaction with 8.0 mg (47 μ mol) copper (II) chloride dihydrate. Yield: 6.1 mg (33%). MALDI: m/z = 718 72Cu⁺ 100%, 781 72 Cu²⁺ 23%. HRMS (*pos.*) calculated 771.0443 ($C_{32}H_{22}O_2N_6CuCl_2S_2 + CH_3OH + H_2O$)*, found 771.0433 ($C_{32}H_{22}O_2N_6CuCl_2S_2 + CH_3OH + H_2O$)*, UV-vis (λ , nm/ ϵ , l mol⁻¹ cm⁻¹): 395/36967. Elemental analysis: calculated (%) for $C_{32}H_{22}Cu_2Cl_4N_6O_2S_2$ C 44.92, H 2.59, N 9.82, found C 44.95, H 2.49, N 9.90.

Preparation of the coordination compound (4Z,4'Z)-2,2'-(ethane-1,2-diyl disulfanediy)bis(4-(2-pyridylmethylidene)-1-(3-chloro-4-fluorophenyl)-2,3-dihydro-4H-imidazol-5-one) 73 with copper (II) chloride dihydrate (73k). 73k was obtained as a dark-brown crystalline precipitate from 15 mg (21 μ mol) of (4Z, 4'Z)-2,2'-(ethane-1,2-diyl disulfandiy)bis(4-(2-pyridylmethylidene)-1-(3-chloro-4-fluorophenyl)-2,3-dihydro-4H-imidazole-5-one) 73 as a result of reaction with 7.1 mg (42 μ mol) of copper (II) chloride dihydrate. Yield: 3 mg (15%). HRMS (*pos.*) calculated 754.9730 ($C_{32}H_{20}Cl_2CuF_2N_6O_2S_2$)*, found 754.9724 ($C_{32}H_{20}Cl_2CuF_2N_6O_2S_2$)*. Elemental analysis: calculated (%) for $C_{32}H_{22}Cu_2Cl_4F_2N_6O_2S_2$ C 43.11, H 2.26, N 9.43, found C 43.42, H 2.51, N 9.35.

AUTHOR INFORMATION

Corresponding Author

* Dr Olga O. Krasnovskaya krasnovskayao@gmail.com

Author Contributions

The manuscript was written through contributions of all authors. All authors have given approval to the final version of the manuscript. *These authors contributed equally.

Funding Sources

Ministry of Education and Science of the Russian Federation, Russian Science Foundation, Russian Foundation for Basic Research.

ACKNOWLEDGMENTS

The synthesis and characterization of coordination compounds was supported by the Ministry of Education and Science of the Russian Federation in the framework of the Increase Competitiveness Program of NUST 'MISIS' implemented by a governmental decree dated 16 March 2013, No. 211.

The Pt-nanoelectrode and spheroid experiments were supported by the Russian Science Foundation (Grant No. 19-74-10059)

The electrochemical study was supported by the Russian Foundation for Basic Research supported (Grant No. 19-29-08007).

The MTT and DNA experiments were supported by the Russian Foundation for Basic Research (Grant No. 18-29-08060).

ABBREVIATIONS

CDDP, Cisplatin; CA-755, Mammary adenocarcinoma cell line; UV-Vis, Ultraviolet-visible spectroscopy; XANES, X-ray absorption near edge structure; eV, Electron Volt; RDE, Rotating Disk Electrode; MCF-7, Michigan Cancer Foundation-7, breast cancer cell line; HEK-293, Human embryonic kidney 293 cell line; A549, Adenocarcinomic human alveolar basal epithelial cell line; Va-13, Human transformed fibroblast cell line; 4T1, murine mammary carcinoma cell line from a BALB/cfC3H mouse; AAS, Atomic absorption spectroscopy; ICP-MS, inductively coupled plasma mass spectrometry; uUc18, Plasmid DNA; EB, Ethidium bromide; FITC/PI, Fluorescein Isothiocyanate/Propidium Iodide; Epa, Anodic peak potential; Epc, Cathodic peak potential; G-SH, Glutathione; i.v., Intravenous; MTS, 3-(4,5-dimethylthiazol-2-yl)-5-(3-carboxymethoxyphenyl)-2-(4-sulfophenyl)-2H-tetrazolium dye; FBS, Fetal bovine serum; EGTA, Ethylene glycol tetraacetic acid; Hepes, N-2-Hydroxyethylpiperazine-N'-2-Ethanesulfonic Acid.

ASSOCIATED CONTENT

Supporting Information

The Supporting Information is available free of charge on the ACS Publications website at DOI:.

UV-Vis data of selected coordination compounds, stability studies of selected coordination compounds, additional crystallographic data for **3k**, **35k**, **41k**, **46k**, **72k**.

XANES Spectra for Type 1, 2 coordination compounds, comparison of different XANES spectra of Type 3 coordination compounds.

Electrochemical data, typical CV and RDE voltammograms of type 1-3 organic ligands and coordination compounds.

EPR spectroscopy data for coordination compounds **56k**, **59k**.

MTT data for organic ligands **1** – **73** after 72h of incubation, cellular accumulation/distribution data of selected coordination compounds in 4T1 cells (ICP-MS), gel electrophoresis data (DNA cleavage assay) of selected coordination compounds, DNA intercalation (competitive binding) data (changes in the fluorescence spectra of human DNA/EB in the presence of increasing concentrations of selected coordination compounds), DNA intercalation constants, BSA binding data (changes in the fluorescence spectra of BSA in the presence of increasing concentrations of selected organic ligands and coordination compounds), concentration constants of stability of the BSA conjugate with selected organic ligands and coordination compounds, the number of binding sites evaluated by Stern-Volmer method, telomerase inhibition rate after incubation with selected coordination compounds, apoptosis analysis of MCF-7 cells (Annexin V-FITC/PI staining) after treatment with selected coordination compounds (values in %).

Fluorescent-based ROS level measurement in MCF-7 cells treated with selected coordination compounds (Fluorescent microphotograph of MCF-7 cells, Cell Rox Deep Red Assay). Calibration line of the platinum electrode used to determine the concentration of H₂O₂ in solution, microphotographs of intracellular measurement of ROS in MCF-7 cells by nanoelectrode, voltammogram before and after penetration of Pt-nanoelectrode into MCF-7 cell, microphotographs of intracellular detection of ROS in MCF-7 spheroids, preincubated with coordination compounds, dose-effect curves for survival of 3D cultures (spheroids).

¹H NMR all target compounds, ¹³C NMR spectra for representative target compounds, and HPLC assessment of purity for target compounds. (PDF)

Molecular formula strings (CSV)

REFERENCES

- (1) Abdel-Mohsen M. A.; Toson E. A.; Helal M. A.; Oncostatic treatment effect of triple negative breast cancer cell line with copper-nicotinate complex. *J. Cell. Biochem.* **2019**, *120*, 3, 4278-4290.
- (2) Chen W.; Yang W.; Chen P.; Huang Y.; Li F. Disulfiram copper nanoparticles prepared with a stabilized metal ion ligand complex method for treating drug-resistant prostate cancers. *ACS Appl. Mater. Interfaces.* **2018**, *10*, 48, 41118-41128.
- (3) Xin C.; Xiaolan Z.; Jinghong C.; Qianqian Y.; Li Y.; Dacai X.; Peiquan Z.; Xuejun W.; Jinbao L. Hinokitiol copper complex inhibits proteasomal deubiquitination and induces paraptosis-like cell death in human cancer cells. *Eur. J. Pharmacol.* **2017**, *815*, 147-155.
- (4) Zeeshan M.; Murugadas A.; Ghaskadbi S.; Rajendran R. B.; Akbarsha M. A. ROS dependent copper toxicity in Hydra-biochemical and molecular study. *Comp. Biochem. Physiol. C: Toxicol. Pharmacol.* **2016**, *185*, 1-12.
- (5) Qin Q.-P.; Meng T.; Tan M.-X.; Liu Y.-C.; Luo X.-J.; Zou B.-Q.; Liang H. Synthesis, crystal structure and biological evaluation of a new dasatinib copper(II) complex as telomerase inhibitor. *Eur. J. Med. Chem.* **2018**, *143*, 1597-1603.
- (6) Fatfat M.; Merhi R. A.; Rahal O.; Stoyanovsky D. A.; Zaki A.; Haidar H.; Kagan V. E.; Gali-Muhtasib H.; Machaca K. Copper chelation selectively kills colon cancer cells through redox cycling and generation of reactive oxygen species. *BMC Cancer.* **2014**, *14*, 527-539.
- (7) Kremer M. L. Mechanism of the Fenton reaction. Evidence for a new intermediate. *Phys. Chem. Chem. Phys.* **1999**, *1*, 3595-3605.
- (8) Sangeetha S.; Murali M. Non-covalent DNA binding, protein interaction, DNA cleavage and cytotoxicity of [Cu(quamol)Cl]·H₂O. *Int. J. Biol. Macromol.* **2018**, *107*, Part B, 2501-2511.
- (9) Cvek B. Comment on 'Cytotoxic effect of disulfiram/copper on human glioblastoma cell lines and ALDH-positive cancer-stem-like cells. *Br. J. Cancer.* **2013**, *108*, 993.
- (10) Beeton M. L.; Aldrich-Wright J. R.; Bolhuis A. The antimicrobial and antibiofilm activities of copper(II) complexes. *J. Inorg. Biochem.* **2014**, *140*, 167-172.
- (11) Shah S.; Dalecki A. G.; Malalasekera A. P.; Crawford C. L.; Michalek S. M.; Kutsch O.; Sun J.; Bossmann S. H.; Wolschendorf F. 8-Hydroxyquinolines are boosting agents of copper-related toxicity in Mycobacterium tuberculosis. *Antimicrob. Agents Chemother.* **2016**, *60*, 10, 5765-5776.
- (12) Gokhale N. H.; Padhye S. B.; Billington D. C.; Rathbone D. L.; Croft S. L.; Kendrick H. D.; Anson C. E.; Powell A. K. Synthesis and characterization of copper(II) complexes of pyridine-2-carboxamidrazones as potent antimalarial agents. *Inorg. Chim. Acta.* **2003**, *349*, 23-29.
- (13) Shoaib A. F.; El-Bindary A. A.; El-Ghamaz N. A.; Rezk G. N. Synthesis, characterization, DNA binding and antitumor activities of Cu(II) complexes. *J. Mol. Liq.* **2018**, *269*, 619-638.
- (14) Hussain A.; Al Ajmi M. F.; Rehman Md. T.; Amir S.; Husain F. M.; Alsalmeh A.; Siddiqui M. A.; AlKhedhairi A. A.; Khan R. A. Copper(II) complexes as potential anticancer and nonsteroidal anti-inflammatory agents: *In vitro* and *in vivo* studies. *Sci. Rep.* **2019**, *9*, 5237.
- (15) Bonnitcha P. D.; Bayly S. R.; Theobald M. B. M.; Betts H. M.; Lewis J. S.; Dilworth J. R. Nitroimidazole conjugates of bis (thiosemicarbazone) ⁶⁴Cu (II) – Potential combination agents for the PET imaging of hypoxia. *J. Inorg. Biochem.* **2010**, *104*, 126-135.
- (16) Lim S. C.; Paterson B. M.; Fodero-Tavoletti M. T.; O'Keefe G. J.; Cappai R.; Barnham K. J.; Villemagne V. L.; Donnelly P. S. A copper radiopharmaceutical for diagnostic imaging of Alzheimer's disease: a bis(thiosemicarbazone)copper(II) complex that binds to amyloid-β plaques. *Chem. Commun.* **2010**, 46, 5437-5439.
- (17) Hickey J. L.; Lim S. C.; Hayne D. J.; Paterson B. M.; White J. M.; Villemagne V. L.; Roselt P.; Binns D.; Cullinane C.; Jeffery C. M.; Price R. I.; Barnham K. J.; Donnelly P. S. Diagnostic imaging agents for Alzheimer's disease: copper radiopharmaceuticals that target Aβ plaques. *J. Am. Chem. Soc.* **2013**, *135*, 16120-16132.
- (18) McInnes L. E.; Noor A.; Kysenius K.; Cullinane C.; Roselt P.; McLean C. A.; Chiu F. C. K.; Powell A. K.; Crouch P. J.; White J. M.; Donnelly P. S. Potential diagnostic imaging of Alzheimer's disease with copper-64 complexes that bind to amyloid-β plaques. *Inorg. Chem.* **2019**, *58*, 5, 3382-3395.
- (19) Krasnovskaya O. O.; Naumov A. E.; Guk D. A.; Gorelkin P. V.; Erofeev A. S.; Beloglazkina E. K.; Majouga A. G. Copper coordination compounds as biologically active agents. *Int. J. Mol. Sci.* **2020**, *21*, 11, 3965.
- (20) Carcelli M.; Tegoni M.; Bartoli J.; Marzano C.; Pelosi G.; Salvalaio M.; Rogolino D.; Gandin V. *In vitro* and *in vivo* anticancer

activity of tridentate thiosemicarbazone copper complexes: Unravelling an unexplored pharmacological target. *Eur. J. Med. Chem.* **2020**, *194*, 112266–112281.

(21) U.S. National Library of Medicine. <https://Clinicaltrials.gov> (Identifier: NCT03323346).

(22) U.S. National Library of Medicine. <https://ClinicalTrials.gov> (Identifier: NCT03950830).

(23) U.S. National Library of Medicine. <https://ClinicalTrials.gov> (Identifier: NCT04265274).

(24) Zhang R.; Qin X.; Kong F.; Chen P.; Pan G. Improving cellular uptake of therapeutic entities through interaction with components of cell membrane. *Drug Deliv.* **2019**, *26*, 1, 328–342.

(25) Haas K. L.; Franz K. J. Application of metal coordination chemistry to explore and manipulate cell biology. *Chem. Rev.* **2009**, *109*, 10, 4921–4960.

(26) Pellei M.; Gandin V.; Cimarelli C.; Quaglia W.; Mosca N.; Bagnarelli L.; Marzano C.; Santini C. Syntheses and biological studies of nitroimidazole conjugated heteroscorpionate ligands and related Cu(I) and Cu(II) complexes. *J. Inorg. Biochem.* **2018**, *187*, 33–40.

(27) Khan S. I.; Ahmad S.; Altaf A. A.; Rauf M. K.; Badshah A.; Azam S. S.; Tahir M. N. Heteroleptic copper(I) halides with triphenylphosphine and acetylthiourea: synthesis, characterization and biological studies (experimental and molecular docking). *New J. Chem.* **2019**, *43*, 19318–19330.

(28) Trachootham D.; Lu W.; Ogasawara M. A.; Nilsa R. D.; Huang P. Redox regulation of cell survival. *Antioxid. Redox Signal.* **2008**, *10*, 8, 1343–1374.

(29) Ambundo E. A.; Deydier M.-V.; Grall A. J.; Agüera-Vega N.; Dressel L. T.; Cooper T. H.; Heeg M. J.; Ochrymowycz L. A.; Rorabacher D. B. Influence of coordination geometry upon copper(II/I) redox potentials. physical parameters for twelve copper tripodal ligand complexes. *Inorg. Chem.* **1999**, *38*, 19, 4233–4242.

(30) Majouga A. G.; Zvereva M. I.; Rubtsova M. P.; Skvortsov D. A.; Mironov A. V.; Azhibek D. M.; Krasnovskaya O. O.; Gerasimov V. M.; Udina A. V.; Vorozhtsov N. I.; Beloglazkina E. K.; Agron L.; Mikhina L. V.; Tretyakova A. V.; Zyk N. V.; Zefirov N. S.; Kabanov A. V.; Dontsova O. A. Mixed valence copper(I,II) binuclear complexes with unexpected structure: synthesis, biological properties and anticancer activity. *J. Med. Chem.* **2014**, *57*, 14, 6252–6258.

(31) Beloglazkina E. K.; Majouga A. G.; Mironov A. V.; Yudina A. V.; Moiseeva A. A.; Lebedeva M. A.; Khlobystov A. N.; Zyk N. V. Synthesis, X-ray crystallography and electrochemistry of three novel copper complexes with imidazole-containing hydantoin and thiohydantoins. *Polyhedron.* **2013**, *63*, 15–20.

(32) Beloglazkina E. K.; Krasnovskaya O. O.; Guk D. A.; Tafeenko V. A.; Moiseeva A. A.; Zyk N. V.; Majouga A. G. Synthesis, characterization and cytotoxicity of binuclear copper(II) complexes with tetradentate nitrogen-containing ligands bis-5-(2-pyridylmethylidene)-3,5-dihydro-4h-imidazol-4-ones. *Polyhedron.* **2018**, *148*, 129–137.

(33) Chen C. L.; Dong C. L.; Asokan K.; Chern G.; Chang C. L. Electronic structure of Cr doped Fe304 thin films by X-ray absorption near-edge structure spectroscopy. *Solid State Commun.* **2018**, *272*, 48–52.

(34) Tougeri A.; Berrier E.; Mamede A.-S.; LaFontaine C.; Briois V.; Joly Y.; Payen E.; Paul J.-F.; Cristol S. Synergy between XANES spectroscopy and DFT to elucidate the amorphous structure of heterogeneous catalysts: TiO₂-supported molybdenum oxide catalysts. *Angew. Chem. Int. Ed.* **2013**, *52*, 6440–6444.

(35) Halvagar M. R.; Solntsev P. V.; Lim H.; Hedman B.; Hodgson K. O.; Solomon E. I.; Cramer C. J.; Tolman W. B. Hydroxo-bridged dicopper(II,III) and (III,III) complexes: models for putative intermediates in oxidation catalysis. *J. Am. Chem. Soc.* **2014**, *136*, 20, 7269–7272.

(36) Schneider J. D.; Smith B. A.; Williams G. A.; Powell D. R.; Perez F.; Rowe G. T.; Yang L. Synthesis and characterization of Cu(II) and mixed-valence Cu(I)Cu(II) clusters supported by pyridylamide ligands. *Inorg. Chem.* **2020**, *59*, 8, 5433–5446.

(37) Prosser K. E.; Walsby C. J. Electron paramagnetic resonance as a tool for studying the mechanisms of paramagnetic anticancer metallodrugs. *Eur. J. Inorg. Chem.* **2017**, 1573–1585.

(38) Kalinina M. A.; Skvortsov D. A.; Rubtsova M. P.; Komarova E. S.; Dontsova O. A. Cytotoxicity test based on human cells labeled with fluorescent proteins: fluorimetry, photography, and scanning for high-throughput assay. *Mol. Imag. Biol.* **2018**, *20*, 368–377.

(39) Chakravarty A. R.; Anreddy P. A. N.; Santra B. K.; Thomas A. M. Copper complexes as chemical nucleases. *J. Chem. Sci.* **2002**, *114*, 4, 391–401.

(40) Zuin Fantoni N.; Molphy Z.; Slator C.; Menounou G.; Toniolo G.; Mitrikas G.; McKee V.; Chatgililoglu C.; Kellett A.

Polypyridyl-based copper phenanthrene complexes: a new type of stabilized artificial chemical nuclease. *Chemistry.* **2019**, *25*, 1, 221–237.

(41) Molphy Z.; Montagner D.; Bhat S. S.; Slator C.; Long C.; Erxleben A.; Kellett A. A phosphate-targeted dinuclear Cu(II) complex combining major groove binding and oxidative DNA cleavage. *Nucleic Acids Res.* **2018**, *46*, 9918–9931.

(42) Alagesan M.; Bhuvanesh N. S. P.; Dharmaraj N. Binuclear copper complexes: synthesis, X-ray structure and interaction study with nucleotide/protein by *in vitro* biochemical and electrochemical analysis. *Eur. J. Med. Chem.* **2014**, *78*, 281–293.

(43) Mansour A. M.; Ragab M. S. DNA/lysozyme binding propensity and nuclease properties of benzimidazole/2,2'-bipyridine based binuclear ternary transition metal complexes. *RSC Adv.* **2019**, *9*, 30879–30887.

(44) Rehman M. T.; Khan A. U. Understanding the interaction between human serum albumin and anti-bacterial/anti-cancer compounds. *Cur. Pharm. Des.* **2015**, *21*, 1785–1799.

(45) Suryawanshi V. D.; Walekar L. S.; Gore A. H.; Anbhule P. V.; Kolekar G. B. Spectroscopic analysis on the binding interaction of biologically active pyrimidine derivative with bovine serum albumin. *J. Pharm. Anal.* **2016**, *6*, 1, 56–63.

(46) Joksimović N.; Baskić D.; Popović S.; Zarić M.; Kosanić M.; Ranković B.; Stanojković T.; Novaković S. B.; Davidović G.; Bugarčić Z.; Janković N. Synthesis, characterization, biological activity, DNA and BSA binding study: novel copper(II) complexes with 2-hydroxy-4-aryl-4-oxo-2-butenolate. *Dalton Trans.* **2016**, *45*, 15067–15077.

(47) Qin Q. P.; Zou B. Q.; Tan M. X.; Wang S. L.; Liu Y. C.; Liang H. Tryptanthrin derivative copper(II) complexes with high antitumor activity by inhibiting telomerase activity, and inducing mitochondria-mediated apoptosis and S-phase arrest in BEL-7402. *New J. Chem.* **2018**, *42*, 15479–15487.

(48) Qin Q. P.; Meng T.; Tan M. X.; Liu Y. C.; Luo X. J.; Zou B. Q.; Liang H. Synthesis, crystal structure and biological evaluation of a new dasatinib copper(II) complex as telomerase inhibitor. *Eur. J. Med. Chem.* **2018**, *143*, 1597–1603.

(49) Hu J.; Liao C.; Mao R.; Zhang J.; Zhao J.; Gu Z. DNA interactions and *in vitro* anticancer evaluations of pyridine-benzimidazole-based Cu complexes. *Med. Chem. Commun.* **2018**, *9*, 337–343.

(50) Dearling J. L. J.; Lewis J. S.; Mullen G. E. D.; Rae M. T.; Zweit J.; Blower P. J. Design of hypoxia-targeting radiopharmaceuticals: selective uptake of copper 64 complexes in hypoxic cells *in vitro*. *J. Eur. J. Nucl. Med.* **1998**, *25*, 788–792.

(51) Fujibayashi Y.; Taniuchi H.; Yonekura Y.; Ohtani H.; Konishi J.; Yokoyama A. Copper-62-ATSM: a new hypoxia imaging agent with high membrane permeability and low redox potential. *J. Nucl. Med.* **1997**, *38*, 7, 1155–1160.

(52) Dearling J. L. J.; Blower P. J. Redox-active metal complexes for imaging hypoxic tissues: structure–activity relationships in copper(II) bis(thiosemicarbazone) complexes. *Chem. Commun.* **1998**, *22*, 2531–2532.

(53) Colombié M.; Gouard S.; Frindel M.; Vidal A.; Chérel M.; Kraeber-Bodéré F.; Rousseau C.; Bourgeois M. Focus on the controversial aspects of (64)Cu-ATSM in tumoral hypoxia mapping by PET imaging. *Front. Med. (Lausanne)*. **2015**, *2*, 58–65.

(54) Anjum R.; Palanimuthu D.; Kalinowski D. S.; Lewis W.; Park K. C.; Kovacevic Z.; Khan I. U.; Richardson D. R. Synthesis, characterization, and *in vitro* anticancer activity of copper and zinc bis(thiosemicarbazone) complexes. *Inorg. Chem.* **2019**, *58*, 20, 13709–13723.

(55) Ngwane A. H.; Petersen R. D.; Baker B.; Wiid I.; Wong H. N.; Haynes R. K. The evaluation of the anti-cancer drug elesclomol that forms a redox-active copper chelate as a potential anti-tubercular drug. *IUBMB Life.* **2019**, *71*, 5, 532–538.

(56) Zhang X.; Liu X.; Phillips D. L.; Zhao C. Mechanistic insights into the factors that influence the DNA nuclease activity of mononuclear facial copper complexes containing hetero-substituted cyclens. *ACS Catal.* **2016**, *6*, 248–257.

(57) Michaels H.; Benesperi I.; Edvinsson T.; Muñoz-García A. B.; Pavone M.; Boschloo G.; Freitag M. Copper complexes with tetradentate ligands for enhanced charge transport in dye-sensitized solar cells. *Inorganics.* **2018**, *6*, 2, 53.

(58) Rezaei A.; Khanamani Falahati-Pour S.; Mohammadzadeh F.; Hajizadeh M. R.; Mirzaei M. R.; Khoshdel A.; Fahmidehkar M. A.; Mahmoodi M. Effect of a copper (II) complex on the induction of apoptosis in human hepatocellular carcinoma cells. *Asian Pac. J. Cancer Prev.* **2018**, *19*, 10, 2877–2884.

(59) Xia L.; Sijia H.; Ailing H.; Yayu Y.; Guozhen F.; Jifeng L.; Shuo W. Intracellular Fenton reaction based on mitochondria-targeted copper(II)-

peptide complex for induced apoptosis. *J. Mater. Chem. B*. **2019**, *7*, 4008-4016.

(60) Jungwirth U.; Kowol C. R.; Keppler B. K.; Hartinger C. G.; Berger W.; Heffeter P. Anticancer activity of metal complexes: involvement of redox processes. *Antioxid. Redox Signaling*. **2011**, *15*, 4, 1085-1127.

(61) Erofeev A.; Gorelkin P.; Garanina A.; Alova A.; Efremova M.; Vorobyeva N.; Edwards C.; Korchev Y.; Majouga A. Novel method for rapid toxicity screening of magnetic nanoparticles. *Sci. Rep.* **2018**, *8*, 7462.

(62) Gomes A.; Fernandes E.; Lima J. L. Fluorescence probes used for detection of reactive oxygen species. *J. Biochem. Biophys. Methods*. **2005**, *65*, 2-3, 45-80.

(63) Jacewicz D.; Siedlecka-Kroplewska K.; Drzeżdżon J.; Piotrowska A.; Wyrzykowski D.; Tesmar A.; Żamojć K.; Chmurzyński L. Method for detection of hydrogen peroxide in HT22 cells. *Sci. Rep.* **2017**, *7*, 45673.

(64) Griendling K. K.; Touyz R. M.; Zweier J. L.; Dikalov S.; Chilian W.; Chen Y. R.; Harrison D. G.; Bhatnagar A. Measurement of reactive oxygen species, reactive nitrogen species, and redox-dependent signaling in the cardiovascular system: a scientific statement from the american heart association. *Circ. Res.* **2016**, *119*, 5, 39-75.

(65) Sheldrick G. M. A short history of SHELX. *Acta. Cryst.* **2008**, *A64*, 112-122.

(66) Brandenburg K. *DIAMOND*. **2000**, Release 2.1d; Crystal Impact GbR, Bonn, Germany.

(67) Mosmann T. Rapid colorimetric assay for cellular growth and survival: application to proliferation and cytotoxicity assays. *J. Immunol. Methods*. **1983**, *65*, 1-2, 55-63.

(68) Friedrich J.; Seidel C.; Ebner R.; Kunz-Schughart L. A. Spheroid-based drug screen: considerations and practical approach. *Nat. Protoc.* **2009**, *4*, 309-324.

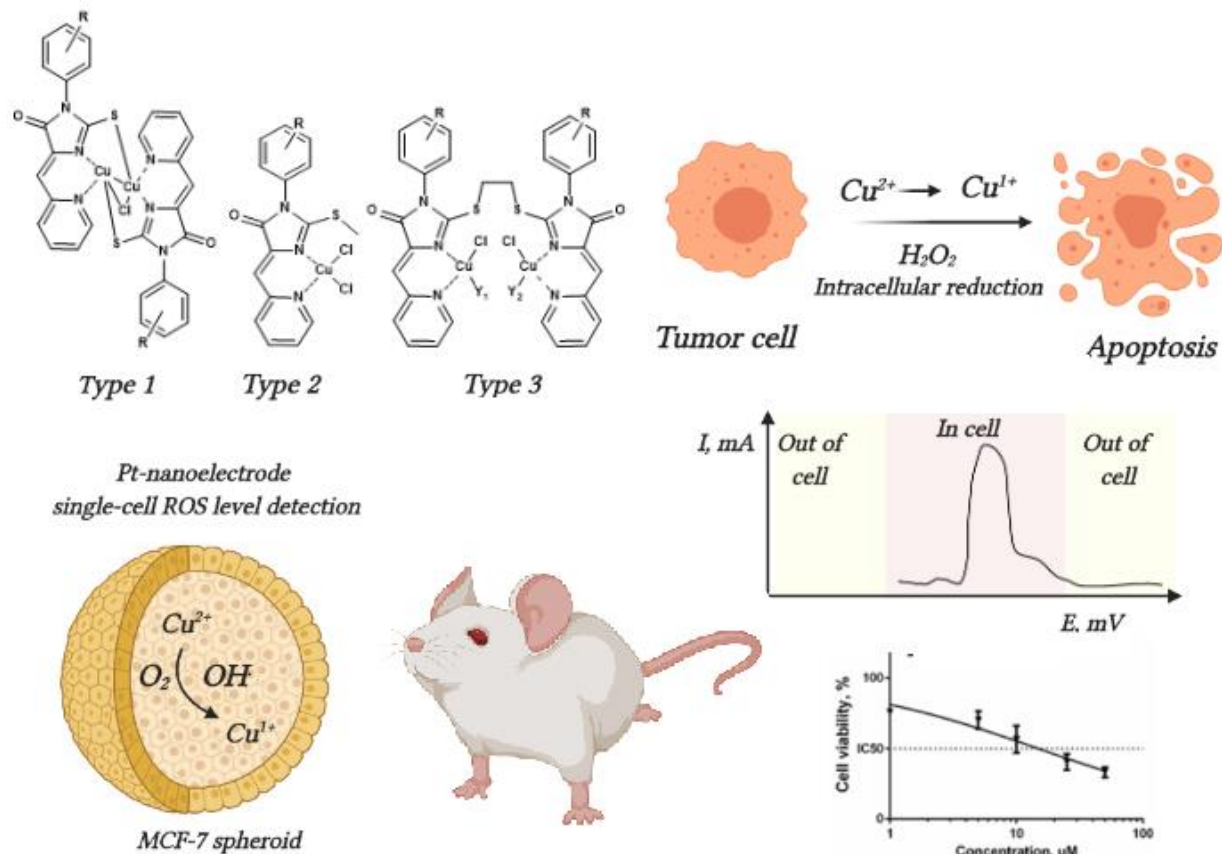
(69) Ryabaya O.; Prokofieva A.; Akasov R.; Khochenkov D.; Emelyanova M.; Burov S.; Markvicheva E.; Inshakov A.; Stepanova E. Metformin increases antitumor activity of MEK inhibitor binimetinib in 2D and 3D models of human metastatic melanoma cells. *Biomed. Pharmacother.* **2019**, *109*, 2548-2560.

(70) Li H.; Le X.-Y.; Pang D.-W.; Deng H.; Xu Z.-H.; Lin Z.-H. DNA-binding and cleavage studies of novel copper(II) complex with L-phenylalaninate and 1,4,8,9-tetra-aza-triphenylene ligands. *J. Inorg. Biochem.* **2005**, *99*, 11, 2240-2247.

(71) Kim N. W.; Piatyszek M. A.; Prowse K. R.; Harley C. B.; West M. D.; Ho P. L.; Coviello G. M.; Wright W. E.; Weinrich S. L.; Shay J. W. Specific association of human telomerase activity with immortal cells and cancer. *Science*. **1994**, *266*, 5193, 2011-2015.

(72) Kuznetsova O. Y.; Antipin R. L.; Udina A. V.; Krasnovskaya O. O.; Beloglazkina E. K.; Terenin V. I.; Koteliansky V. E.; Zyk N. V.; Majouga A. G. An improved protocol for synthesis of 3-substituted 5-arylidene-2-thiohydantoins: Two-step procedure alternative to classical methods. *J. Heterocycl. Chem.* **2015**, *53*, 5, 1570-1577.

Table of Contents graphic



1
2
3
4
5
6
7
8
9
10
11
12
13
14
15
16
17
18
19
20
21
22
23
24
25
26
27
28
29
30
31
32
33
34
35
36
37
38
39
40
41
42
43
44
45
46
47
48
49
50
51
52
53
54
55
56
57
58
59
60